

Book of Abstract

Characterisation of Crack/Notch Tip Fields

Edited by
G. Meneghetti, A. Campagnolo, M. Ricotta,
M. Vormwald, Y. Hong, T. Palin-Luc, L. Susmel



Prima edizione 2024, Padova University Press

Titolo originale: Book of Abstract. Characterisation of Crack/Notch Tip Fields

Tutti i diritti di traduzione, riproduzione e adattamento, totale o parziale, con qualsiasi mezzo (comprese le copie fotostatiche e i microfilm) sono riservati.

ISBN 978-88-6938-408-0

©2024 Padova University Press
Università degli Studi di Padova
Via 8 Febbraio 2, Padova
www.padovauniversitypress.it

Le immagini del frontespizio sono distribuite con licenza Unsplash (<https://unsplash.com/it/licenza>)

Autore:

https://unsplash.com/it/@filos_photo

Immagine:

<https://unsplash.com/it/foto/uno-specchio-dacqua-con-edifici-sullo-sfondo-l-nTYEA2fVk>

Autore:

<https://unsplash.com/it/@marcostevanon> https://unsplash.com/it/@filos_photo

Immagine:

<https://unsplash.com/it/foto/edificio-in-cemento-bianco-vicino-allo-specchio-dacqua-durante-la-notte-FpCHxPyG7MU>



<https://www.padovauniversitypress.it/en/publications/9788869384080>



This work is licensed under a Creative Commons Attribution International License
<https://creativecommons.org/licenses/by-nc-nd/4.0/>



UNIVERSITÀ
DEGLI STUDI
DI PADOVA



DIPARTIMENTO
DI INGEGNERIA
INDUSTRIALE

SEVENTH IJFATIGUE & FFEMS
JOINT WORKSHOP

Characterisation of Crack/Notch Tip Fields



Book of abstracts



The University of Padua, University Language Centre CLA
5-7 June 2024 | Padua, Italy

Sponsored by



Authors' index

Aguilera J. A.	1, 15	Hong Y.	25, 77
Aghabeigi M.	9	Hu X.-K.	17
Akbardoost J.	9	Jacquemound C.	41
Almuhanna H.	3	Jin P.	27
Antunes F. V.	5, 51, 65	Jivkov A.	67
Askes H.	7	Kalina M.	29
Ayatollahi M. R.	9	Kästner M.	29
Baer J.	13	Kockelmann W.	41
Beretta S.	55	Kotousov A.	73
Borrego L.	15	Liu M.	47
Branco R.	15	Liu Z.	27
Breitbarth E.	11	Livieri P.	31, 33
Brighenti R.	69	Lopez-Crespo P.	1, 15
Buffiere J.-Y.	23	Maragoni L.	59
Burzic Z.	61	Marghitas M.	35
Buslaps T.	1	Markham M.	37
Buttin P.	45	Marsavina L.	35
Campagnolo A.	13, 43	Matvienko Y.	39
Carraro P. A.	59	Mayorga L. G.	45
Cerezo P. M.	1, 15	McDowell D.	79
Chen R.	17, 19	McKendrey S.	41
Chen X.	27	Meggiolaro M. A.	47
Cicero S.	21	Meneghetti G.	13, 43
Cornetti P.	49	Merot P.	45
Coules H.	41	Miranda A. C.	47
Cova M.	55	Mirzaei A. M.	49
Cruces A. S.	1, 15	Montanari M.	69
Dammass F.	29	Morel F.	45
D'Andrea A.	55	Mostafavi M.	41
Díaz F. A.	5	Neto D. M.	5, 51, 65
Du L.	25	Nowell D.	53
Eleonsky S.	39	Palin-Luc T.	23
Engelberg D.	67	Pan X.	25
Fatemi A.	37	Patriarca L.	55
Garcia-Gonzalez A.	1, 15	Paysan F.	11
González G. G.	5	Pegritz M.	57
Hansen-Dörr A.	29	Perkovic S.	61
Hebrard L.	23	Pessard E.	45
Hohenwarter A.	57	Pinho de Castro J. T.	47



Authors' index

Pippan R.	57	Zhu T.	79
Pisarev V.	39	Zirkle T.	79
Popa C.-F.	35		
Qian G.	25, 77		
Quaresimin M.	59		
Radakovic Z.	61		
Ramadhan R.	41		
Ranc N.	23		
Robert C.	45		
Rusnati L.	55		
Sapora A.	49		
Schneider T.	29		
Sedmak A.	61		
Sehitoglu H.	63		
Seibert P.	29		
Sérgio E. R.	5, 51, 65		
Sheen B.	53		
Shi P.	67		
Smith M.	67		
Spagnoli A.	69		
Steuwer A. T.	1		
Susmel L.	3		
Tao Z.	25		
Tatar F.	69		
Torelli G.	3		
Tovo R.	33		
Tsakmakis A.	71		
Van-Heule X.	41		
Vasco-Olmo J. M.	5		
Vecchiato L.	13		
Vidler J.	73		
Visentin A.	43		
Vormwald M.	71		
Walch L.	57		
Withers P. J.	1		
Xuan F.-Z.	17, 19		
Zappalorto M.	59, 75		
Zhang N.	77		
Zhu M.-L.	17, 19		



Workshop program

5th of June (Day 1)

- 08.15-08.45 Registration
08.45-09.00 Workshop Opening

Session I – *Chairman: Luca Susmel*

- 09.00-09.20 **Puyu Shi, Dirk Engelberg, Michael Smith, Andrey Jivkov.**
On the effect of triple line disclinations in intergranular cracking..... p. 67
- 09.20-09.40 **Huseyin Sehitoglu.**
Dislocation Glide Theories (CRSS) Relevant to Fatigue..... p. 63
- 09.40-10.00 **Rong Chen, Xiao-Kai Hu, Ming-Liang Zhu, Fu-Zhen Xuan.**
Towards a strain-based approach to fatigue cracking p. 17
- 10.00-10.20 **Rong Chen, Ming-Liang Zhu, Fu-Zhen Xuan.**
In-situ observation of notch-induced fatigue crack initiation and growth behavior in a magnesium alloy. p. 19
- 10.20-10.40 **Youshi Hong, Zhiqiang Tao, Leiming Du, Xiangnan Pan, Guian Qian.**
Crack surface contacting behaviour at initiation region of very-high-cycle fatigue for high-strength alloys..... p. 25
- 10.40-11.20 Coffee break

Session II – *Chairman: Giovanni Meneghetti*

- 11.20-11.40 **Diogo Mariano Neto, Edmundo Rafael Sérgio, Fernando Ventura Antunes.**
Predicting the fatigue crack growth rate using the plastic strain damage at the crack tip. p. 51
- 11.40-12.00 **Edmundo Rafael Sérgio, Fernando Ventura Antunes, Diogo Mariano Neto.**
Fatigue crack growth: Effect of micro-voids damage p. 65
- 12.00-12.20 **Fernando Ventura Antunes, Diogo Mariano Neto, Edmundo Rafael Sérgio, Giancarlo Gómez Gonzáles, Jose Manuel Vasco-Olmo, Francisco Alberto Díaz.**
Fatigue crack growth: a close look to crack tip phenomena using the CTOD..... p. 5
- 12.20-12.40 **Louis Hebrard, Nicolas Ranc, Thierry Palin-Luc, Jean-Yves Buffiere.**
Influence of environment on the propagation of internal fatigue cracks in a Ti alloy..... p. 23
- 12.40-13.00 **Reinhard Pippan, Michael Pegritz, Lukas Walch, Anton Hohenwarter.**
Residual Stress Fields of Pre-Cracks and Impact on Fracture Mechanics Properties..... p. 57

13.00-14.30 Lunch Break

Session III – *Chairman: Youshi Hong*

- 14.30-14.50 **James Vidler, Andrei Kotousov.**
Effect of wake of plasticity on the residual crack closure and determination of crack tip opening loads using compliance-based methods..... p. 73
- 14.50-15.10 **Pierre Merot, Franck Morel, Camille Robert, Etienne Pessard, Linamaria Gallegos Mayorga, Paul Buttin.**
A unified non local approach to interpret defect size and shape effects on fatigue strength..... p. 45
- 15.10-15.30 **Simon McKendrey, Xavier Van-Heule, Rangi Ramadhan, Winfried Kockelmann, Harry Coules, Clementine Jacquemound, Mahmoud Mostafavi.**
Validating residual stress reconstruction via finite element analysis using neutron imaging..... p. 41
- 15.30-15.50 **Jose A. Aguilera, Pablo M. Cerezo, Alejandro S. Cruces, Antonio Garcia-Gonzalez, Axel Steuwer, T. Buslaps, Philip J. Withers, Pablo Lopez-Crespo.**
Characterisation of the cyclic plastic zone in the crack-tip of a fatigued specimen by synchrotron diffraction..... p. 1
- 15.50-16.10 **Eric Breitbarth, Florian Paysan.**
Characterisation of crack closure mechanisms with robot-assisted high-resolution digital image correlation..... p. 11
- 16.10-16.40 Coffee break

Session IV – *Chairman: Michael Vormwald*

- 16.40-17.00 **Alberto Campagnolo, Luca Vecchiato, Jurgen Baer, Giovanni Meneghetti.**
Multi-probe potential drop technique to estimate the geometry, location and size of a crack propagating in cylindrical specimens..... p. 13
- 17.00-17.20 **Michele Zappalorto.**
Analytical stress field solutions for radiused notches in orthotropic solids..... p. 75
- 17.20-17.40 **Amir Mohammad Mirzaei, Pietro Cornetti, Alberto Sapore.**
Fatigue life prediction of holed laminated composites based on Finite Fracture Mechanics. p. 49
- 18.00-18.20 **Yury Matvienko, Vladimir Pisarev, Sviatoslav Eleonsky.**
Verification of a non-destructive method for quantitative analysis of damage accumulation proceeding from notch border displacements..... p. 39

End of Day 1

6th of June (Day 2)

08.30-09.00 Registration

Session V – *Chairman: Thierry Palin-Luc*

- 09.00-09.20 **Matthew Markham and Ali Fatemi.**
Mixed-Mode Small Crack Growth Behaviours in Additively Manufactured Metals..... p. 37
- 09.20-09.40 **Ningyu Zhang, Youshi Hong, Guian Qian.**
Microstructure-based fatigue life prediction of additively manufactured AlSi10Mg specimens..... p. 77
- 09.40-10.00 **Harm Askes.**
Generalised continuum models for periodic beam lattice structures with distributed mass..... p. 7
- 10.00-10.20 **Mihai Marghitas, Cosmin-Florin Popa, Liviu Marsavina.**
On the size and notch effect in AM photo-polymerised components..... p. 35
- 10.20-10.40 **Pablo M. Cerezo, Jose A. Aguilera, Alejandro S. Cruces, Antonio Garcia-Gonzalez, Ricardo Branco, Luis Borrego, Pablo Lopez-Crespo.**
Digital image correlation for monitoring stress intensity factor in 18Ni300 additively manufactured samples..... p. 15
- 10.40-11.20 Coffee break

Session VI – *Chairman: David Nowell*

- 11.20-11.40 **Antonio Carlos de Oliveira Miranda, Mengen Liu, Marco Antonio Meggiolaro, Jaime Tupiassú Pinho de Castro.**
Why does the theory of critical distance work?..... p. 47
- 11.40-12.00 **Majid Reza Ayatollahi, Javad Akbardoost, Mahya Aghabeigi.**
Evaluating size effects using a modified energy-based fracture criterion..... p. 9
- 12.00-12.20 **Markus Kästner, Arne Hansen-Dörr, Franz Dammass, Martha Kalina, Tom Schneider, Paul Seibert.**
Phase-field modelling of fracture – inelasticity, heterogeneity, and fatigue..... p. 29
- 12.20-12.40 **Aris Tsakmakis, Michael Vormwald.**
Analysis of crack tip fields in a phase field model for ductile fracture..... p. 71
- 12.40-13.00 **Sergio Cicero.**
Assessment of structural materials containing notch-type defects: A comprehensive validation of the FAD-TCD methodology on metallic and non-metallic materials... p. 21
- 13.00-14.30 Lunch Break

Session VII – *Chairman: Alberto Campagnolo*

- 14.30-14.50 **Luca Patriarca, Antonio D’Andrea, Matteo Cova, Lorenzo Rusnati, Stefano Beretta.**
Cyclic R-curve measurements for structural metallic alloys..... p. 55
- 14.50-15.10 **David Nowell, Bemim Sheen.**
Fatigue Crack Propagation under Non-proportional Multiaxial Loading p. 53
- 15.10-15.30 **Andrea Spagnoli, Matteo Montanari, Roberto Brighenti, Farzad Tatar.**
On the puncturing of flawed soft membranes..... p. 69
- 15.30-15.50 **Pengfei Jin, Zheng Liu, Xu Chen.**
Analysis of crack-tip field in orthotropic compact-tension-shear specimens..... p. 27
- 15.50-16.10 **Marino Quaresimin, Paolo A. Carraro, Lucio Maragoni, Michele Zappalorto.**
A comprehensive damage-based strategy to predict fatigue damage evolution in composite laminates. p. 59
- 16.10-16.40 Coffee break
- 18.00-19.30 Guided tour of Palazzo Bo (Palazzo Bo is the historical headquarters of the University of Padova since 1493)

19.45 Workshop Dinner

End of Day 2

7th of June (Day 3)

Session VIII – *Chairman: Thierry Palin-Luc*

- 9.00-9.20 **Aleksandar Sedmak, Srdja Perkovic, Zijah Burzic, Zoran Radakovic.**
Notch vs. crack effects on impact toughness of a duplex steel p. 61
- 9.20-9.40 **Giovanni Meneghetti, Alberto Visentin, Alberto Campagnolo.**
Implementation of the Peak Stress Method for the automated FEA-assisted design of welded structures subjected to variable amplitude multiaxial fatigue loads p. 43
- 9.40-10.00 **Paolo Livieri, Roberto Tovo.**
Review of the design fatigue strength for steel butt welded joints: influence of geometrical factors and shape defects..... p. 33
- 10.00-10.20 **Paolo Livieri.**
Simplified analysis of stress intensity factors at weld toe..... p. 31
- 10.20-10.50 Coffee break

10.50-11.50 **Discussion Session & Closure – *Chairman: Michael Vormwald & Youshi Hong***

End of Day 3

Characterisation of the cyclic plastic zone in the crack-tip of a fatigued specimen by synchrotron diffraction

Jose A. AGUILERA¹, Pablo M. CERESO¹, Alejandro S. CRUCES¹, Antonio GARCIA-GONZALEZ¹, Axel STEUWER^{2,3}, T. BUSLAPS⁴, Philip J. WITHERS⁵, Pablo LOPEZ-CRESPO¹

¹ Department of Civil and Materials Engineering, University of Malaga, C/Dr Ortiz Ramos s/n, 29071, Malaga, Spain

² EISCAT Scientific Association, Bengt Hultqvists väg 1, SE-981 92 Kiruna, Sweden

³ Nelson Mandela University, Gqeberha, 6031 South Africa

⁴ ESRF, 71, avenue des Martyrs, CS 40220, 38043 Grenoble Cedex 9, France.

⁵ Henry Royce Institute, Department of Materials, The University of Manchester, M13 9PL, UK

plc@uma.es

The analysis of crack-tip stresses and Plastic Zones (PZ) under cyclic and variable amplitude loading is a vital aspect of fracture mechanics. Its significance lies in its ability to advance engineering designs for lightweight constructions that are susceptible to fatigue. Even though Linear Elastic Fracture Mechanics (LEFM) has been effective in predicting Fatigue Crack Growth (FCG), the primary force behind this phenomenon is the damage mechanism near the crack tip, which is usually non-linear [1]. In accordance with the commonly acknowledged understanding, the first phase of loading leads to the genesis of the monotonic PZ which is subsequently followed by the formation of a relatively smaller secondary PZ when the material is unloaded. As the material continues to undergo cyclic loading, a distinct plastic zone, known as the Cyclic Plastic Zone (CPZ), is established [2,3]. To understand FCG better, we need to investigate the damage parameters that control it and quantify different PZs. Synchrotron X-ray diffraction (S-XRD) is a useful experimental technique that enables precise measurement of stress fields and elastic strain distributions at the crack tip while studying the effects of overloads (OLs) on FCG [4]. Despite the fact that S-XRD studies can identify the strain or stress fields at the crack tip in the bulk of materials, only a limited number of studies have expanded their focus beyond the process zone located in front of the crack tip [5]. The need for new insights into the plasticity near the crack tip has been highlighted, specifically in regard to the size of the plastic zone. We have developed a comprehensive approach for evaluating the plastic zone in a thin (~plane stress) specimen under various stages of fatigue. Our aim is to accurately delineate both the fatigue-crack plastic zone and the background plastic zone, with unprecedented accuracy.

The study comprises a series of important stages, illustrated in Fig. 1a. The main objective is to precisely measure the elastic strain fields located in the region preceding a fatigue crack, particularly under conditions where plastic strains exert a considerable influence. This necessitated a meticulous selection of materials and specimen geometry, in addition to carrying out in-situ fatigue testing while recording X-ray diffraction patterns at each stage. Analysing the data to generate comprehensive strain maps and resultant stresses is also a key stage in determining the PZ. This process is outlined below. An in-situ cyclic loading test is conducted following ASTM E647 recommendations on a bainitic steel Compact Tension specimen ($W = 50$ mm and $B = 3.3$ mm) having Young's modulus, $E = 220$ GPa, a yield stress of 699 MPa and a Poisson's ratio of 0.33. The experiment, with a ΔK for precracking of 29.4 MPa \sqrt{m} , R of 0.03 and OL of 67%, with a constant load amplitude for further cycles, was undertaken at the European

Synchrotron Radiation Facility in Grenoble, France. Two solid-state Energy Dispersive detectors were situated so as to measure the strains in perpendicular in-plane directions; the crack growth and opening direction following [6]. The resulting diffraction patterns are analysed with GSAS-II [7] after conversion from energy dispersive to artificial angle dispersive scale. The Pawley-type refinement allows for the obtention of lattice parameters that are converted into elastic strains when compared to the determined stress-free lattice parameter. Assuming plane stress conditions, stress in each direction is inferred, and with the external input of shear stress from a Finite Element Model, equivalent Von Mises stresses are calculated. Lastly, using von Mises yield criterion the PZ is characterized. The results of this work shed new light on the PZ shape and size in the crack tip, Fig. 1b (estimated error ± 20 MPa). Resulting PZs are having a mixed shape between plane strain and plane stress analytic boundaries, what might be in line with the state of stress in the mid plane of a thin sample. Further it can identify the CPZ under K_{min} , which it has not been possible to explore previously experimentally in the bulk of a CT.

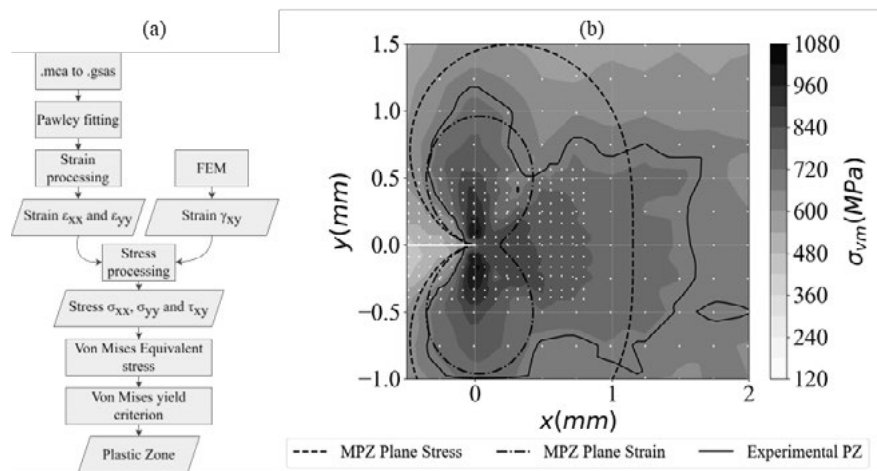


Figure 1. (a) Flow chart of process followed. (b) Von Mises equivalent stress field near the crack tip for OL event at maximum load. Plane stress, plane strain and experimental PZs indicated.

REFERENCES

1. Ritchie, R.O. Mechanisms of fatigue-crack propagation in ductile and brittle solids. *Int. J. Fracture*, 100, 55–83 (1999).
2. Park, H.-B.; Kim, K.-M.; Lee, B.-W. Plastic zone size in fatigue cracking. *Int. J. Pres. Ves. Pip.*, 68, 279–285 (1996).
3. Park, H.-B.; Kim, K.-M.; Lee, B.-W. A new method for cyclic crack-tip plastic zone size determination under cyclic tensile load. *Eng. Fract. Mech.*, 126, 141–154 (2014).
4. Steuwer, A.; Santisteban, J.R.; Turski, M.; Withers, P.J.; Buslaps, T. High-resolution strain mapping in bulk samples using full-profile analysis of energy-dispersive synchrotron X-ray diffraction data. *J. Appl. Crystallogr.*, 37, 883–889 (2004).
5. Carrera, M.; Cruces, A.S.; Kelleher, J.F.; Tai, Y.; Yates, J.R.; Withers, P.J.; Lopez-Crespo, P. Characterisation of the crack tip plastic zone in fatigue via synchrotron X-ray diffraction. *Fatigue Fract. Eng. M.*, 45, 2086–2098 (2022).
6. Steuwer, A.; Rahman, M.; Shterenlikht, A.; Fitzpatrick, M. E.; Edwards, L.; Withers, P. J. The evolution of crack-tip stresses during a fatigue overload event. *Acta Mater.*, 58, 4039–4052 (2010).
7. Toby, B.H.; Von Dreele, R.B. GSAS-II: the genesis of a modern open-source all purpose crystallography software package. *J. Appl. Crystallogr.*, 46, 544–549 (2013).

The use of the Theory of Critical Distances to Estimate the Static failure of Double-Lap Shear Bolted Connections

Hasan ALMUHANNA¹, Giacomo TORELLI¹, Luca SUSMEL¹

¹Department of Civil and Structural Engineering, The University of Sheffield, Mapping Street, Sheffield S1 3JD, UK

l.susmel@sheffield.ac.uk

This study examines the static behaviour of 316L stainless steel double-lap shear bolted connections under uniaxial tensile loading, with a primary focus on applying the Theory of Critical Distances (TCD). The use of TCD, employing linear elastic stress fields, has consistently proven reliable in estimating static failure around stress raisers, with error percentages typically falling within a range of $\pm 20\%$ [1, 2]. The main aim of this investigation is to explore whether the Point Method (PM) (i.e., the simplest formalisation of the TCD) can be used to perform the static assessment of bolted connections, with this approach being applied by directly post-processing the local linear-elastic stress fields in the vicinity of the holes in the joint inner plates.

The experimental tests involved connections with single and double bolts. Following the Eurocode 3 (EC3) design procedure, key design parameters such as thickness, breadth, end distance, edge distance, and horizontal pitch distance were identified as influential variables affecting the failure mechanism significantly [3]. Therefore, the inner plates being tested were designed with different combinations of these parameters to exhibit various failure modes. The test results were then compared to the design estimations obtained by applying the EC3 procedure, revealing significant discrepancies in failure predictions.

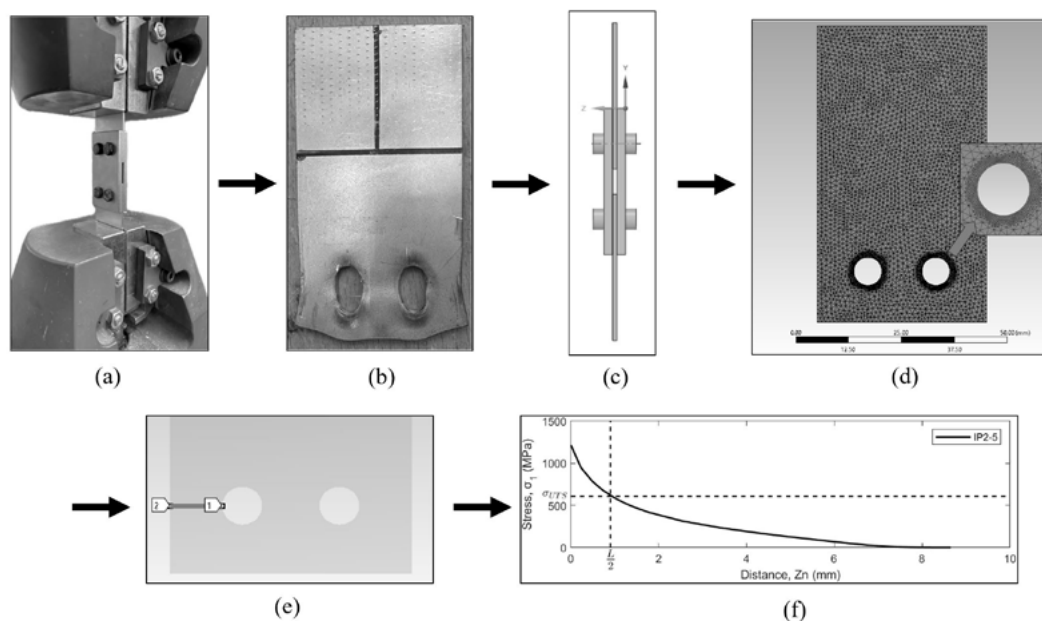


Figure 1. Procedure followed to apply the PM: (a) experimental test, (b) failure induced on the inner plate, (c) FE modelling, (d) mesh refinement around the holes, (e) definition of the focus path and associated stress-distance curve, and (f) application of the PM method.

To overcome the limitations associated with the standard design approach, the TCD was applied in the form of the PM, treating the holes in the inner plates as conventional stress concentrators. Fig. 1 summarises the procedure that was followed to use the PM to post-process the results being generated. The relevant stress fields in the vicinity of the holes were determined through three-dimensional Finite Element (FE) models solved using ANSYS Workbench. These linear-elastic models were assembled by using tetrahedral elements (TET10). The bolts and nuts were created separately and combined with the plates by making the most of the ANSYS assembly tool. Finally, the regions at the interface between plates were modelled using frictional contact.

According to Fig. 1e, the focus path for determining the relevant linear-elastic stress-distance curves was assumed to originate from the hot-spot and extend perpendicular to the direction of the applied loading.

The critical distance was estimated using the following well-known formula [1]:

$$L = \frac{1}{\pi} \left(\frac{K_c}{\sigma_{UTS}} \right)^2 \quad (1)$$

The fracture toughness, K_c , associate with the stainless steel being investigated was eastimated to be equal to $45.6 \text{ MPa}\cdot\text{m}^{0.5}$ for a thickness of 2 mm [4]. Together with a ultimate tensile strength, σ_{UTS} , of 608.4 MP, the above value for K_c returned a critical length, L , equal to 1.8 mm.

The application of the TCD in the form of the PM proved successful, yielding estimates characterized by a mean error of 17% (with a standard deviation of 11.1%) for joints with one bolt and of 18.8% (with a standard deviation of 9.5%) for connections with two bolts. These results are indeed promising, suggesting that the TCD can be reliably utilised for designing bolted joints. Moreover, this critical length-based design approach demonstrates a higher level of accuracy compared to the standard approach recommended by EC3.

REFERENCES

1. Susmel, L.; Taylor, D. On the use of the Theory of Critical Distances to predict static failures in ductile metallic materials containing different geometrical features, *Eng. Fract. Mech.*, 75(15), 4410–4421 (2008).
2. Ameri, A. A. H.; Davison, J. B.; Susmel, L. On the use of linear-elastic local stresses to design load-carrying fillet-welded steel joints against static loading. *Eng. Fract. Mech.*, 136, 38–57 (2015).
3. EN 1993-1-8 (2005) (English): Eurocode 3: Design of steel structures - Part 1-8: Design of joints. The European Union Per Regulation 305/2011, Directive 98/34/EC, Directive 2004/18/EC.
4. Broek, D. Elementary engineering fracture mechanics. Kluwer Academic, Boston, US (1986).

Fatigue crack growth: a close look to crack tip phenomena using the CTOD

Fernando Ventura ANTUNES¹, Diogo Mariano NETO¹, Edmundo Rafael SÉRGIO¹,
Giancarlo Gómez GONZÁLES², Jose Manuel VASCO-OLMO², Francisco Alberto DÍAZ²

¹ CEMMPRE, ARISE, Department of Mechanical Engineering, University of Coimbra, Portugal

² Departamento de Ingeniería Mecánica y Minera, University of Jaén, Jaén, Spain

fernando.ventura@dem.uc.pt

Fatigue crack growth (FCG) is usually studied using ΔK , which is a linear elastic parameter, however several limitations have been found in the use of da/dN - ΔK curves. In fact, FCG is linked to non-linear and irreversible mechanics happening at the crack tip, therefore, non-linear parameters must be used to study FCG instead of ΔK . In here, we propose the use of CTOD to study crack tip phenomena.

Figure 1 presents a typical curve of CTOD versus applied load, measured numerically at the first node behind crack tip. In this curve it is possible to identify the minimum load (point A), crack opening (point B) and crack closure (point F), the transition between elastic and plastic regimes (point C), the elastic and plastic deformations (δ_e and δ_p , respectively) and the energy dissipated (dashed area).

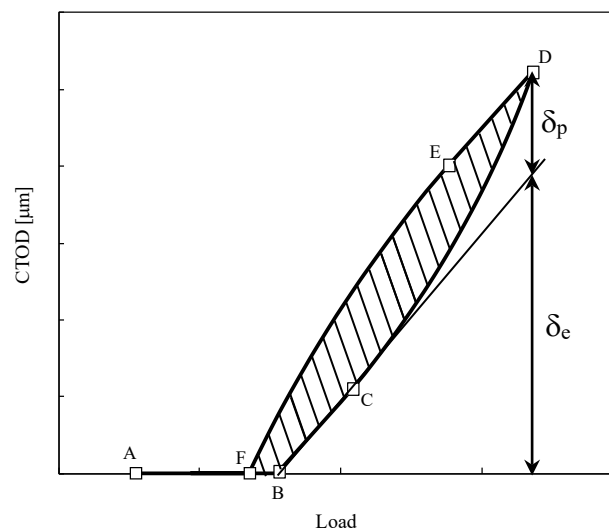


Figure 1. A typical curve of CTOD versus load.

Usually only the crack closure level is quantified through the CTOD curve, however much more information can be obtained from the CTOD analysis. Therefore, the objective of the present study is to explain how to use CTOD parameters for a better understanding of FCG. This way, a wider use of CTOD plots is expected in both experimental and numerical studies.

Linear correlations of da/dN with plastic CTOD, δ_p , were obtained for different materials using DIC [1] and FEM analysis [2], as can be seen in Figures 2a and 2b. The plastic CTOD includes the effects of crack closure, crack tip blunting, partial closure and residual stresses. Figure 2b shows that, using the plastic CTOD as crack driving force, the effect of stress ratio no

longer exists. The da/dN -plastic CTOD curve, which is supposed to be a material property, was used to predict the effect of different load parameters on FCG rate, namely, loading parameters (overloads, load blocks, etc.) and material parameters (Young’s modulus, isotropic and kinematic hardening parameters) [3-5].

The CTOD was also used to predict fatigue threshold in vacuum [6] and the limits of small-scale yielding [7]. SSY conditions were shown to dominate when the elastic component of CTOD is $>75\%$ of the total CTOD measured at a distance of $8\ \mu\text{m}$ (the finite element mesh size) behind the crack tip, i.e., $\delta_e/\delta_t > 75\%$. Large-scale yielding, LSY, conditions become dominant for relatively large values of plastic CTOD, $\delta_e/\delta_t < 60\%$.

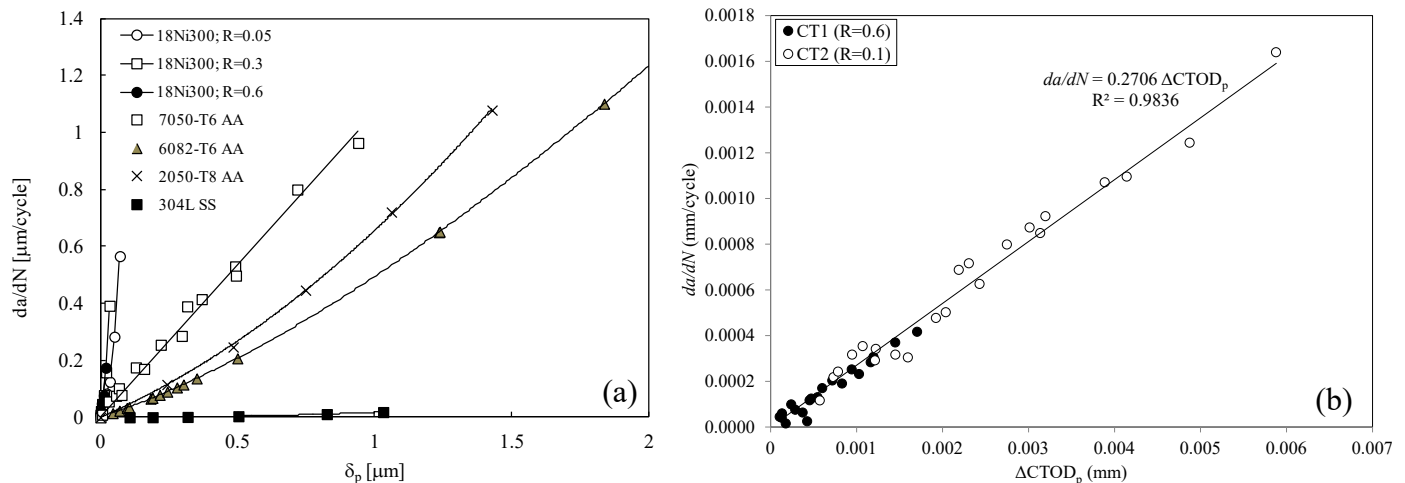


Figure 2. da/dN versus plastic CTOD. (a) FEM results for different materials. (b) DIC results for two stress ratios (CT specimens made of titanium).

REFERENCES

1. Vasco-Olmo, J.M.; Díaz, F.A.; Antunes, F.V.; James, M.N. Plastic CTOD as fatigue crack growth characterising parameter in 2024-T3 and 7050-T6 aluminium alloys using DIC. *Fatigue Fract Eng Mater Struct*, 43, 1719–1730 (2020).
2. Antunes, F.V.; Santos, L.; Capela, C.; Ferreira, J.M.; Costa, J.D.; Jesus, J.; Prates, P. Fatigue Crack Growth in Maraging Steel obtained by Selective Laser Melting. *Applied Science*, 9, 4412 (2019).
3. Borges, M.F.; Antunes, F.V.; Prates, P.A.; Branco, R.; Vojtek, T. Effect of Young’s modulus on Fatigue Crack Growth. *Int J Fatigue*, 132, 105375. (2020).
4. Borges, M.F.; Antunes, F.V.; Prates, P.A.; Branco, R.; Cruces, A.S.; Lopez-Crespo, P. Effect of Kinematic Hardening Parameters on Fatigue Crack Growth. *Theor Appl Fract Mech*, 106, 102501 (2020).
5. Borges, M.F.; Antunes, F.V.; Prates, P.A.; Branco, R. A Numerical Study of the Effect of Isotropic Hardening Parameters on Mode I Fatigue Crack Growth. *Metals*, 10 (2), 177 (2020).
6. Antunes, F.V.; Prates, P.A.; Camas, D.; Sarrazin-Baudoux, C.; Gardin, C. Numerical prediction of fatigue threshold of metallic materials in vacuum. *Engng Fract Mech*, 216, 106491 (2019).
7. Marques, B.; Borges, M.F.; Antunes, F.V.; Vasco-Olmo, J.M.; Díaz, F.A.; James, M.N. Boundaries of Small-Scale Yielding regime. *Engng Fracture Mechanics*, 252 (2021).

Generalised continuum models for periodic beam lattice structures with distributed mass

Harm ASKES¹

¹Faculty of Engineering Technology, University of Twente, Netherlands

h.askses@utwente.nl

The use of a standard elasticity model for modelling the stress and strain fields around sharp cracks poses some challenges to the analyst. Namely, the stresses and strains tend to exhibit singularities at the crack tip, which limits the usefulness of these fields in the interpretation of the structural integrity of the component. However, other continuum formulations are available that avoid these problematic features of standard elasticity. Typically, such alternative models belong to the category of so-called “generalised continuum models” and they are equipped with additional terms including microstructural length parameters.

For instance, the gradient elasticity theory suggested by Aifantis and coworkers in the early 1990s [1, 2, 3] includes higher-order spatial derivatives of the strain in the stress-strain relation and has been used to predict singularity-free crack-tip fields. An alternative approach is to take the spatial average of stress or strain over a (limited) volume around the crack tip, such as done in the theory of critical distances proposed by Taylor and coworkers [4, 5]. What these theories have in common is the appearance of an intrinsic material length scale, either in the coefficient that accompanies the higher-order spatial derivatives (as in gradient elasticity) or in the parameter that sets the averaging volume (as in the theory of critical distances). Indeed, it is possible to derive gradient elasticity theory from the theory of critical distances [6, 7], thereby establishing a linear relation between the respective length scale parameters [7].

Generalised continuum models are thus versatile and robust modelling tools in the analysis of notch and crack-tip fields. This is demonstrated for instance in [8], covering a diverse set of experimental results from the literature that include fatigue and static fracture as well as a wide range of relative crack lengths. Interestingly, simply taking the gradient elasticity length scale equal to the grain size of the material led to the best correspondence between experimental results and modelling results throughout. Thus, a proper quantification of the intrinsic length scale is of paramount importance.

Identification of the intrinsic length scale is simplified importantly when materials with a periodic microstructure are considered. It is often possible to derive the intrinsic length scale of a generalised continuum as a closed-form expression of the microstructural geometry. However, care must be taken that such derivation procedures lead to generalised continuum models that are thermodynamically stable – a requirement that is not straightforward to fulfil if realistic wave propagation predictions are desired at the same time [9]. In addition, the dynamic versions of generalised continuum models are typically equipped with multiple length scales, with (at least) one appearing in the stress-strain relations as explained above and (at least) one appearing in the equivalent enrichment of the inertia terms [9].

In this contribution, the focus will be on the derivation of a suitable generalised continuum model for periodic beam lattice structures. A number of interrelated challenges are taken into account. Firstly, applicability to both statics and dynamics means that the model needs to satisfy the requirements of singularity-free crack-tip stresses and strains as well as realistic wave

propagation predictions. Secondly, thermodynamic stability of such models is imperative but not trivial [10, 11, 12]. Thirdly, in a dynamic context a modelling choice must be made as to whether the mass is assumed to be concentrated in the beam connections or whether the mass is considered to be distributed evenly across the length the individual beam elements. The latter would appear to be more realistic but requires a number of additional operations in achieving thermodynamic stability, as will be shown.

REFERENCES

1. Aifantis, E.C. On the role of gradients in the localization of deformation and fracture. *Int. J. Engng. Sci.* 30, 1279–1299 (1992).
2. Altan, S.B.; Aifantis, E.C.. On the structure of the mode III crack-tip in gradient elasticity. *Scripta Metall. Mater.* 26, 319–324 (1992).
3. Ru, C.Q. ; Aifantis, E.C.. A simple approach to solve boundary-value problems in gradient elasticity. *Acta Mech.* 101, 59–68 (1993).
4. Taylor, D. *The Theory of Critical Distances: A New Perspective in Fracture Mechanics.* Elsevier (2007).
5. Susmel, L.; Taylor, D. On the use of the Theory of Critical Distances to predict static failures in ductile metallic materials containing different geometrical features. *Engng. Fract. Mech.* 75, 4410-4421 (2008).
6. Askes, H.; Susmel, L.; Livieri, P.; Tovo, R.; Taylor, D. Intrinsic material length, theory of critical distances and gradient mechanics: Analogies and differences in processing linear-elastic crack tip stress fields. *Fatigue Fract. Engng. Mater. Struct.* 36, 39-55 (2013).
7. Susmel, L.; Askes, H.; Bennett T.; Taylor, D. Theory of Critical Distances versus Gradient Mechanics in modelling the transition from the short to long crack regime at the fatigue limit. *Fatigue Fract. Engng. Mater. Struct.* 36, 861-869 (2013).
8. Askes, H.; Susmel, L. Understanding cracked materials: Is Linear Elastic Fracture Mechanics obsolete? *Fatigue Fract. Engng. Mater. Struct.* 38, 154-160 (2015).
9. Askes, H.; Aifantis, E.C. Gradient elasticity in statics and dynamics: An overview of formulations, length scale identification procedures, finite element implementations and new results. *Int. J. Solids Struct.* 48, 1962-1990 (2011).
10. Bažant, Z.P.; Christensen, M. Analogy between micropolar continuum and grid frameworks under initial stress. *Int. J. Solids Struct.* 8, 327–346 (1972).
11. Kumar, R.S.; McDowell, D.L. Generalized continuum modeling of 2-D periodic cellular solids. *Int. J. Solids Struct.* 41, 7399–7422 (2004).
12. Bacigalupo, A.; Gambarotta, L. A dynamic high-frequency consistent continualization of beam lattice materials. *Composite Struct.* 272, 114146 (2021).

Evaluating size effects using a modified energy-based fracture criterion

Majid Reza AYATOLLAHI¹, Javad AKBARDOOST², Mahya AGHABEIGI¹

¹ Fatigue and Fracture Laboratory, Center of Experimental Solid Mechanics and Dynamics, School of Mechanical Engineering, Iran University of Science and Technology, Narmak, Tehran, Iran

² Faculty of Engineering, Kharazmi University, Mofatteh Avenue, Tehran, Iran

m.ayat@iust.ac.ir

The applicability of laboratory-size specimens for predicting the fracture resistance of large structures has been investigated over the past few decades [1] for brittle and quasi-brittle materials. While most of these studies are restricted to pure mode I loading, the importance of mixed-mode loading in engineering structures emphasizes the need for further exploration under such loading conditions.

To evaluate the size dependency, the theoretical fracture models often involve employing the stress or strain field at a critical distance (r_c) from the crack tip, which is assumed to be elastically equivalent to the FPZ length. However, in quasi-brittle materials where this distance is relatively large, accurate results may not be achieved by considering only the singular term of the Williams’ series expansion, and it is necessary to account for the higher-order terms. Recently, a modified maximum tangential stress (MMTS) criterion was proposed [2] to investigate the size-dependent fracture toughness in quasi-brittle materials under mixed-mode I/II loading. This stress-based criterion considers the first and second non-singular terms, along with the singular term in the Williams’ series expansion. The finite element over deterministic (FEOD) method was also utilized to determine the second non-singular term. Despite the fact that the MMTS criterion is capable of estimating both size and geometry effects simultaneously under various mode mixities (M_c), the calculation process for the second non-singular term of Williams’ series expansion is generally complicated and requires high coding skills. Thus, it is preferred to adopt an approach that is capable of appropriately estimating size-dependent fracture toughness with no need to calculate the second or higher order non-singular terms.

The aim of this paper is to present a novel approach that utilizes a modified version of the conventional strain energy density (SED) criterion [3], named the modified strain energy density (MSED) criterion. By focusing exclusively on the singular and first non-singular (T-stress) terms of the Williams’ series expansion, which can be conveniently derived from finite element codes, the size effect can be estimated using the MSED criterion. According to the SED and the MSED criterion, the crack growth initiates along θ_0 where the magnitude of the strain energy density factor (S) attains its minimum value at the distance r_c from the crack tip. Furthermore, the onset of brittle fracture takes place when the MSED factor along θ_0 attains its critical value (S_{cr}), which is dependent on the T-stress too. Taking all these conditions into account, the size-dependent fracture curves under mixed-mode I/II loading based on the MSED criterion can be obtained using the following equation:

$$\frac{K_{Ic}}{K_{eff}} = \sqrt{\frac{A_1 K_I^{*2} + A_2 K_{II}^{*2} + A_3 K_I^* K_{II}^* + A_4 \left(4\sqrt{\frac{r_c}{R}} T^*\right) K_I^* + A_5 \left(4\sqrt{\frac{r_c}{R}} T^*\right) K_{II}^* + A_6 \left(4\sqrt{\frac{r_c}{R}} T^*\right)^2}{\left[\frac{1-\nu}{2\pi G} + \frac{1-\nu}{2\pi G} \left(4\sqrt{\frac{r_c}{R}} \frac{T^*}{K_I^*}\right)\right] + \frac{1-\nu}{8\pi G} \left(4\sqrt{\frac{r_c}{R}} \frac{T^*}{K_I^*}\right)^2} (K_I^{*2} + K_{II}^{*2})} \quad (1)$$

in which, K_{Ic} , K_{eff} , ν , G and R are the apparent fracture toughness, the effective stress intensity factor, the Poisson’s ratio, the modulus of rigidity and a characteristic dimension of the cracked specimen, respectively. The constant coefficients $A_{i(i=1:6)}$ are functions of θ_0 . In addition, K_I^* , K_{II}^* and T^* are defined as dimensionless geometry factors. Meanwhile, determining the value of r_c and its correlation with the specimen size is a crucial aspect of this criterion. Indeed, the size-dependent fracture resistance of quasi-brittle materials under mixed-mode (I/II) loading can be estimated by substituting the size-dependent value of r_c into Eq. (1). To this end, a new strain-based formulation is used for estimating the value of r_c :

$$r_c = \frac{[(1+\nu)(1-2\nu)]^2}{2\pi} \left(\frac{K_{Ic}}{f_t}\right)^2 \quad (2)$$

where f_t is the tensile strength of material. For the sake of verification, the theoretical estimates of the MSED criterion are compared with a number of experimental results available in the literature [2] for semi-circular bend (SCB) specimens made of Guiting limestone with various sizes (Figure. 1a). Very good agreement is shown to exist between the results of the proposed size-dependent fracture criterion and the test results (Figure 1b)

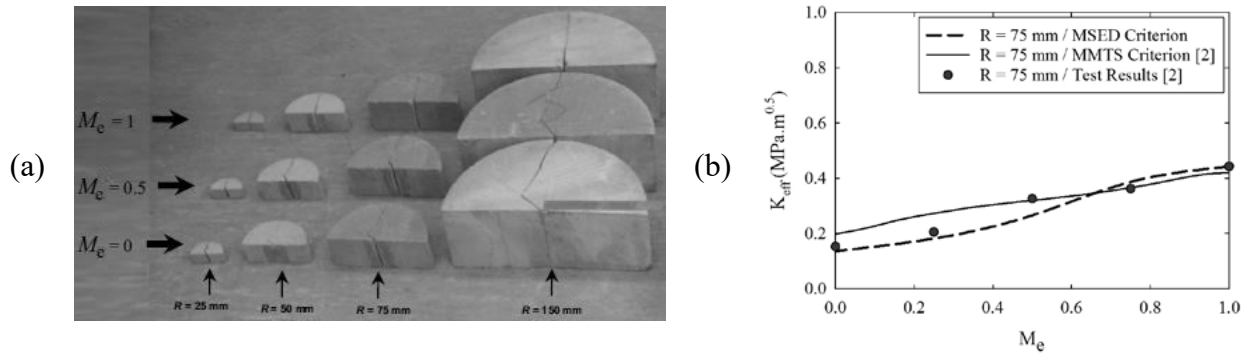


Figure 1. (a) Mixed mode fracture in the tested SCB specimens of various sizes [2] and (b) a comparison between the estimated fracture curves of MMTS and MSED criteria and the experimental results for the specimen radius R of 75 mm. $M_c=0$ for pure mode II and $M_c=1$ for pure mode I.

REFERENCES

1. Bažant, ZP. Size effect in blunt fracture: concrete, rock, metal. *J. Eng. Mech.*, 110, 518-35, (1984).
2. Akbardoost, J.; Ayatollahi, MR.; Aliha, MRM.; Pavier, M.; Smith, D. Size-dependent fracture behavior of Guiting limestone under mixed mode loading. *Int. J. Rock Mech. Min.*, 71, 369-80 (2014).
3. Sih, GC. Strain-energy-density factor applied to mixed mode crack problems. *Int. J. Fract.*, 10, 305-21 (1974).

Characterisation of crack closure mechanisms with robot-assisted high-resolution digital image correlation

Eric BREITBARTH¹, Florian PAYSAN¹

¹ German Aerospace Center (DLR), Institute of Materials Research, Linder Hoehe, 51147 Cologne, Germany

eric.breitbarth@dlr.de

New experimental techniques have historically led to new scientific knowledge. In this context, we present our robot-based high-resolution Digital Image Correlation (DIC) setup designed to capture time-series data of the crack tip field during fatigue crack propagation [1]. Using this data, we determine the plastic zone, stress intensity factors and investigate fatigue crack closure. This technological advancement extends traditional fracture mechanics by seamlessly integrating robotics, multi-scale DIC, data storage, evaluation algorithms, and explainable artificial intelligence (XAI) [2,3].

Figure 1a depicts our servo-hydraulic testing rig, where a robot manipulates a light optical microscope to precisely follow the crack tip on the MT(160) sample. With a 1.6x magnification and a field of view of 10.2 x 6.4 mm², we achieve a spatial resolution of approximately 0.05 mm for DIC. The machine controller orchestrates the test sequence, and TCP data streams enable seamless communication between different systems. Employing our open-source Python framework, "CrackPy" (<https://github.com/dlr-wf/crackpy>, [4]), we standardize DIC data, detect the crack tip, and evaluate crack tip loadings using various methods, including the over-deterministic approach, J- and interaction integral, Buckner-Chen integral [5], and the CJP model.

Our investigation focused on fatigue crack propagation in 2-mm-thick AA2024-T3 aluminum specimens under constant amplitude loading parallel (T-L) and perpendicular (L-T) to the rolling direction [6]. The robot systematically scans the surface in a checkerboard pattern for every 0.2 mm crack extension, enabling crack tip loading and plastic zone measurements [6]. At 10 mm intervals, the robot captures 30 images during loading and unloading, allowing for a detailed analysis of crack closure with high spatial and temporal resolution. The crack opening kinetics, based on local crack opening displacement measurements from high-resolution DIC (Fig. 1b), illustrate distinct variations along the crack path, confirming location-dependent K_{opening} values [8].

Introducing a new method, we identify plasticity-induced crack closure (PICC) as a predominant shielding mechanism and determine K_{opening} at the crack front in our fatigue crack experiments. Our findings contribute to the ongoing discussion regarding the shielding effect of PICC, demonstrating its negligible influence on fatigue damage in the plastic zone when the crack closure contact is directed towards the surface.

In conclusion, our study reveals a clear location dependence of the K_{opening} value along the crack path. The presented methodology enables the direct determination of both $K_{\text{opening,cm0d}}$ and $K_{\text{opening,ct0d}}$. Remarkably, at approximately 50 % of $K_{I,\text{max}}$, $K_{\text{opening,ct0d}}$ is found to be twice as high as the expected $K_{\text{opening,cm0d}}$ value obtained using the crack-mouth-opening-displacement (CMOD) extensometer. This research advances our understanding of fatigue crack behavior and opens up opportunities for further research in this area.

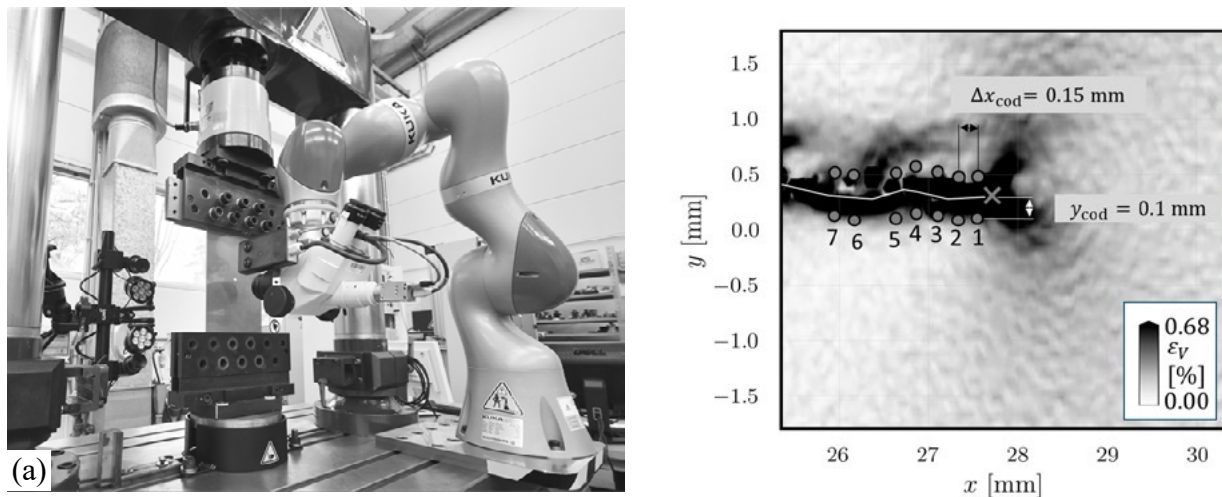


Figure 1. Experimental fatigue crack growth setup with multi-scale digital image correlation (a) and crack tip equivalent strain field to investigate fatigue crack closure (b).

REFERENCES

1. Paysan, F.; Dietrich, E.; Breitbarth, E. A Robot-Assisted Microscopy System for Digital Image Correlation in Fatigue Crack Growth Testing. *Experimental Mechanics*, 63(6), 975–986 (2023).
2. Melching, D.; Strohmann, T.; Requena, G.; Breitbarth, E. Explainable machine learning for precise fatigue crack tip detection. *Scientific Reports*, 12(1), 9513 (2022).
3. Melching, D.; Schultheis, E.; Breitbarth, E. Generating artificial displacement data of cracked specimen using physics-guided adversarial networks. *Machine Learning: Science and Technology*, 4(4), 045063 (2023).
4. Strohmann, T.; Melching, D.; Paysan, F.; Klein, A.; Dietrich, E.; Requena, G.; Breitbarth, E. Crack Analysis Tool in Python - CrackPy (2022).
5. Melching, D.; Breitbarth, E. Advanced crack tip field characterization using conjugate work integrals. *International Journal of Fatigue*, 169, 107501 (2023).
6. Kalina, M.; Schöne, V.; Spak, B.; Paysan, F.; Breitbarth, E.; Kästner, M. Fatigue crack growth in anisotropic aluminium sheets — phase-field modelling and experimental validation. *International Journal of Fatigue*, 176, 107874 (2023).
7. Breitbarth, E.; Besel, M. Energy based analysis of crack tip plastic zone of AA2024-T3 under cyclic loading. *International Journal of Fatigue*, 100, 263–273 (2017).
8. Paysan, F.; Breitbarth, E. Towards three dimensional aspects of plasticity-induced crack closure: A finite element simulation. *International Journal of Fatigue*, 163, 107092 (2022).

Multi-probe potential drop technique to estimate the geometry, location and size of a crack propagating in cylindrical specimens

Alberto CAMPAGNOLO¹, Luca VECCHIATO¹, Juergen BAER²,
Giovanni MENEGHETTI¹

¹ Department of Industrial Engineering, University of Padova, Via Venezia, 1 – 35131 Padova, Italy

² Institute for Materials Science, University of the Bundeswehr Munich, D-85577 Neubiberg, Germany

giovanni.meneghetti@unipd.it

Crack initiation life of a fatigue tested component often needs to be defined at a certain (short) crack length. The size of an initiated crack can be estimated by employing different experimental methods, one of which is the direct current potential drop (DCPD) technique, which exploits the change in electrical resistance of the cracked component resulting from an increase in the crack size to measure the crack size itself.

In the case of cylindrical specimens subjected to fatigue loadings, the crack geometry in terms of configuration (circumferential or semi-elliptical, Fig. 1) and the shape (aspect ratio c/a , Fig. 1), location (θ , Fig. 1) and size (a , Fig. 1) can be singled out by means of the potential drop method (PDM) operating with more than one potential probe, while the single-probe DCPD would be useless to this aim.

In the present contribution, three potential probes are adopted to overcome this issue, as sketched in Fig. 1. First, experimental fatigue tests under pure axial loading have been performed using plain, blunt and sharp notched bars made of steel and titanium alloy; in all experimental tests the multi-probe potential drop technique has been used, consisting of three potential probes. Afterwards, for comparison purposes the three experimental potential drops have been post-processed by adopting three different methods based on: (i) the average potential drop ratio [1]; (ii) a vectorial representation of the potential drop ratios [2] and (iii) a Probability-Based Diagnostic Imaging (PDI) algorithm.

More in detail, the procedure proposed in [1] takes advantage of the average potential drop ratio to estimate the cracked area, while a comparison of the potential drop ratios allows an approximate estimation of the crack configuration and location.

According to the method proposed in [2], the three potential drop ratios represent the length of three vectors originating at the potential measurement point and directed along the axis of the specimen. On the tips of such three vectors, a plane as well as its normal vector are defined. Finally, the orientation and the length of the normal vector allow to estimate the crack location and size, respectively.

The procedure based on a Probability-Based Diagnostic Imaging (PDI) algorithm takes advantage of a database generated from finite element analyses and experimental measurements and allows to estimate the crack geometry, i.e. the configuration (circumferential or semi-elliptical) and the shape (aspect ratio c/a), location and size.

The comparison of the three different techniques shows that the method based on a PDI algorithm seems to be the most promising since it is more efficient for defining the crack geometry, location and size, which are necessary for structural durability calculations.

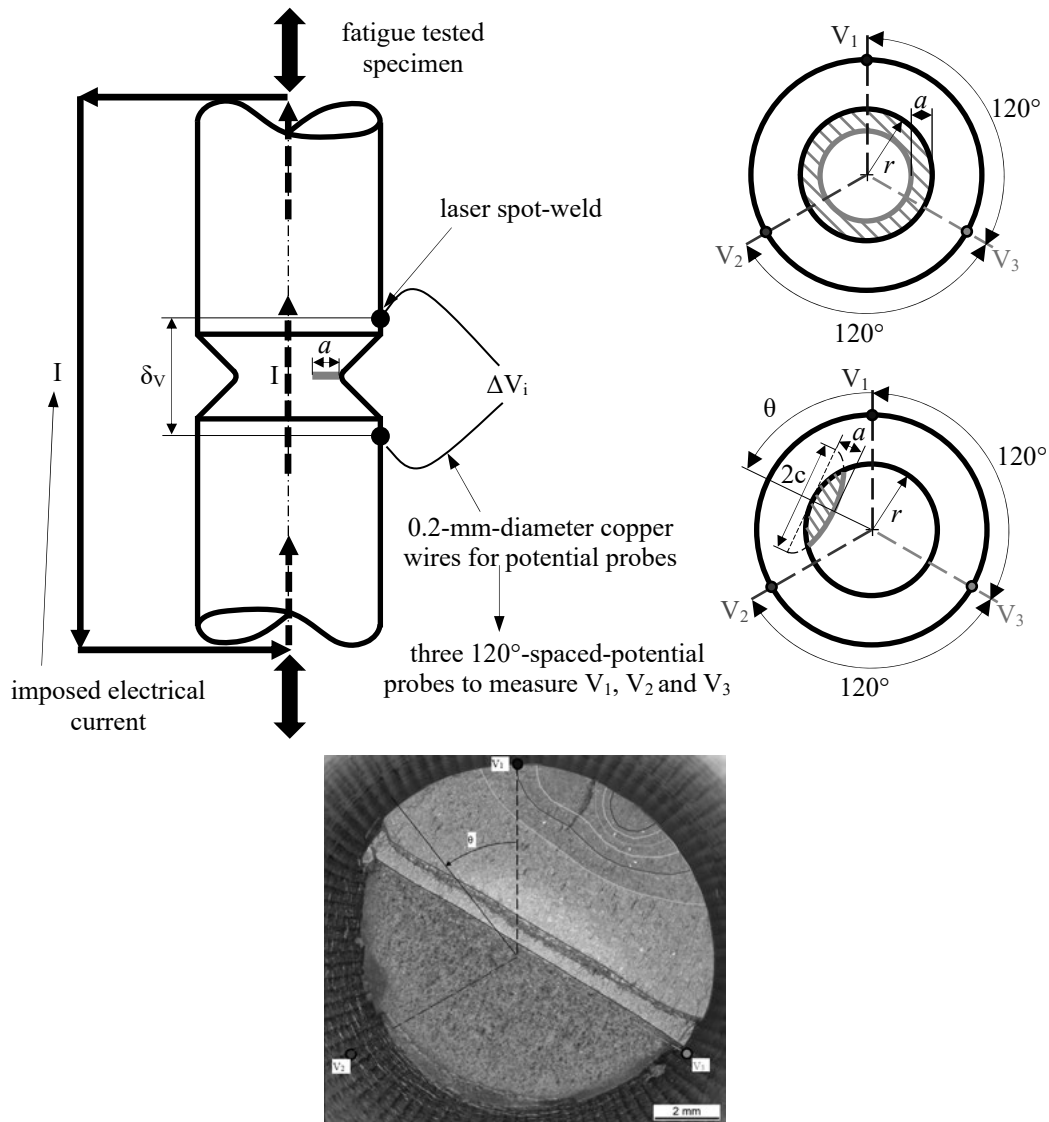


Figure 1. Experimental setup of the direct current potential drop method with three 120°-spaced potential probes. Examples of a circumferential and a semi-elliptical surface crack initiated at the notch tip. Example of experimental crack fronts generated by fatigue testing a blunt notched steel specimen under axial loading.

REFERENCES

1. Campagnolo, A.; Bär, J.; Meneghetti, G. Analysis of crack geometry and location in notched bars by means of a three-probe potential drop technique. *Int. J. Fatigue*, 124, 167–187 (2019).
2. Bär, J.; Nahbein, M. Multiple potential drop measurement – A new method for crack detection and crack length measurement. *Theoretical and Applied Fracture Mechanics* 129, 104226 (2024) DOI: 10.1016/j.tafmec.2023.104226

Digital image correlation for monitoring stress intensity factor in 18Ni300 additively manufactured samples

Pablo M. CEREZO¹, Jose A. AGUILERA¹, Alejandro S. CRUCES¹, Antonio GARCIA-GONZALEZ¹, Ricardo BRANCO², Luis BORREGO^{2,3}, Pablo LOPEZ-CRESPO¹

¹ Department of Civil and Materials Engineering, University of Malaga, C/Dr Ortiz Ramos, s/n, 29071 Malaga

² CEMMPRE, Department of mechanical engineering, University of Coimbra, Rua Luís Reis Santos 3030-788 Coimbra, Portugal

³ Department of mechanical engineering, Coimbra Polytechnic- ISEC, Rua Pedro Nunes, 3030-199 Coimbra, Portugal

plc@uma.es

Additive manufacturing (AM) technologies have garnered increasing attention due to their potential advantages compared to conventional subtractive manufacturing methods. The method employed in the creation of diverse components is exceptionally versatile and boasts a low material consumption rate, rendering it a compelling alternative for the manufacturing of superior components [1], [2]. Nevertheless, it is imperative to carry out a fatigue analysis of said components to guarantee their resilience against various loads.

Digital Image Correlation (DIC) is a straightforward and easily implemented method, which is particularly useful in fracture mechanics due to its direct application and lack of need for sophisticated sample preparation. One of its key advantages is its scale-free nature, allowing for measurements to be taken across a wide range of scales, from micro- [3] to macro- [4] levels.

The Stress Intensity Factor (SIF) is a crucial metric utilized to anticipate the fatigue life of engineering components that are susceptible to linear elastic failure. The assessment of SIF via crack tip fields presents a significant advantage since it eliminates the need for prior information on crack length, applied force, or specimen geometry. As a result, it is an ideal method for evaluating engineering components in-service. DIC has proven to be a valuable tool in analysing the effects of crack closure and crack tip plasticity on SIF assessment. Previously, assessing the SIF was a complicated process that involved an over-deterministic approach. An analysis of experimental data was conducted to create a model of the displacement field in the vicinity of the crack tip. This method facilitated the tracking of the SIF progression throughout the loading sequences. More recently, the use of DIC on C-specimens and 3-point-bend specimens has demonstrated encouraging results in the estimation of SIF. Advancements in digital photography have improved SIF estimation precision for both pure mode I and mixed-mode conditions. Additionally, DIC has facilitated the evaluation of other crack parameters, such as T-Stress and Crack Tip Opening Angle, on double cantilever specimens [5]. Various methodologies were employed to assess the elastic-plastic properties of the crack. To assess the mechanisms behind crack growth and closure in varying thicknesses of aluminium alloy, high magnification DIC was employed to measure COD [6]. To facilitate the monitoring of crack growth rate, the plastic zone preceding the crack was evaluated utilizing the technique of DIC on specimens exhibiting both artificial and real fatigue cracks.

The study aims to evaluate the effectiveness of SIF against cyclic loading in a steel plate fabricated by additive manufacturing. The analysis of SIF is performed using the DIC

methodology for different values of ΔK (10, 15, 20, 25, and 30 $MPa \cdot \sqrt{m}$) as shown in Fig. 1B. The samples have various printing orientations (0° , 45° , and 90°) also shown in Fig. 1.

Through experimental analysis utilizing Williams' model, the SIF was assessed during cyclic loading. As the loading amplitude increased, a discrepancy between the experimental and nominal estimations of SIF became evident. This discrepancy was due to the crack tip plasticity effect, a factor not accounted for in the nominal evaluation. Further investigation using Irwin's approach revealed that monitoring the evolution of SIF in a sample under cyclic loading could continue until the sample experienced a sudden fracture.

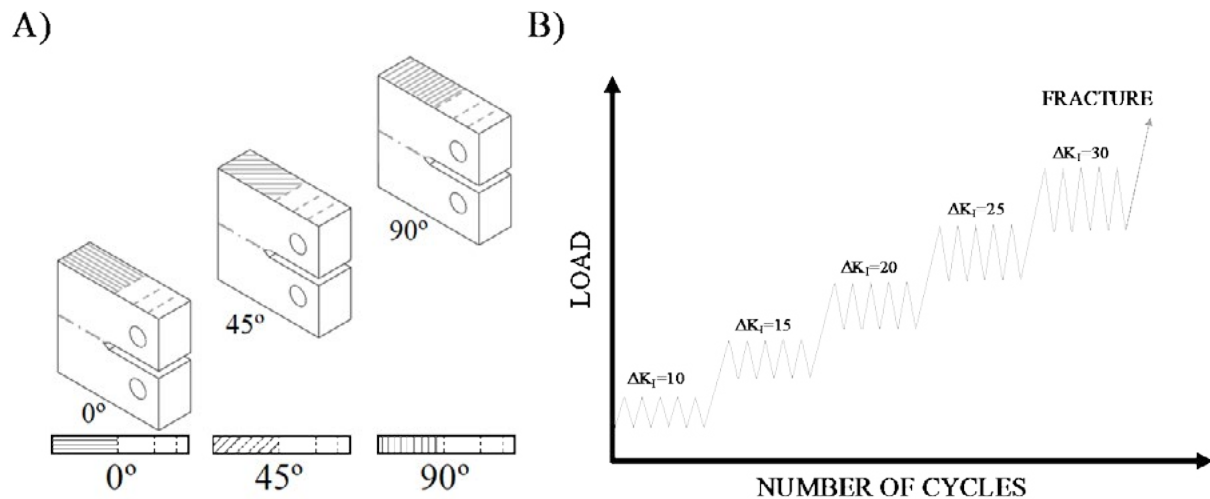


Figure 1. A) Geometry of the CT Specimen Manufacturing for 0° , 45° and 90° orientations (the top lines indicate the orientation of the weld beads, while the striped lines indicate the crack plane) and B) schema of the loading sequences.

REFERENCES

1. Demir, A.G; Previtali, B. Investigation of remelting and preheating in SLM of 18Ni300 maraging steel as corrective and preventive measures for porosity reduction. *Int. J. Adv. Manuf. Technol.*, 93, 5–8, (2017).
2. Rivalta, F.; Ceschini, L.; Jarfors, A.E.W.; Stolt, R. Effect of Scanning Strategy in the L-PBF Process of 18Ni300 Maraging Steel. *Metals*, 11, 5, (2021).
3. Sutton, M.A.; Li, N.; Joy, D.C.; Reynolds, A.P.; Li, X. Scanning Electron Microscopy for Quantitative Small and Large Deformation Measurements Part I: SEM Imaging at Magnifications from 200 to 10,000. *Exp Mech*, 47, 6, 775–787, (2007).
4. Yoneyama, S.; Kitagawa, A.; Iwata, S.; Tani, K.; Kikuta, H. Bridge deflection measurement using digital image correlation. *Exp Tech*, 31, 1, 34–40, (2007).
5. Yates, J.R.; Zanganeh, M.; and Tai, Y.H. Quantifying crack tip displacement fields with DIC. *Eng. Fract. Mech.*, 77, 11, 2063–2076, (2010).
6. de Matos, P.F.P.; Nowell, D. Experimental and numerical investigation of thickness effects in plasticity-induced fatigue crack closure. *Int. J. Fatigue*, 31, 11–12, 1795–1804, (2009).

Towards a strain-based approach to fatigue cracking

Rong CHEN¹, Xiao-Kai HU¹, Ming-Liang ZHU¹, Fu-Zhen XUAN¹

¹East China University of Science and Technology, Shanghai, China

mlzhu@ecust.edu.cn

Strain localization or accumulation correlates well with fatigue cracking while near crack-tip strain characterization is rather significant. In this work, a high-resolution method to decorate nano-gold particles as speckles was proposed, and its effectiveness was verified by comparing strain measurement errors with microstructures and Al₂O₃ particles under in-situ tensile test. Near-tip strain was characterized and statistically analyzed to develop a strain-based yielding criterion for crack-tip plasticity evaluation which was found applicable to both tensile and fatigue loadings. The near-tip strain of face centered cubic 304 stainless steel satisfied lognormal distribution whereas body centered cubic 25Cr steel obeyed gauss distribution, and was found evolving logistic-gauss-lognormal with fatigue crack growing and plasticity increasing. The role of strain ratchetting in fatigue cracking was modelled, and found the relative strain increasing rate could well represent branch or stable growth mode, and thus drive fatigue cracking. The strain ratchetting associated cracking speed parameter was able to quantitatively interpret cross-scale fracture down to atomic level.

The microstructural damage analysis near crack-tip illustrated that fatigue crack growth of 25Cr steel was governed by breakdown of lathy martensites and formation of fine grains while the cracking of 304ss underwent austenite-to-martensite transformation process occurred at a near-tip strain of approximately 13%. In the case of fatigue cracking of 25Cr, the microstructure is a mixture of lath martensite and bainites, as shown in Figs. 1(b-c). The numerous fine grains can be observed near crack-tip while the matrix far away are almost intact. Similarly, the fatigue cracking mechanism of 25Cr is described by step 2-3 in Fig. 1(e). Note that the 25Cr is dominated by transgranular growth, however, the mode of crack growth can be intergranular based on the fatigue crack and grain boundary interaction behavior [1].

In the case of 304ss, the martensitic transformation in front of crack-tip seems to be a pre-requisite for crack extension and is thus believed to be an added stage for the whole cracking process, when compared with 25Cr steel. The bcc martensite was transformed from fcc austenite by the displacive atom collective movements [2]. The physics of macro fatigue fracture is closely related to atomic movement and microstructural damage, which at atomic scale could be interpreted in terms of strain ratchetting for cracking of atoms. It appears the phase transformation followed by microstructural damage in 304ss results in a growing fatigue crack in a locally hardened martensites with surrounding austenites. A further correlation of FCG rate at macro-scale with local cyclic strain accumulation and associated modelling are needed to illustrate the contribution of phase transformation to the overall fatigue crack growth resistance and fatigue lifetime.

The main conclusions are listed as follows.

(1) A method for preparation of micro-nano-scale speckles with little agglomeration was proposed which could be applied for characterization of near crack-tip strain at high precision under both tensile and cyclic loadings.

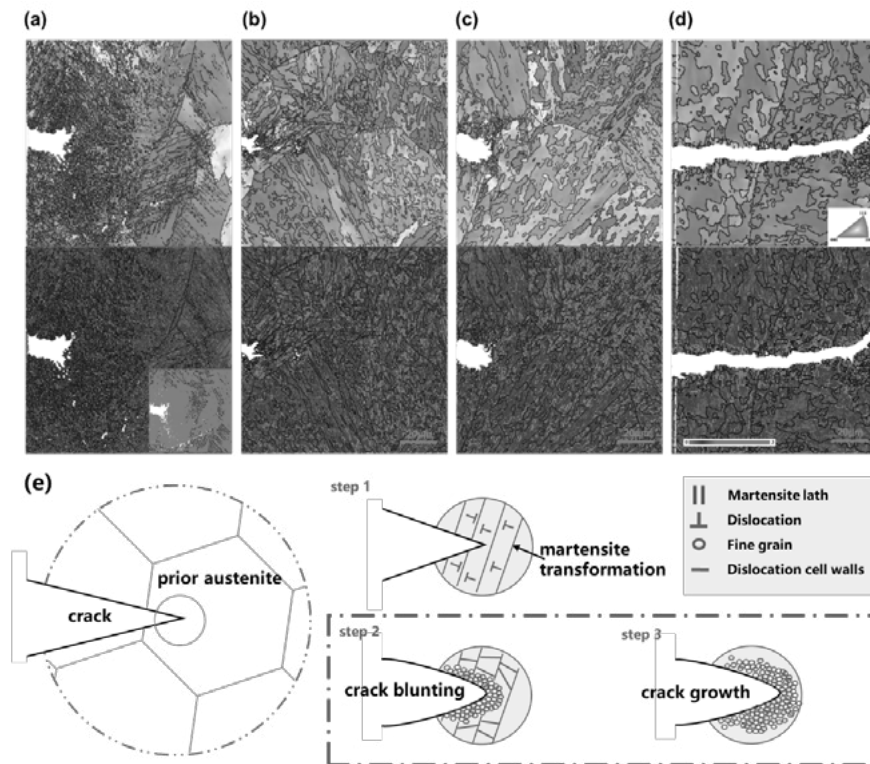


Figure 1. The IPF-Z and KAM maps obtained by EBSD for the three types of fatigue test

(2) A strain-based yielding criterion was proposed to evaluate plasticity at crack-tip under tensile and cyclic loadings, which informed a sound correlation among cyclic plasticity, strain ratchetting and damage mechanisms for fatigue cracking. With plasticity increasing and crack growing, the strain distribution around crack-tip evolved under the statistical pattern of logistic-gauss-lognormal.

(3) The relative strain increasing rate was found indicative of static or growing fatigue crack, crack path branch or stable growth, and the associated cracking speed parameter in terms of strain ratchetting was able to quantitatively interpret cross-scale fracture down to atomic level.

(4) A mechanistic understanding of near-tip fatigue cracking was proposed by microstructural damage analysis, where fatigue crack growth of 25Cr steel was by breakdown of lathy martensites and formation of fine grains while the cracking of 304ss underwent austenite-to-martensite transformation process occurred at a near-tip strain of approximately 13%.

REFERENCES

1. Zeng, X.; Zhang, C.; Zhu, W.; Zhu, M.; Wang, Y.; Zhang, X. Quantitative characterization of short fatigue crack and grain boundary interaction behavior in zirconium, *Int. J. Fatigue*, 161, 106894 (2022).
2. Yang, X.-S.; Sun, S.; Ruan, H.-H.; Shi, S.-Q.; Zhang, T.-Y. Shear and shuffling accomplishing polymorphic fcc $\gamma \rightarrow$ hcp $\epsilon \rightarrow$ bct α martensitic phase transformation, *Acta Mater.* 136, 347-354 (2017).

In-situ observation of notch-induced fatigue crack initiation and growth behavior in a magnesium alloy

Rong CHEN¹, Ming-Liang ZHU¹, Fu-Zhen XUAN¹

¹East China University of Science and Technology, Shanghai, China

1374676966@qq.com; chenrong9606@163.com

The assessment of fatigue life of magnesium alloys is a hot topic due to light weight design and manufacturing of engineering components. The investigation on the fatigue behavior of magnesium alloy notched components is important to improve its fatigue performance as the geometric discontinuity cannot be avoided in engineering practice. Notches can affect fatigue performance by generating i) stress concentration, and ii) multi-axial fatigue. The commonly used methods for notch fatigue life assessment are: local strain method, energy method, damage mechanics method, strain gradient method and critical distance method. Although the short crack initiation and growth stages occupy more than 70% of the total fatigue life, the research on fatigue short cracking of rare earth magnesium alloys is still lacking, especially in the case of notched specimen.

In this paper, the single edge notch specimen (SENT) with Mg-RE alloy was studied to explore the cracking mechanism of short crack. The specimens were mounted on an in-situ loading module with a 2kN load capacity (Deben Co. Ltd, UK). A suitable loading rate of 0.5 mm/min was selected by taking into account the strength and plasticity of the material. The loading module was then assembled into the SEM (EVO MA15, Zeiss, Germany) to conduct the in-situ tensile and fatigue tests. The crack growth rate undergoes a process of decreasing and the increasing, similar to the overload retardation effect. It can be observed that the crack growth path is zigzag in the stage of decreasing crack growth rate, which is closely related to the microstructure of magnesium alloy. However, deflection also occurs at the rapid growth stage, considering crack-tip shielding effects by deflection and branching of the crack may also be responsible for the decrease in growth rate.

Statistics of strain at different stages of the specimen are crucial in understanding the extent of damage accumulation in the material. As the plastic deformation of the specimen increases, the strain field distribution law obeys a Logistic-Gauss-Lognormal distribution, where plastic strain dominates the evolution of the strain field distribution law. Imagine that the crack growth rate may be associated with the strain gradient near the crack, which is related to the transfer of compressive stresses. Therefore, the strain field near the crack-tip was further analyzed. At the stage of decreasing crack growth rate, the strain at the crack-tip continues to decrease when the crack tip gets closer to the compressive strain region. It should be clear that the residual compressive stresses are transferred from the crack-tip to the crack-wake during crack propagation, accompanied by the strain redistribution.

In addition, the grain and active slip orientation were analyzed based on EBSD technique. It was observed that crack was dominated by non-basal slip with transgranular at the stage of decreasing growth rate. However, the small crack effect is related to the microstructure but is limited, the weakening of the crack growth drive force by compressive strain may be the determining factor.

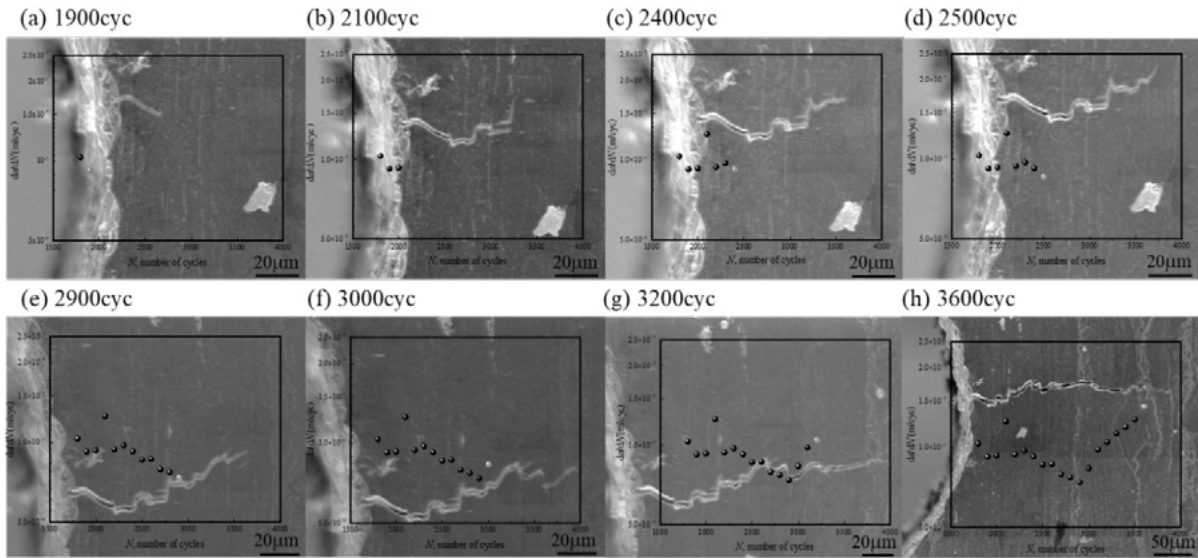


Figure 1. Fatigue crack growth rate and associated crack morphology

Assessment of structural materials containing notch-type defects: A comprehensive validation of the FAD-TCD methodology on metallic and non-metallic materials

Sergio CICERO¹

¹ LADICIM, Departamento de Ciencia e Ingeniería del Terreno y de los Materiales, University of Cantabria, Avenida de los Castros, 44, 39005 Santander, Spain

ciceros@unican.es

This work provides a description, and the subsequent validation, of a structural integrity assessment methodology of structural materials containing notch-type defects. The approach is based on the combination of Failure Assessment Diagrams (FAD) and the Theory of Critical Distances (TCD). The former provides the general assessment tool, which is exactly the same one as that used for crack-like defects, whereas the latter provides the notch effect correction required for the analysis of this type of defects. The proposed methodology is validated on a number of metallic and non-metallic structural materials, with 1106 experimental results on different types of testing specimens, covering four structural steels, aluminium alloys 7075-T651 and 6060-T66, PVC, PMMA, PA6, fibre-reinforced PA6, 3D printed (Fused Filament Fabrication) ABS, PLA and graphene reinforced PLA, granite and limestone (Table 1).

Table 1. Summary of the experimental conditions analysed in this research. n: number of specimens; ρ : notch radius; L: critical distance; $K_{mat,0.95}$: fracture toughness (5% failure prob.).

Material	Geometry	n	ρ (mm)	E (GPa)	Yield or proof stress (MPa)	σ_u (MPa)	$K_{mat,0.95}$ (MPam ^{1/2})	L (mm)
S275JR (-120 °C)	CT	23	0-2.0	213	398	613	40.4	0.0137
S275JR (-90 °C)	CT	24	0-2.0	211	380	597	61.5	0.0062
S275JR (-50 °C)	CT	24	0-2.0	209	349	564	48.4	0.0049
S275JR (-30 °C)	CT	24	0-2.0	208	344	548	59.1	0.0061
S275JR (-10 °C)	CT	34	0-2.0	207	337	536	74.8	0.0083
S275JR (+40 °C)	CT	24	0-2.0	205	331	504	387	0.1697
S275JR (+70 °C)	CT	23	0-2.0	203	331	492	599	0.3421
S355J2 (-196°C)	CT	24	0-2.0	218	853	922	29.3	0.0291
S355J2 (-150°C)	CT	21	0-2.0	215	527	759	51.7	0.0084
S355J2 (-120°C)	CT	22	0-2.0	212	459	671	72.0	0.0168
S355J2 (-100°C)	CT	35	0-2.0	212	426	646	93.7	0.0140
S355J2 (-50°C)	CT	24	0-2.0	209	395	602	262	0.0778
S355J2 (-20°C)	CT	24	0-2.0	208	385	587	561	0.3156
S460M (-140°C)	SENB	24	0-2.0	214	702	795	39.8	0.0028
S460M (-120°C)	SENB	24	0-2.0	213	647	758	46.6	0.0075
S460M (-100°C)	SENB	33	0-2.0	212	605	726	56.5	0.0053
S690Q (-140°C)	SENB	24	0-2.0	214	1004	1111	46.2	0.0069
S690Q (-120°C)	SENB	24	0-2.0	213	949	1060	55.9	0.0131
S690Q (-100°C)	SENB	34	0-2.0	212	907	1015	70.1	0.0170
Al7075 T651 (LT)	CT	23	0-2.0	71.6	554	612	25.8	0.0150
Al7075 T651 (TL)	CT	24	0-2.0	74.4	539	602	25.6	0.0215
Al6060 T66	Tube	3	0.8-1.5	70.7	215	264	51.1	0.12
PVC	Tube	3	0.8-1.5	3.47	38.6	51.1	6.40	0.08

PMMA	SENB	32	0-2.5	3.42	48.5	71.9	1.75	0.105
PA6	SENB	25	0-2.0	2.85	54.2	54.2	1.86	0.190
ABS _{0/90}	SENB	11	0-2.0	2.24	47.7	51.7	1.89	2.68
ABS _{30/-60}	SENB	11	0-2.0	2.32	59.0	59.3	1.65	2.84
ABS _{45/-45}	SENB	11	0-2.0	2.38	55.6	60.8	1.87	3.22
PLA _{0/90}	SENB	19	0-2.0	3.76	51.2	52.0	3.20	0.57
PLA _{30/-60}	SENB	19	0-2.0	3.31	38.0	42.0	2.91	0.38
PLA _{45/-45}	SENB	20	0-2.0	2.75	35.3	41.1	2.62	0.24
PLA _{pl}	Plate	39	0.9-1.3	2.75	35.3	41.1	2.62	0.24
SGRF ₅ -PA6	SENB	25	0-2.0	3.30	66.9	72.0	1.63	0.157
SGRF ₁₀ -PA6	SENB	25	0-2.0	3.55	70.1	78.1	1.88	0.168
SGRF ₃₀ -PA6	SENB	24	0-2.0	6.45	105	128	4.34	0.261
SGRF ₅₀ -PA6	SENB	25	0-2.0	12.6	161	192	8.38	0.599
SGRF ₁₀ -PA6(2)	SENB	25	0-2.0	2.00	31.0	63.4	3.59	1.290
SGRF ₁₀ -PA6(5)	SENB	23	0-2.0	0.95	22.5	47.6	3.46	0.450
SGRF ₅₀ -PA6(2)	SENB	25	0-2.0	6.92	63.4	112	7.32	1.438
SGRF ₅₀ -PA6(4)	SENB	24	0-2.0	6.20	46.5	92.2	5.23	8.838
PLA-Gr _{0/90}	SENB	20	0-2.0	4.13	50.5	51.0	2.88	0.85
PLA-Gr _{30/-60}	SENB	20	0-2.0	4.06	41.0	44.3	3.57	2.28
PLA-Gr _{45/-45}	SENB	20	0-2.0	3.97	47.5	49.0	4.77	1.11
PLA-Gr _{pl}	Plate	39	0.9-1.3	3.97	47.5	49.0	4.77	1.11
Granite	SENB	41	0-10	45.6	9.0	9.0	1.18	6.04
Limestone	SENB	41	0-10	64.1	7.8	7.8	0.71	2.71

The approach, referred to as FAD-TCD approach, is theoretically justified, and consists in maintaining the FAL ($f(L_r)$) and limit load (P_L) solutions used in the analysis of cracks (defined in structural integrity assessment procedures) and applying the notch effect correction on K_r by considering the apparent fracture toughness estimation derived from the Theory of Critical Distances, instead of the fracture toughness value obtained from cracked specimens.

As seen in Figure 1, the application of the FAD-TCD approach to 1106 specimens, 895 of which have notch radii larger than 0 mm), significantly reduces the conservatism associated to the evaluation of notches as crack-like defects, with the assessment points much closer to the limiting condition defined by the FAL, yet maintaining the safety of the analysis. There are 32 notched specimens out of 895 (less than 3.5%) unsafely evaluated through the FAD-TCD approach. These results are in very good concordance with the 5% probability of failure assumed for the material fracture toughness K_{mat} .

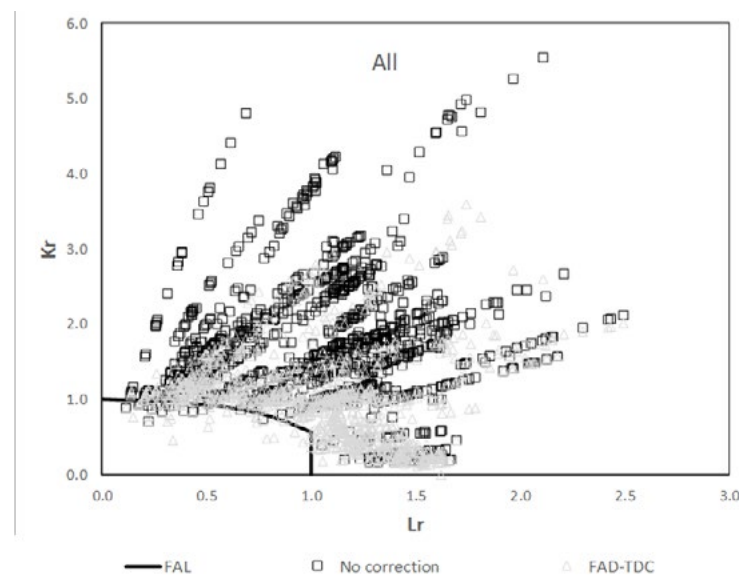


Figure 1. FAD assessments of all the specimens and materials, without (crack-like assessment) and with FAD-TDC notch correction.

Influence of environment on the propagation of internal fatigue cracks in a Ti alloy

Louis HEBRARD^{1,2,3}, Nicolas RANC², Thierry PALIN-LUC^{3,4}, Jean-Yves BUFFIERE¹

¹ INSA LYON Lab. MATEIS

² Laboratoire PIMM, Arts et Métiers, Paris (12 point)

³ Univ. Bordeaux, CNRS, Bordeaux INP, I2M, F-33400, Talence, France.

⁴ Arts et Metiers Institute of Technology, CNRS, Bordeaux INP, HesamUniversite, I2M, F-33400 Talence, France.

jean-yves.buffiere@insa-lyon.fr

In the Very High Cycle Fatigue regime (low-stress amplitudes and $N_{\text{failure}} \sim 10^8 - 10^{10}$ cycles), metallic engineering materials like high strength steels, Ti or Ni alloys, tend to fail from fatigue cracks initiated in the bulk where they propagate in "vacuum" condition. In this type of environment, the crack growth rates are expected to be much slower than in air but *direct* measurements of $da/dN = f(\Delta K)$ curves remain scarce in the literature [1]. For designing against fatigue, therefore, engineers have to resort to propagation curves established for surface cracks growing in (ultra) high vacuum. The relevance of ultra high vacuum for simulating the environment seen by internal fatigue cracks has been debated in the literature [2]; another issue is the stress state at the tip of a fully internal crack which might be different from that of a through crack in, for example, a CT sample.

To address this last issue we have used an in situ ultrasonic fatigue machine [3] to study in situ the propagation of internal fatigue cracks growing from an artificial defect in a Ti-6Al4V alloy cycled at 20 kHz [4]. A laser vibrometer and a real-time FFT analysis are used to detect crack initiation and synchrotron X-ray micro-tomography allows to image the internal crack propagation in the sample under load. Two sets of samples have been produced. The first one contains a central canal along the specimen axis which brings air from the laboratory to the internal notch; in the second series the notches are not connected to the surface.

The specimens failure occurs systematically from an internal crack initiated at the artificial defect regardless of its environment. The number of cycles to failure and the crack growth rates are compared for both types of defects. In the case of samples containing a defect isolated from air, internal cracks propagate at a much slower rate than when the defect is connected with ambient air. For isolated defects, microstructural features observed by SEM on the fracture surfaces are in good agreement with the findings of the literature for natural internal cracks in Ti-6Al-4V. For defects connected to air a supplementary region surrounding the defects appears on the fracture surface with a pronounced faceted / crystallographic aspect.

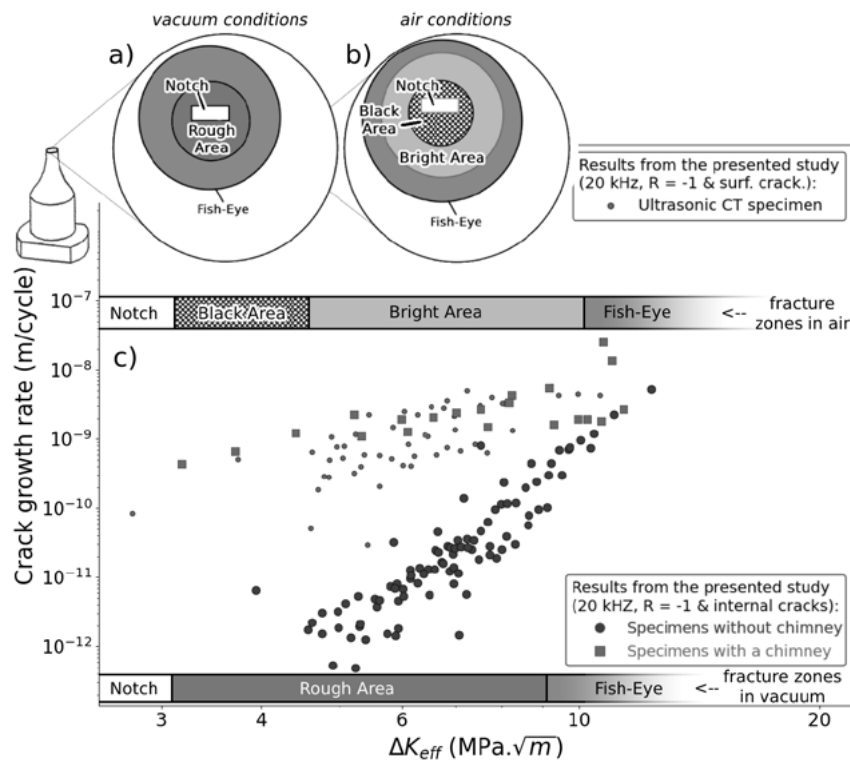


Figure 1. Fig. 9. Scheme of the fracture surface for a crack which propagated in vacuum (a) and air (b). (c) Crack growth rate data (larger symbols: tomography data, smaller symbols: CT data). The SIF range corresponding to the different regions of the fracture surfaces in vacuum and in air are shown by the colored bars respectively at the bottom and at the top of the curve as explained in Section 4.4. For a colour version of this figure see [4]

REFERENCES

1. Nakamura, T.; Yoshinaka, F.; Oguma, H.; Shiozawa, D.; Nakai, Y.; Uesugi, K. Detection of small internal fatigue cracks in Ti-6Al-4V by using synchrotron radiation μ CT imaging. *Mech. Eng. Letters*, 2, 16–00233 (2016).
2. Sinha, V.; Larsen, JM. Vacuum Levels Needed to Simulate Internal Fatigue Crack Growth in Titanium Alloys and Nickel-Base Superalloys: Thermodynamic Considerations. *Metall. Mat. Trans. A*, 43, 3433-41 (2012).
3. Messenger, A.; Junet, A.; Palin-Luc, T.; Buffiere, JY.; Saintier, N.; Ranc, N.; May, M.; Gaillard, Y.; King, A.; Bonnin, A.; Nadot, Y. In situ synchrotron ultrasonic fatigue testing device for 3D characterisation of internal crack initiation and growth. *Fat. Fract. Eng. Mat. Struct.*, 43, 558-567 (2020).
4. Hébrard, L.; Buffiere, JY.; Palin-Luc, T.; Ranc, N.; Majkut, M.; King, A.; Weck, A. Environment effect on internal fatigue crack propagation studied with in-situ X-ray microtomography. *Mar. Sc. Eng. A*, 882, 145462 (2023).

Crack surface contacting behaviour at initiation region of very-high-cycle fatigue for high-strength alloys

Youshi HONG¹, Zhiqiang TAO^{1,2}, Leiming DU¹, Xiangnan PAN¹, Guian QIAN¹

¹ Institute of Mechanics, Chinese Academy of Sciences, Beijing 100190, China

² College of Robotics, Beijing Union University, Beijing 100020, China

hongys@imech.ac.cn

In very-high-cycle fatigue (VHCF) of high-strength alloys, crack initiation mainly from internal defects and a distinct feature at crack initiation region prevails, which is fine granular area (FGA) in high-strength steels or rough area (RA) in titanium alloys. FGA or RA is regarded as the characteristic region of crack initiation for VHCF because it is derived as a function of shear modulus and Burgers vector of material, and its formation process consumes more than 95% of total fatigue life [1]. Experiments show that substantial microstructure refinement down to nanograins underneath the surfaces of FGA or RA region, which mainly happened under the cases of negative stress ratios [2-4]. We considered that the microstructure refinement in the crack initiation region is due to the contacting between crack surfaces in crack initiation region, and proposed the model of “numerous cyclic pressing (NCP)” to explain the mechanism of microstructure refinement and nanograin formation in the crack initiation region of VHCF, which is attributed to the sufficient cycles of repeated compressive stress at the localized field of initiated crack surfaces [2]. Figure 1 shows a recent example of RA feature for an additively manufactured Ti-6Al-4V [5]. Interestingly, substantial grain refinement occurred not only at the main crack surface layer but also along the banks of the sub-crack in crack initiation region.

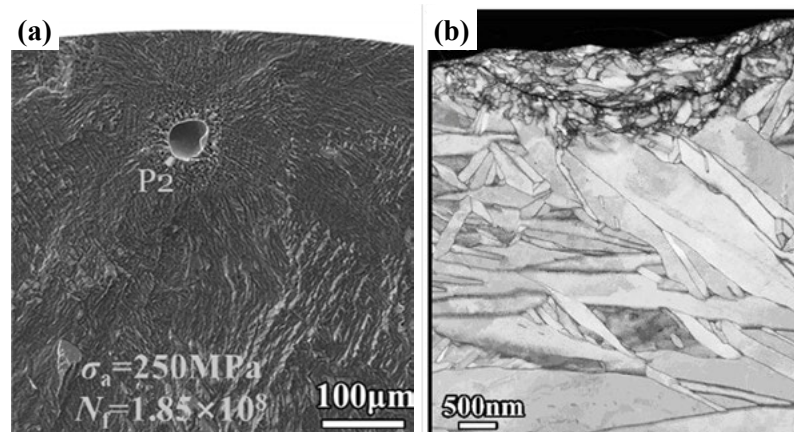


Figure 1. (a) SEM image showing crack initiation region with RA feature of an additively manufactured Ti-6Al-4V, short rectangular bar being the location of profile sample, and (b) TEM image of the profile sample showing microstructure refinement in RA surface layer [5].

A numerical analysis was performed to further address the process of microstructure refinement and nanograin formation in relation with the contact actions at crack surfaces in FGA or RA region. The material for this analysis is a high-strength steel. 4-node bilinear axisymmetric quadrilateral elements from Abaqus CAE element library with a minimum

element size of $0.5\ \mu\text{m}$ were used in the analysis. A spherical defect as crack origin was inserted in the model. Figure 2 illustrates the calculation results of the maximum contact stresses as a function of crack length for the stress ratio (R) values of -1 , -0.5 , 0.1 and 0.3 . It is seen that the status of contact stress is dependent on the applied stress ratio (or mean stress) and the maximum contact stress decreases with increasing value of stress ratio. For negative stress ratios, a contact stress peak appears at crack tip. Then, the value decreases gradually to a constant for $R = -1$ but again increases to a constant for $R = -0.5$. In general, the value for $R = -1$ is much larger than that for $R = -0.5$. On the contrast, the results show contact stress vanishing for the positive stress ratio cases of $R = 0.1$ and 0.3 . This implies that the repeated contact stress caused by the remote cyclic tensile and compressive loading will result in the microstructure refinement even nanograin formation in the surface layer of crack initiation region. It should be emphasized that the contact stress between the crack surfaces will cause the localized shear deformation thus to induce the microstructure refinement, and the distribution of contact stress at crack surfaces is in relation to crack closure behavior. In short, this result is in support of the NCP model [2] to further understand the formation mechanism of FGA or RA in high-strength alloys.

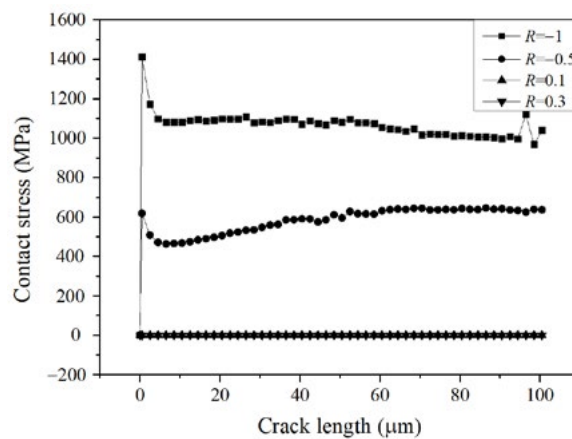


Figure 2. Calculation results showing contact stress versus crack length at crack initiation region for different R values of a high-strength steel.

REFERENCES

- Hong, Y.; Lei, Z.; Sun, C.; Zhao, A. Propensities of crack interior initiation and early growth for very-high-cycle fatigue of high strength steels. *Int. J. Fatigue*, 58, 144–151 (2014).
- Hong, Y.; Liu, X.; Lei, Z.; Sun, C. The formation mechanism of characteristic region at crack initiation for very-high-cycle fatigue of high-strength steels. *Int. J. Fatigue*, 89, 108–118 (2016).
- Su, H.; Liu, X.; Sun, C.; Hong, Y. Nanograin layer formation at crack initiation region for very-high-cycle fatigue of a Ti-6Al-4V alloy. *Fatigue Fract. Eng. Mater. Struct.*, 40, 979–993. (2017).
- Ritz, F.; Stäcker, C.; Beck, T.; Sander, M. FGA formation mechanism for X10CrNiMoV12-2-2 and 34CrNiMo6 for constant and variable amplitude tests under the influence of applied mean loads. *Fatigue Fract. Eng. Mater. Struct.*, 41, 1576–1587 (2018).
- Du, L.; Pan, X.; Hong, Y. New insights into microstructure refinement in crack initiation region of very-high-cycle fatigue for SLM Ti-6Al-4V via precession electron diffraction. *Materialia*, 33, 102008 (2024).

Analysis of crack-tip field in orthotropic compact-tension-shear specimens

Pengfei JIN¹, Zheng LIU¹, Xu CHEN¹

¹ School of Chemical Engineering & Technology, Tianjin University, Tianjin, China

xchen@tju.edu.cn

The absence of relevant standards or normative methods compels engineers to treat orthotropic materials as isotropic for structural integrity analysis and design. However, this practice can introduce significant errors [1], resulting in considerable safety risks. Furthermore, in practical conditions, cracks often exhibit mixed-mode fracture behaviours, and the combination of orthotropy gives rise to an even more complex stress field in the vicinity.

In this context, conducting Compact-Tension-Shear (CTS) tests proves to be a promising research methodology for determining the fracture toughness of orthotropic materials in mixed-mode I & II [2]. It requires only one specimen to generate all in-plane mixed-mode loading conditions. Moreover, taking composite materials as an example, CTS tests are not only applicable for determining interlaminar fracture toughness but can also be employed for translaminar or intralaminar fracture assessments [3]. Despite having significant advantages, the lack of characterization of crack-tip fields or fracture parameters in orthotropic CTS specimens has impeded the further application of CTS tests.

Therefore, it is crucial to incorporate orthotropy into the characterization of crack-tip fields, develop solutions of fracture parameters, addressing the gap in the existing researches. This study conducted a comprehensive two-dimensional finite element analysis (2D FEA) on orthotropic CTS specimens to assess critical parameters in fracture toughness including stress intensity factor (SIF), T -stress and crack mouth opening displacement (CMOD) compliance. The SIF reflects the strength of the singular stress term at the crack-tip. Meanwhile, the T -stress, which is the first constant term in the Williams' series expansion, is commonly employed as an in-plane constraint correction parameter. Additionally, CMOD-compliance serves as a metric for crack propagation but also facilitates the assessment of structural toughness.

For orthotropic CTS specimen as shown in Figure 1, the analysis matrix encompassed a wide range of material orthotropy ($\lambda=0.02-40$ and $\rho=0-10$), crack length ratios ($a/W=0.2-0.8$), and loading angles ($\beta=0^\circ-90^\circ$). Results (some of the results are shown in Figure 2) show the coupled effects of orthotropy, geometry, and loading angle on the fracture parameters. Compared to long cracks under pure mode I loading, the effect of λ and ρ on fracture parameters of CTS specimen is equally significant. The impact of orthotropy varies under different geometries and loading angles, while different fracture parameters exhibit varying degrees of sensitivity to orthotropy.

In summary, this study conducted an investigation into the crack-tip fields of orthotropic CTS specimens under mixed-mode loading, successfully establishing a multi-parameter characterization of K_I , K_{II} , and T . Furthermore, the obtained fracture parameters including CMOD-compliance would contribute to the development of fracture toughness testing methods for orthotropic materials under mixed-mode loading and provide a reference for standardization in the process.

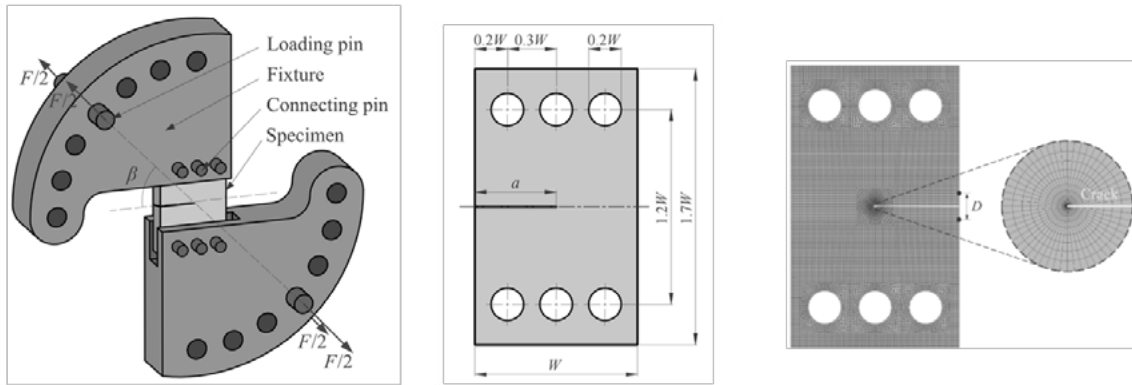


Figure 1. Structure diagram of CTS loading device and finite element model mesh for CTS specimen.

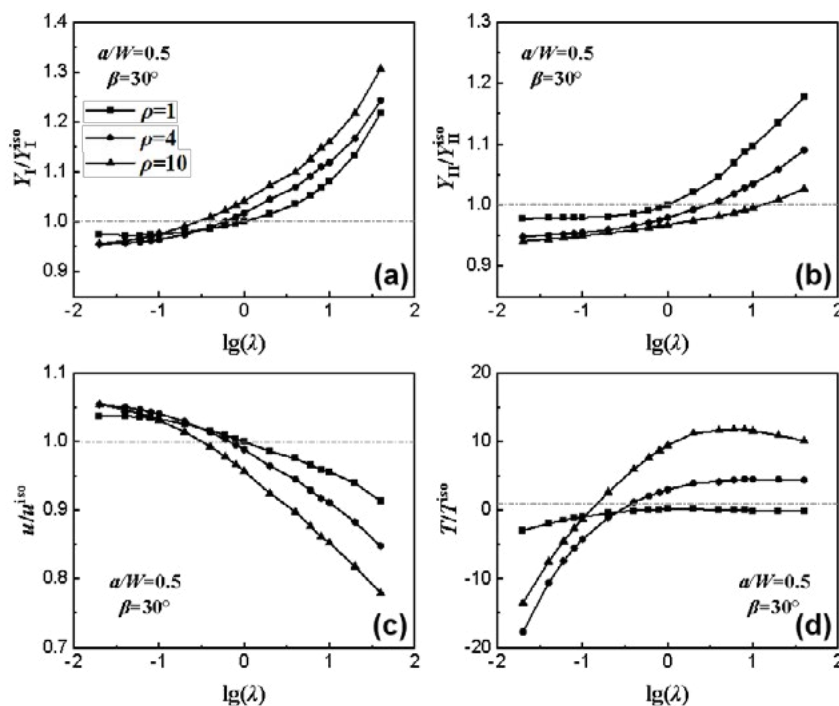


Figure 2. The effects of orthotropy on the fracture parameters at $a/W=0.5$ and $\beta=30^\circ$: (a) Normalized mode I SIF; (b) Normalized mode II SIF; (c) Normalized T -stress; (d) Normalized CMOD-compliance.

REFERENCES

1. Le-Ngoc, L.; McCallion, H. On the fracture toughness of orthotropic materials, *Eng. Fract. Mech.*, 58, 355–362 (1997).
2. Rikards, R.; Buchholz, F.G.; Wang, H.; Bledzki, A.K.; Korjakin, A.; Richard, H.A. Investigation of mixed mode I/II interlaminar fracture toughness of laminated composites by using a CTS type specimen, *Eng. Fract. Mech.*, 61, 325–342 (1998).
3. Jamali, J.; Mahmoodi, M.J.; Hassanzadeh-Aghdam, M.K.; Wood J.T. A mechanistic criterion for the mixed-mode fracture of unidirectional polymer matrix composites, *Compos. Part B Eng.*, 176, 107316 (2019).

Phase-field modelling of fracture – inelasticity, heterogeneity, and fatigue

Markus KÄSTNER^{1,2}, Arne HANSEN-DÖRR, Franz DAMMASS¹, Martha KALINA¹,
Tom SCHNEIDER¹, Paul SEIBERT¹

¹ TU Dresden, Institute of Solid Mechanics, 01062 Dresden, Germany

² DCMS – Dresden Center for Computational Materials Science, 01062 Dresden, Germany

markus.kaestner@tu-dresden.de

In the last fifteen years, the phase-field method has developed into a powerful approach for simulating various fracture phenomena. The method uses a diffuse, implicit representation of cracks in terms of an additional field variable d . The regularisation allows for a numerically favourable representation of the crack compared to explicitly changing a finite element mesh. On the other hand, it results in a coupled field problem. The method is able to account for various crack phenomena such as crack initiation, crack branching and coalescence without additional conditions. In this contribution, current developments of the method for the simulation of crack propagation in materials with rate-dependent ductile behavior, in heterogeneous materials and under cyclic loading are presented. For this purpose, a general, modular energy functional is introduced

$$\Pi_\ell = \int_{\Omega} g(d)\psi^e(\varepsilon) + \beta_{vi}g_{vi}(d)\psi^{vi}(\varepsilon) dV + \int_{\Omega} \alpha(D)G_c(\mathbf{x}) \frac{1}{2\ell} (d^2 + \ell^2 |\nabla d|^2) dV \quad (1)$$

The first term is the elastic energy density, which is reduced with crack propagation by the degradation function $g(d)$. The second is a contribution of accumulated inelastic dissipation. Heterogeneities are modeled by a spatial variation of the critical energy release rate G_c . To account for fatigue, the crack resistance can be reduced by a fatigue degradation function $\alpha(D)$.

Ductile fracture: When using the phase-field method to model and simulate crack propagation in inelastic materials, it is crucial to consider the dissipative mechanisms in the base material and crack as well as their coupling. As an example, a generalized phase field model for the fracture of viscoelastic materials is presented here [1]. The formulation assumes a bidirectional coupling between crack phase field and relaxation mechanisms, i.e. viscous internal variables are explicitly included in the evolution of the phase-field and vice versa. More recently, the role of a rate-dependent fracture toughness G_c has been investigated [2]. The model has been applied to simulate the temperature- and rate dependent fracture behavior of natural materials [3].

Heterogeneities and interface fracture: In, e.g., fiber-reinforced polymers or grain-like metallic structures, crack propagation is guided by the local heterogeneous material structure. To model the fracture processes, which are essentially determined by the material boundaries, a phase-field model for brittle fracture is combined with a diffuse representation of the microstructure. The critical energy release rate $G_c(\mathbf{x})$ is reduced at interfaces to represent the generally weaker material. We have observed that the regularizations of the crack with the characteristic length l and the interface l_i interact. To enable quantitative predictions, a numerical compensation was developed in [4].

The approach was implemented and the simulation is compared with an analytical reference solution of linear-elastic fracture mechanics in [5]. The results are shown in Figure 1. A very good

agreement was found with regard to the prediction of the fracture behavior depending on the ratio of the fracture toughnesses in bulk and interface. The findings from the simulations can be used specifically for the development of damage-resistant materials in terms of materials design.

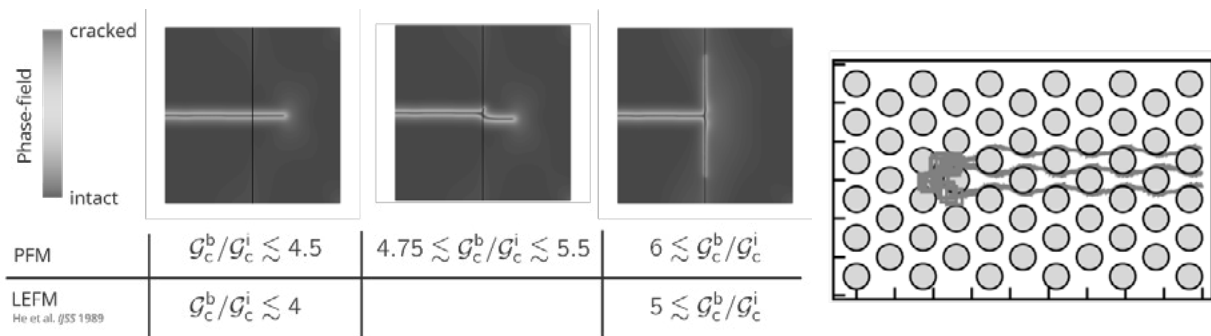


Figure 1. *Left* – Simulation of a crack approaching an interface. Depending on the ratio of the fracture toughness of bulk (b) and interface (i) three different phenomena are observed. *Right* – simulation of a cracked heterogeneous microstructure.

Fatigue: The modeling of fatigue phenomena is still a challenging task. Our phase-field model was developed in particular with regard to an efficient simulation of high numbers of load cycles of $N > 10^4$ [6]. The standard phase field formulation is extended by introducing a scalar reduction function $\alpha(D) \in [0;1]$, which models the progressive material weakening due to fatigue by a local reduction of the fracture toughness G_c depending on the fatigue damage $D \in [0;1]$, which is determined classic fatigue concepts. The parameterization and application for the quantitative prediction of fatigue crack propagation are explained in [7] where it is also shown that the model can be used to simulate accelerated and retarded crack growth due to residual stresses. Recently, the model was applied to predict tooth flank fracture where it is essential to account for the heterogeneous material properties resulting from case hardening [8].

REFERENCES

1. Dammaß, F.G.; Ambati, M.; Kästner A generalised phase-field model of fracture in viscoelastic materials. *Cont. Mech. Thermo.* (2021).
2. Dammaß, F.G.; Kalina, K.A.; Ambati, M.; Kästner, M. Phase-field modelling and analysis of rate-dependent fracture phenomena at finite deformation. *Comput. Mech.* (2023).
3. Dammaß, F.G. et al. Rate-and temperature-dependent ductile-to-brittle fracture transition: Experimental investigation and phase-field analysis for toffee. *Eng. Fract. Mech.* (2024).
4. Hansen-Dörr, A.C.; Hennig, P.; De Borst, R.; Kästner, M. Phase-field modeling of interface failure in brittle materials. *Comput. Methods in Appl. Mech. Eng.* 346:25–42 (2018).
5. Hansen-Dörr, A.C.; Dammaß, F.G.; De Borst, R.; Kästner, M. Phase-field modeling of crack branching and deflection in heterogeneous media. *Eng. Frac. Mech.* 232, 107004 (2020).
6. Seiler, M.; Linse, T.; Hantschke, P.; Kästner, M. An efficient phase-field model for fatigue fracture in ductile materials. *Eng. Fract. Mech.* 106807 (2020).
7. Seiler, M.; et al. Phase-field modelling for fatigue crack growth under laser-shock-peening-induced residual stresses. *Arch. Appl. Mech.* 1-18 (2021).
8. Schneider, T.; Müller, D.; Seiler, M.; Tobie, T.; Stahl, K.; Kästner, M. Phase-field modeling of fatigue crack growth during tooth flank fracture in case-hardened spur gears. *Int. J. Fatigue* 163, 107091 (2022).

Simplified analysis of stress intensity factors at weld toe

Paolo LIVIERI¹

¹Department of Engineering, University of Ferrara, Via Saragat 1, 44100 Ferrara (Italy)

paolo.livieri@unife.it

The J-integral is a path-independent integral introduced by Rice [1] and Cherepanov [2], that established a simple relationship between the path integral and the stress intensity factors (SIF) of a crack subjected to mode I, mode II and mode III loadings. Successively, Chiarelli and Frediani [3] and Huber et al. [4] considered the extension from a 2D to 3D model by considering an integral in a plane perpendicular to the crack front starting from Eshelby’s energy momentum tensor.

The J-integral applied to a V-notch in a plate (namely J_V) is not constant if the initial and final integration points are moved along the side but the path independence of the integral is always verified. If we consider a path with fixed points at each end at the same distance ρ from the origin (see Figure 1), the J_V assume a simplified formulation [5,6]:

$$J_V = J_{V1} + J_{V2} + J_{V3} = \bar{J}_1 \frac{K_{N,1}^2}{E'} \rho^{2\lambda_1-1} + \bar{J}_2 \frac{K_{N,2}^2}{E'} \rho^{2\lambda_2-1} + \bar{J}_3 \frac{K_{N,3}^2}{2G} \rho^{2\lambda_3-1} \quad (1)$$

where K_N are the notch stress intensity factors, \bar{J}_i are parameters that only depend on the opening angle 2α , E' is equal to the elastic modulus E for plane stress and $E'=E/(1-\nu^2)$ for plane strain, and G is the shear modulus. Furthermore, each J_V mode is proportional to the corresponding mode (I, II or III) of the classic J_i integral of a virtual embedded crack lying along the bisector of the V-notch and with a length equal to ρ (see Figure 2):

$$\frac{J_i \Big|_a}{J_{V,i} \Big|_{r=\rho}} = v_i \quad i = 1, 2, 3 \quad (2)$$

The parameters v_i are reported in Table 1 for an opening angle of 135 degrees. So that, the stress intensity factors of a crack behind a sharp V-notch can be calculated by means of the J_V evaluated for the V-notch without modelling the crack with the same external load and boundary conditions. Table 3 reports the values of v_i for a selected opening angle.

The aim of this paper is to verify the use of the J_V integral in welded structures for the evaluations of the stress intensity factors of a crack at the weld toe by means of the three-dimensional FE model without modelling the crack. Figure (2) shows a hollow section subjected to tensile loading (F) and torque (M_t). The opening angle is of 135 degrees. When the size of the weld toe tends to zero, accurate FE analysis show that the v_i parameters tend to that reported in table 1. Figure 2 shows the trend of v_i .

Table 1. v_i parameters for an opening angle of 135 degrees

2α	v_1	v_2	v_3
135°	1.74	2.12	1.23

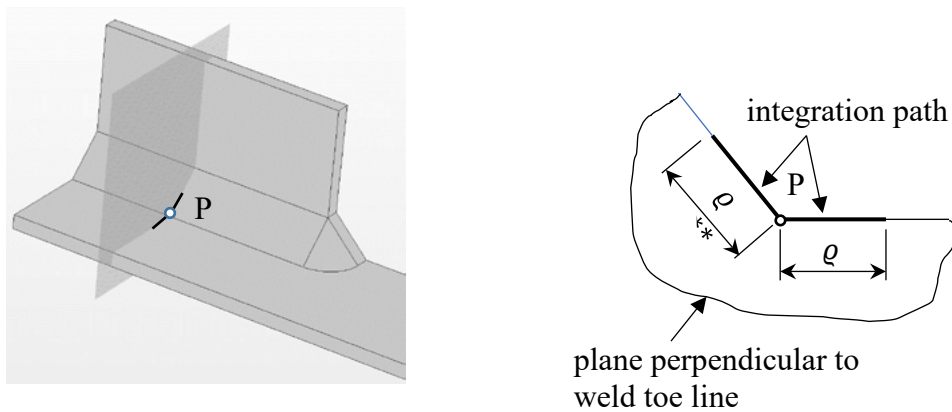


Figure 1. J_V for a welded joint with a sharpe V-notch.

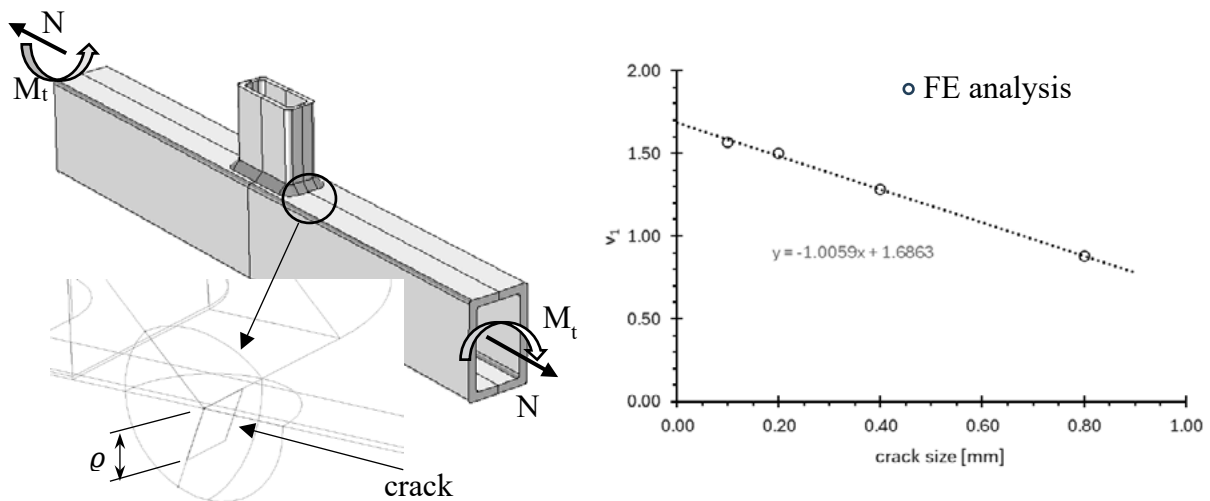


Figure 2. Value of the parameter ν_l at the weld toe obtained with a three-dimensional FE analysis.

REFERENCES

1. Rice, J.R. A path independent integral and the approximate analysis of strain concentration by notches and cracks. ASME J. App. Mech., 35, 379-386, (1968)
2. Cherepanov, G. P. Prickladnaia Matematika i Mekhanika. 31, 476-488, (1967)
3. Chiarelli, M.; Frediani, A. A computation of the three-dimensional J-integral for elastic materials with a view to applications in fracture mechanics. Eng. Fract. Mech., 44, 763–788, (1993)
4. Huber, O.; Nickel, J.; Kuhn, G. On the decomposition of the J-integral for 3D crack problems. Int. J. of Fract., 64, 339–348, (1993)
5. Livieri, P. Use of J–integral to predict static failures in sharp V-notches and rounded U-notches. Eng. Fract. Mech., 75, 1779-1793, (2008)
6. Livieri, P. Fatigue strength assessment of three-dimensional welded joints with the J_V parameter. Theor. Appl. Fract. Mech., 119, (2022)

Review of the design fatigue strength for steel butt welded joints: influence of geometrical factors and shape defects

Paolo LIVIERI¹, Roberto TOVO¹

¹Department of Engineering, University of Ferrara, Italy

roberto.tovo@unife.it

During last two decades, the studies on fatigue strength of welded joint progressively moved from the nominal and structural stress approaches to the local stress methods, by acknowledging the dominating position of the notch effects at toes, roots or other stress raisers related to defects or geometrical irregularities.

The peculiarity of the weld geometry is the significant presence of sharp stress concentrations, compared to other structural details, and the related problems in estimating the actual notch sensitivity. The local stress investigations proposed several methods to address and overcome such criticality. The most largely used local method is the “1 mm fictitious radius”; however, even different methods have been used in the literature as well as the Strain Energy Density SED, the Peak Stress Method, the Critical Distance or the Implicit Gradient approaches. Similarly, even the Fracture Mechanics based approaches, by investigating the crack thresholds or propagating condition in the weldments, deal with the stress field affected by the overall local weld geometry.

The proposed methodology, somehow, determine an effective stress value by averaging the local stress field at the tip of the stress raisers. Each method has its advantages and overcomes. At this stage, several investigations have been carried out and it is not convenient to focus on which method could be more effective, but it is more practical to take advantage of the evidence coming out from the investigations and to develop updated design guidelines more accurately considering the effects of weld geometry parameters and properties. Also the actual decrease caused by defects and irregularities can be conveniently be included in a comprehensive approach. The “FAT Categories” suggested in design standards, consider a reduced number of influencing parameters and the proposed corrections can now probably been improved according with the scientific literature.

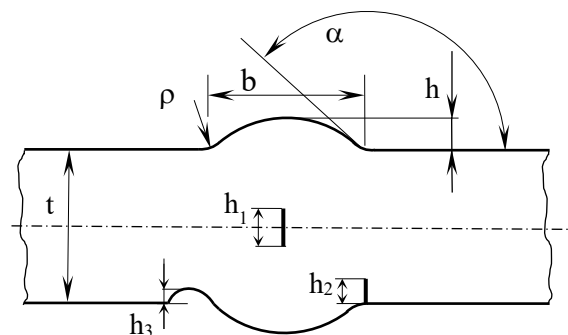


Figure 1. definition of the weld geometrical parameters and of main defect dimensions: inner lack of penetration, crack like defect at toe, rounded undercuts.

This paper focuses on butt weldment made of steel under cyclic tensile loading. It aims to take advantage of the local stress methods and to summarise main outcomes in a reformulation of influencing factors as a contribution for upcoming design guidelines.

In this direction, a representing contribution has been recently given in [1] where parametrical formulas for design curve assessment are proposed. Other contributions, for butt welds are, for instance in [2]. In this paper, starting from the outcomes [3], a larger comparison with the literature is given, by suggesting new criteria and formulation of the geometrical parameters influence. Even the acceptability of common defects is addressed. Used reference geometry and parameter definitions are shown in fig. 1.

The main effort is to order the principal influencing parameter starting from the most affecting ones. According to the literature they are the size effect and the h/b value. In this paper, considering the size effect, the fundamental role of the weld angle “ α ” is highlighted, so that, the influence of the h and h/t values, are mainly associated to their relationship with “ α ”.

In figure 2, the new formulated size effect, based on main plate thickness, is given. In the same figure also the usual Fat categories definition of the size effect is shown together with some confirming data taken from the literature, obtained with the fictitious radius approach.

In the second part of the figure 2, an example of the effect of a lack of fusion is proposed. Other crack like or notch like defects, are considered in the paper.

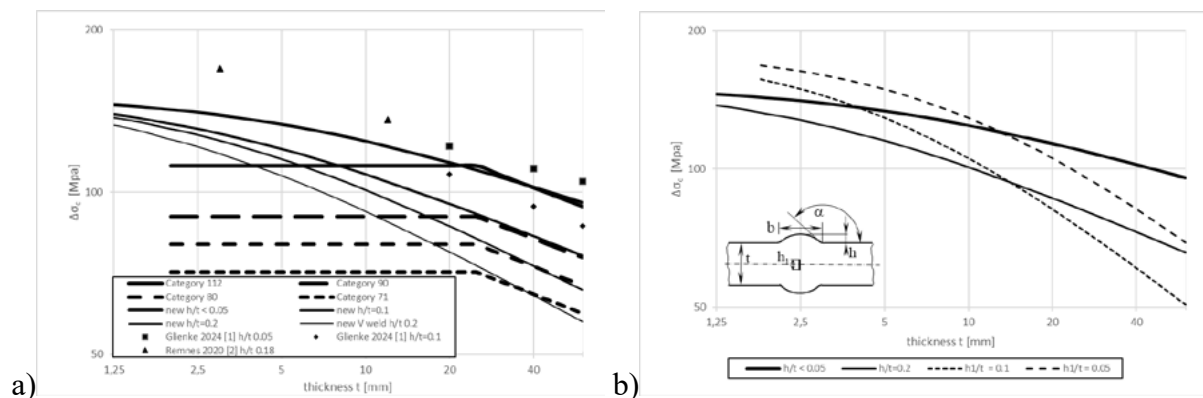


Figure 2. a) new formulation of the size effect compared to FAT categories and data from literature; b) the influence of the inner lack of penetration.

REFERENCES

1. Glienke, R.; Kalkowsky, F.; Hobbacher, A.F.; Holch, A.; Thiele, M.; Marten, F.; Kersten, R.; Henkel, K.-M. Evaluation of the Fatigue Resistance of Butt-Welded Joints in Towers of Wind Turbines - a Comparison of Experimental Studies with Small Scale and Component Tests as Well as Numerical Based Approaches with Local Concepts. *Weld. World*. (2024).
2. Remes, H.; Gallo, P.; Jelovica, J.; Romanoff, J.; Lehto, P. Fatigue Strength Modelling of High-Performing Welded Joints. *Int. J. Fatigue*, 135, (2020).
3. Livieri, P.; Tovo, R. Overview of the Geometrical Influence on the Fatigue Strength of Steel Butt Welds by a Nonlocal Approach. *Fat. Fract. Eng. Mater. Struct.*, 43(3), 502–514, (2020).

On the size and notch effect in AM photo-polymerised components

Mihai MARGHITAS¹, Cosmin-Florin POPA¹, Liviu MARSAVINA^{1,2}

¹ University Politehnica Timisoara, Department of Mechanics and Strength of Materials, Romania

² CCTFA, Romanian Academy – Timisoara Branch, Romania

liviu.marsavina@yahoo.com

The Additive Manufacturing (AM) technologies have completely renewed the production processes in the last decades, allowing to obtain parts of complex geometry with precisions not achievable with traditional manufacturing technologies such as machining, cast, and molding [1]. One of these technologies uses the photopolymerisation of an initial liquid monomer resin with a light-induced polymerization reaction. The Digital Light Processing (DLP) technology, which operates by directly projecting the UV-light image of the entire cross-section of the object being printed, belong to this AM categories.

The mechanical and fracture properties of components obtained through DLP are strongly influenced by process parameters (exposure time, specimen orientation, curing treatment, and so on), [1-2]. On the other hand, the 3D printed component with DLP technology show a brittle behavior, [2].

In this work, we investigated the size and the notch effect on DLP components obtained using Anycubic Photon printer. Considering our previous studies for manufacturing the specimens, we consider the parameters that provided higher mechanical and fracture properties (exposure time 20 s, layer thickness 0.05 mm, spatial orientation 45⁰, cleaning in Isopropyl Alcohol for 5 minutes and UV curing for 5 minutes). For the size effect, we considered a Semi-Circular Bend (SCB) specimen having different radius (R=10, 20, 30 and 40 mm), a sharp notch a=R/2 and a constant thickness t=6 mm). While for the notch effect SCB specimens with radius R=40 mm were manufactured with round notches of radius 0.8 and 2.2 mm.

Tests were performed at room temperature with 2 mm/min loading speed on a Zwick Proline Z005 testing machine.

The data for the size effect were interpreted according with Bazant [3,4] representing the nominal strength σ_N versus the specimen radius R:

$$\sigma_N = \frac{\sigma_{N0}}{\sqrt{1 + \frac{R}{R_0}}} \quad (1)$$

where σ_{N0} and R_0 are fitting parameters, which were obtained from a plot of $1/(\sigma_N)^2$ versus R, Fig. 1:

$$\sigma_{N0} = \sqrt{C} \quad \text{and} \quad R_0 = \frac{1}{A \sigma_{N0}^2} \quad (2)$$

A and C are the parameters of a linear fitting.

The fitting parameters allow determining the energy release rate G_f , respectively the fracture toughness K_{Ic} , where E represents the Young modulus:

$$G_f = \frac{1}{AE} \quad \text{and} \quad K_{Ic} = \sqrt{G_f E} \quad (3)$$

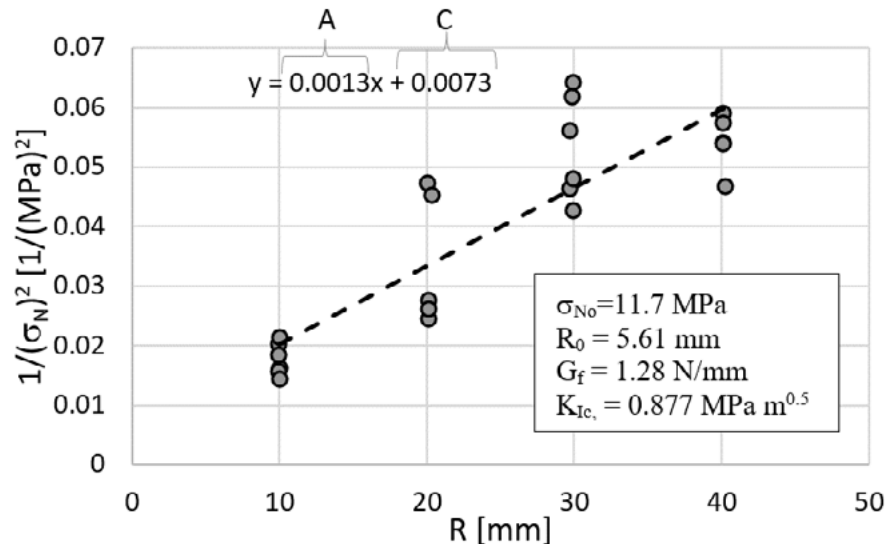


Figure 1. The size effect for DLP printed SCB specimens.

The resulted fracture toughness has a value of $0.877 \text{ MPa m}^{0.5}$, which is in accordance with the fracture toughness obtained using Single Edge Notched Bend (SENB) specimens.

The notch effect is plotted in Fig. 2 as load versus notch radius.

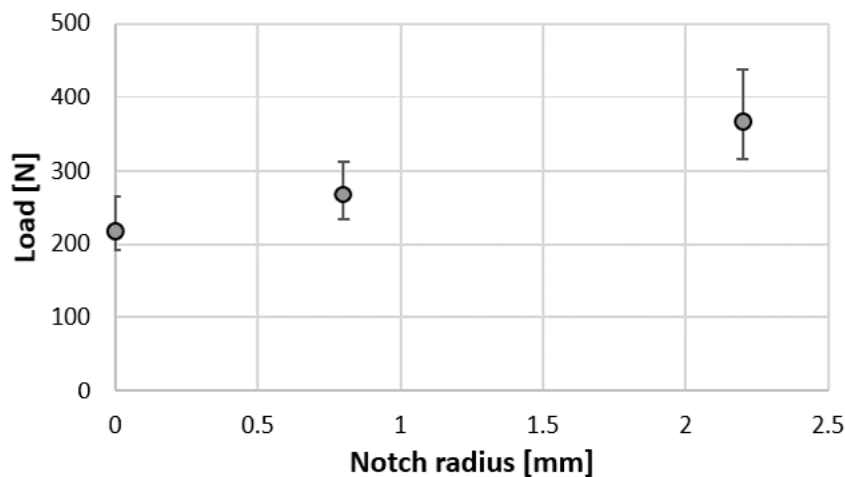


Figure 2. The notch effect for DLP printed SCB specimens.

REFERENCES

1. Brighenti, R.; Cosma, M.P.; Marsavina, L.; Spagnoli, A.; Terzano, M. Laser-based additively manufactured polymers: a review on processes and mechanical models. *Journal of Materials Science*, 56, 961-998 (2020).
2. Brighenti, R.; Marsavina, L.; Marghitas, M.P.; Montanari, M.; Spagnoli, A.; Tatar F. The effect of process parameters on mechanical characteristics of specimens obtained via DLP additive manufacturing technology. *Materials Today: Proceedings*, 78, 331 – 336 (2023).
3. Bažant, Z.P. *Scaling of Structural Strength*. Hermes-Penton, London, (2002).
4. Zdenek, P.; Z.P. Bažant, Z.; Yong, Z.; Goangseup, M.D. Isaac, Size effect and asymptotic matching analysis of fracture of closed-cell polymeric foam. *Int. J. of Sol. and Struc.* 40, 7197–7217 (2003).

Mixed-Mode Small Crack Growth Behaviours in Additively Manufactured Metals

Matthew MARKHAM¹, Ali FATEMI¹

¹The University of Memphis, Memphis, TN, USA

afatemi@memphis.edu

Over the past decade, Additive Manufacturing (AM) has made the transition from being used primarily for rapid prototyping to the production of service parts in structural applications. The rapid adaptation of this manufacturing process is likely due to the advantages it offers over conventional manufacturing methods, including: fabrication of complex geometries in near net shape, on-site manufacturing of replacement parts, and reduced cost for small production runs.

Despite these advantages, the defect content is much more variable in AM components than conventionally manufactured parts. In fact, the defect content within a single part may vary significantly due to the unique thermal history of different areas of the component. As a result, test coupons may not be representative of AM parts, even when fabricated alongside the part during the same build.

Traditional crack initiation approaches for fatigue life predictions determine the life of micro-crack nucleation plus small crack growth up to typically about 2 mm in length. Defects in AM parts can exist at sizes similar to micro-cracks (~50-100 μm) and in various orientations with respect to critical locations, depending on the orientation of the part on the build plate. These defects can act as small cracks, making crack nucleation life negligible, and the majority of crack initiation life in these parts can be thought to consist of small crack growth.

Multiaxial stress states in most service parts are unavoidable due to the applied loading conditions, and even cases where uniaxial stress states exist, part geometry can result in multiaxial stress states at critical locations. With these considerations in mind in addition to the variable size and orientation of manufacturing defects, there is a clear need for mixed-mode characterization of crack growth in AM metals due to these multiaxial stress states. The main purpose of this study is to document and characterize mixed-mode small crack growth behaviors in two AM metals, L-PBF Ti-6Al-4V and L-PBF 17-4 PH stainless steel.

Three different geometries (solid square cross-section specimens, standard thin-walled tubular specimens, and compact thin-walled tubular specimens) were tested as a part of this study. All three geometries were used to characterize small crack growth in L-PBF Ti-6Al-4V, and only standard thin-walled tubular specimens were used in 17-4 PH stainless steel. Some specimens of all three geometries were induced with artificial Femtosecond Laser Ablation (FLA) defects. Small crack growth behaviors under constant amplitude uniaxial, pure torsion, torsion with static compression, and in-phase axial-torsion loadings from both artificial and natural defects were characterized as a part of this study.

Small crack paths in both L-PBF materials were found to be torturous for all loading cases. There were multiple events of secondary crack growth, crack coalescence, and crack branching behaviors. It was found that even in cases where macroscopic crack growth indicated Mode I growth, local crack extension tended to occur in either Mode II/III or mixed-mode. One example displaying many of these characteristics is shown in Figure 1. Torsion with static compression loading was applied to this L-PBF Ti-6Al-4V compact tubular specimen, and small crack growth

was monitored until the crack growing from a vertically oriented FLA artificial defect reached a length of about 1300 μm . At this point loading was changed to in-phase axial-torsion, causing the small crack to slowly change direction before continuing growth along this new path.

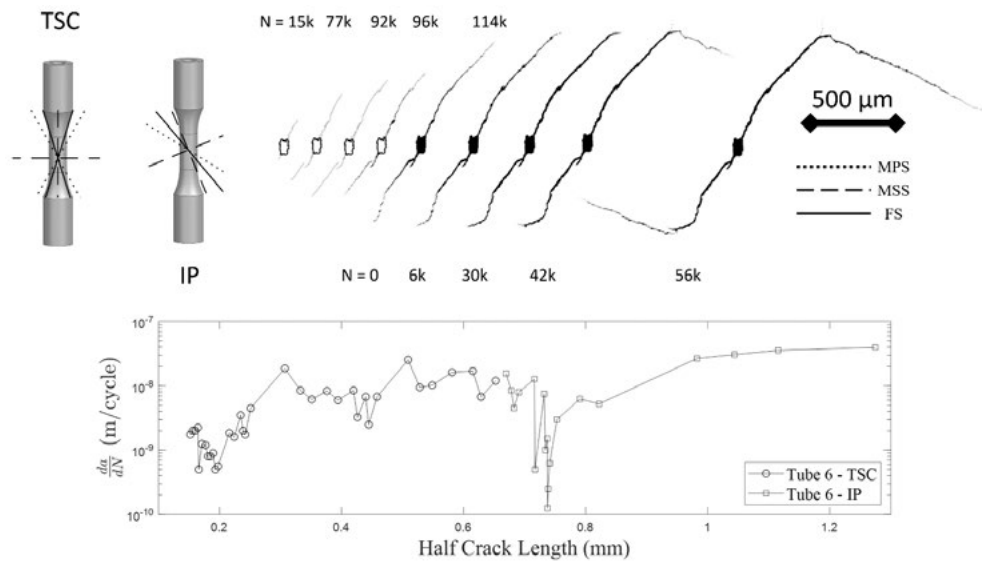


Figure 1. Crack paths in L-PBF Ti-6Al-4V specimen from FLA artificial defect. Initial loading was torsion with static compression. After crack reached a total length of about 1300 μm , testing continued with in-phase axial-torsion loading.

Roughness-induced crack closure was found to play a significant role in governing mixed-mode small crack growth behaviors, both in the form of asperity interlocking and friction-induced closure. This effect was most evident in specimens tested under pure torsion loadings, wherein crack face interactions resulted in either the arrest of small shear cracks, or the formation of Mode I branches. In both materials, rough crack faces were observed to abrade as the cracks grew out of the small crack growth regime, suggesting a reduction in roughness-induced closure by the time the crack grew to the size of a large crack. Evidence of crack face destruction as a result of roughness-induced closure in 17-4 PH and Ti-6Al-4V in specimens both with and without artificial defects under fully-reversed pure torsion loading is shown in Figure 2.

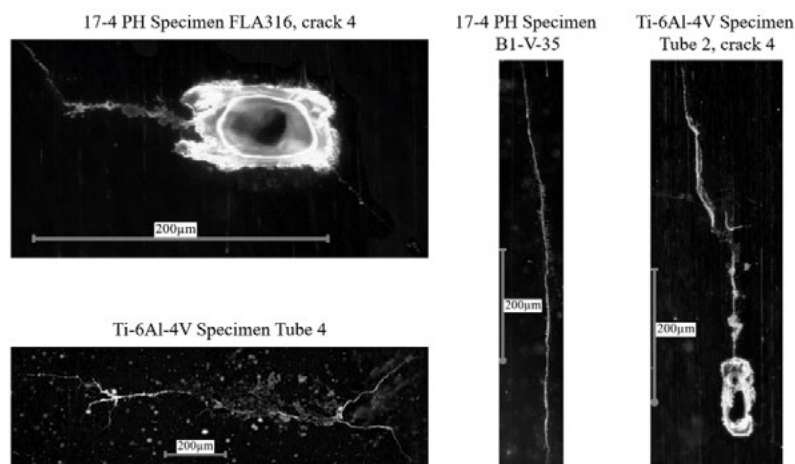


Figure 2. Evidence of crack face destruction as a result of roughness-induced closure in 17-4 PH and Ti-6Al-4V in specimens both with and without artificial defects under cyclic torsion loading.

Verification of a non-destructive method for quantitative analysis of damage accumulation proceeding from notch border displacements

Yury MATVIENKO¹, Vladimir PISAREV², Sviatoslav ELEONSKY²

¹ Mechanical Engineering Research Institute of the Russian Academy of Science, 101000 Moscow, Russia

² Central Aero-Hydrodynamics Institute named after Prof. N.E. Zhukovsky, 140180 Zhukovsky, Moscow Region, Russia

ygmatvienko@gmail.com

Quantitative description of low-cycle fatigue damage accumulation is of great interest [1, 2]. Employing experimental, especially non-destructive techniques, can significantly contribute to solving this problem. That is why novel non-destructive method for quantitative analysis of damage accumulation in stress concentration area under low-cycle fatigue conditions is developed and verified. Created approach is based on optical interferometric measurements of plastic dimple diameter in two orthogonal directions. Required dimple is caused by spherical ball indentation under prescribed external load. This procedure is performed near through-thickness hole in plane rectangular specimens with different levels of damage accumulation. Main scientific novelty of the approach resides in involving current damage indicators, which can be reliably derived on a base of simplest measurements of two in-plane displacement components by speckle-pattern interferometry. Evolution of each damage indicator over lifetime provides the damage accumulation function in an explicit form [3, 4].

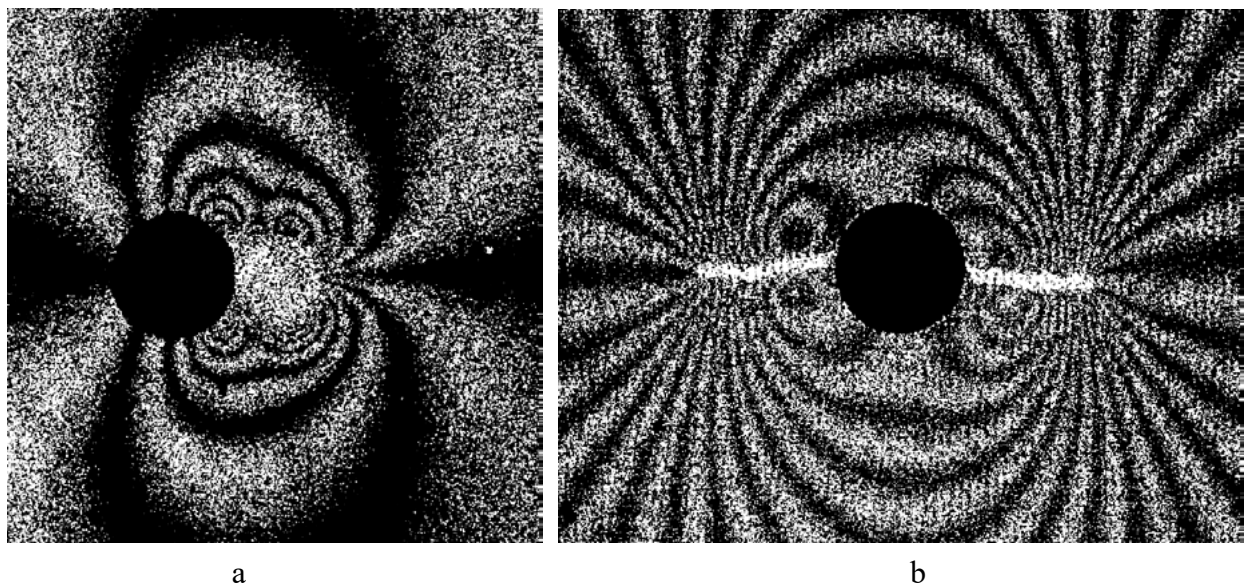


Figure 1. Interference fringe patterns obtained after ball indentation (a) and narrow notch inserting in the specimen subjected to $N = 1550$ cycles (42% of lifetime).

Objects of present research consist of eight 2024 aluminium plates of dimensions $180 \times 24.2 \times 5$ mm with a centred through-thickness hole of diameter $2r_0 = 3.0$ mm. All specimens are manufactured from a single material bar by the same technology. Mechanical properties are the following, namely, Young’s modulus $E = 74,000$ MPa, yield stress $\sigma_y = 330$ MPa and Poisson’s ratio $\mu = 0.33$. The specimens are tested under uniaxial push-pull loading with the stress range 350 MPa and stress ratio -0.40 . The experimental procedure includes the following steps. The first specimen is tested in initial state before low-cycle fatigue. The second specimen serves for failure lifetime ($N_F = 3687$). Other six specimens are subjected to low-cycle fatigue loading with different number of cycles to reach different fatigue damage levels. Dimples, which are performed along horizontal symmetry axis by pressing the steel ball of 7.2 mm diameter with 175 kN force, are located closely to the hole edge as it is shown in Figure 1a.

Comparison of the results following from proposed method with analogous data obtained by known destructive approach provides a mean to estimate the reliability of non-destructive technique. There is unique way for comparing two approaches by using the same specimens because plastic dimples belong to the single external face of each specimen. Opposite face can be successively used for registration of fringe patterns, which are attributed by inserting narrow notch. Fracture mechanics parameters, which are related to artificial notch and obtained on different stages of low-cycle fatigue, provide the damage accumulation function in an explicit form. The details of developed procedure are given in Ref. [3–5]. Typical interferogram describing displacement field near the notch is shown in Figure 1b. Experimental dependencies of the notch mouth opening displacement and the stress intensity factor from cycle number are constructed by the data of fringe patterns interpretation for all eight specimens. Constructed damage accumulation functions proceeding from ball indentation technique and inserting artificial notch method are in good agreement. Thus, high efficiency of non-destructive ball indentation approach with respect to quantitative analysis of damage accumulation is clearly substantiated.

REFERENCES

1. Ellyin, F. Fatigue damage, crack growth and life prediction, Chapman & Hall, (1997).
2. Murakami, S. Continuum Damage Mechanics, Springer Dordrecht Heidelberg London New York, (2012).
3. Matvienko, Y.G.; Pisarev, V.S.; Eleonsky, S.I. Evolution of fracture mechanics parameters relevant to narrow notch increment as a measure of fatigue damage accumulation. *Int. J. Fatigue*, 149, 106310 (2021).
4. Matvienko, Y.G.; Pisarev, V.S.; Eleonsky, S.I. Low-cycle fatigue damage accumulation near the cold-expanded hole by crack compliance data. *Int. J. Fatigue*, 155, 106590 (2022).
5. Pisarev, V.S.; Matvienko, Y.G.; Eleonsky, S.I.; Odintsev I.N. Combining the crack compliance method and speckle interferometry data for determination of stress intensity factors and T-stresses. *Engineering Fracture Mechanics*, 179, 348–374 (2017).

Validating residual stress reconstruction via finite element analysis using neutron imaging

Simon MCKENDREY¹, Xavier VAN-HEULE¹, Ranggi RAMADHAN^{1,2}, Winfried KOCKELMANN², Harry COULES^{1,3}, Clementine JACQUEMOUND^{1,4}, Mahmoud MOSTAFAVI¹

¹ University of Bristol, Queens Building, University Walk, Bristol, UK BS8 1TR

² ISIS Neutron and Muon Source, Harwell, Didcot, UK OX11 0QX

³ Jacobs, 601 Faraday Street, Birchwood Park, Warrington, UK WA3 6XF

⁴ CEA, Paris-Saclay - Bât.607 - Pce 182, 91191 Gif-sur-Yvette Cedex, France

simon.mckendrey@bristol.ac.uk

Residual stresses are self-equilibrated that are formed because of strain-incompatibility. They can be induced by mechanical and thermal processes such as: phase transformation, local plastic deformation, or manufacturing. Of particular interest to safety critical industries are residual stresses induced by welding. It is therefore desirable to simulate their effects on various damage mechanisms. To this aim, the key is correct reconstruction of residual stress in finite element models. The issue is that rarely are full residual stress tensors measured within the full volume of a component. Thus, upon the insertion of the limited residual stress into a finite element model it redistributes to maintain compatibility resulting in a different field from that is measured.

Residual stress reconstructions using measured data have been successfully created in previous works. Residual stress distributions were found by Korsunsky et al. [1] used high energy x-ray diffraction as input into an FE model using an inverse eigenstrain method. However this method required knowledge of the Green’s function for the given geometry, which can be difficult to determine for industrial components. Uzun et al. proposed a method which does not rely on Green’s functions to determine the distribution of eigenstrains in weld bead- on-plate components [3], and instead uses a least to predict residual stress that best match the contour measured displacements, allowing for residual stress predictions throughout the whole body.

Do et al. [4] used combined neutron diffraction and deep hole drilling residual stress measurements as input data for an iterative FE method. This method takes known stress values and applies them to the model before allowing them to reach equilibrium. It then takes the new equilibrated stresses and combines them with the known measured values and allows the model to reach equilibrium again. This step is then repeated until the measured values maintain their initial value. This method works well when multiple components of stress within the incompatible region are known. Coules et al. [5] compared the two different methods of reconstructing full field residual stresses in FE using limited experimental residual stress measurements. They showed that using the iterative method and only two components of the stress tensor it is possible to achieve errors of as little as approximately 15%.

This work proposes a simple method for reconstructing residual stresses in a welded pipe. It relies on a single line scan measurement of residual stress along the axial direction at mid-thickness of a pipe. A single line scan was chosen as this is a common dataset which is collected during residual stress measurements, and typically only the hoop and axial components of strain are measured. These measured residual strain components are then used to calculate the residual

stresses present in the pipe. These calculated residual stresses are amplified and applied to the FE model uniformly both radially and in the hoop. The amplification of the stress state is performed so that during a step to establish equilibrium, the stress at the mid-thickness relaxes to the measured value. The method applied by the Abaqus software to establish equilibrium applies both to the stress field defined by the user and to a set of stresses created by Abaqus of opposite sign but of equal magnitude to the user defined stresses. Abaqus then linearly reduces the magnitude of the artificial stresses over an initial equilibrium step. The stresses that remain are the equilibrium stresses. An iterative approach is taken to find the optimal amplification value. As the problem is essentially a line-search for a minimum with no expected local minimum, a golden section optimisation algorithm was implemented. The optimisation algorithm is used to find the amplification factor which provides the lowest root mean squared error to the measured strain values. The RMS error is calculated as the average RMS error of each equilibrium state elastic strain component in the model and the corresponding measured strain component; taken from Gauss points along a line in the model at a location representative of the experimentally measured elastic strain location. The proposed method was validated using synchrotron X-ray diffraction and neutron Bragg edge imaging.

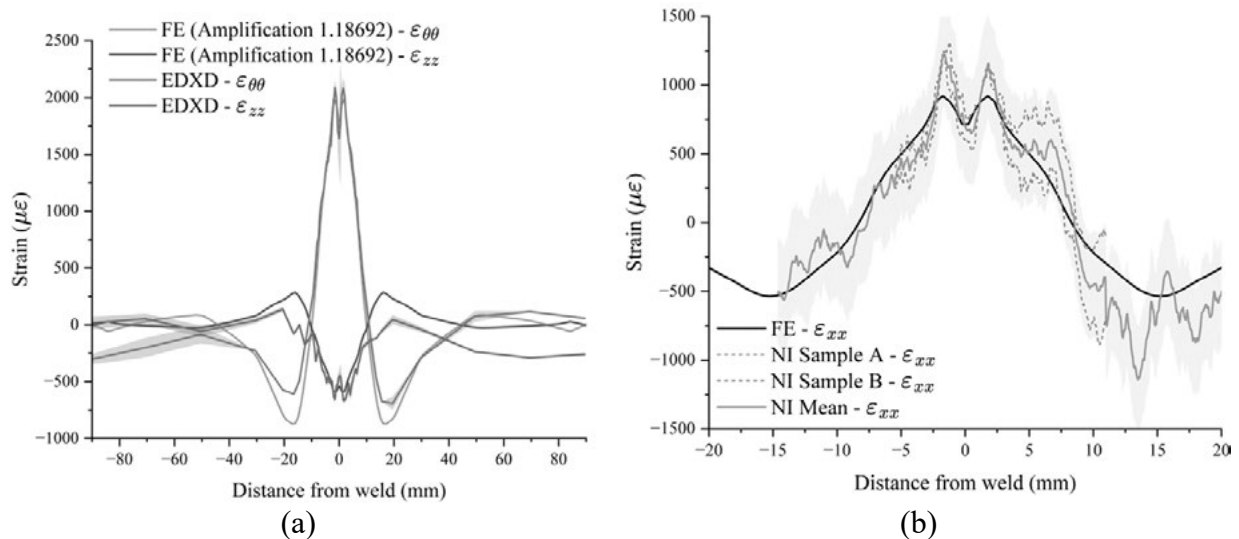


Figure 1. Residual stress in a welded pipe (a) measured and simulated by X-ray diffraction (b) estimated and validated by neutron Bragg edge imaging.

REFERENCES

1. Korsunsky, A.M.; Regino, G.M.; Nowell, D. Reconstruction of Residual Stress in a Welded Plate Using the Variational Eigenstrain Approach. *Engineering, Materials Science, Physics*, 10 (2005)
2. Uzun, F.; Korsunsky, A.M. On the identification of eigenstrain sources of welding residual stress in bead-on-plate inconel 740H specimens. *Int. J. Mech. Sciences*, 9, S. 231–245, 145 (2018)
3. Do, S; Serasli, K.; Smith, D. Combined Measurement and Finite Element Analysis to Map Residual Stresses in Welded Components. *American Society of Mechanical Engineers, Pressure Vessels and Piping Division 6 B* (2014)
4. Coules, H.E.; Smith, D.J.; Abburi Venkata, K.; Truman, C.E. A method for reconstruction of residual stress fields from measurements made in an incompatible region. *Int. J. Solids and Structures*, 5(10), 51-63 (2014)

Implementation of the Peak Stress Method for the automated FEA-assisted design of welded structures subjected to variable amplitude multiaxial fatigue loads

Giovanni MENEGHETTI¹, Alberto VISENTIN¹, Alberto CAMPAGNOLO¹

¹ Department of Industrial Engineering, University of Padova, Via Venezia, 1 – 35131 Padova, Italy

giovanni.meneghetti@unipd.it

The Peak Stress Method (PSM) is a FE-oriented method to rapidly estimate the Notch Stress Intensity Factors (NSIFs) K_1 , K_2 and K_3 from the opening, in-plane shear and out-of-plane shear peak stresses calculated at the notch tip by means of a linear-elastic FE analysis adopting relatively coarse FE meshes [1]. The PSM adopts the averaged Strain Energy Density (SED) criterion to perform fatigue lifetime estimations of welded structures, where the weld toe and weld root geometries are idealized and are assumed as sharp V-shaped notches with null tip radius. In this perspective, the PSM allows to re-formulate the averaged SED as a function of the relevant singular peak stresses, which are combined into an equivalent peak stress [1]. The equivalent peak stress can be adopted to estimate the fatigue lifetime of welded structures, in conjunction with known PSM fatigue design curves [1]. To date, the proposed PSM design scatter bands for steel welded joints and aluminium welded joints have been validated against approximately 1300 and 330 experimental fatigue results, respectively. Moreover, the PSM has been recently extended to variable amplitude (VA) fatigue loadings by combining the equivalent peak stress with Miner’s Linear Damage Rule (LDR) and it has been successfully validated against 320 VA fatigue data taken from the literature [2]. In order to support the FE analyst in automating the fatigue design of complex welded structures, an interactive analysis tool has been developed in Ansys[®] Mechanical [3]. A single linear elastic FE analysis is first required, wherein each unit load must be applied to the model using separate load steps, and then the time-history of each applied load must be imported. The developed PSM analysis tool accomplishes the following tasks in a fully automated way (Fig. 1).

- a. Analyzes the CAD geometry of the model to identify all sharp V-notches of the structure.
- b. Generates a FE mesh by adopting 10-node tetrahedral elements and a proper element size in compliance with PSM requirements.
- c. Calculates the PSM-related coefficients [1] as a function of the notch opening angle 2α and material elastic properties, by using specifically developed polynomial expressions.
- d. After solving the FE analysis, calculates the relevant peak stress time-histories tied to mode I, mode II and mode III relevant to each applied VA load. Sum the peak stress time-histories relevant to each analysed node to define mode I, mode II and mode III peak stress time-histories.
- e. Applies the Rainflow cycle counting to obtain peak stress spectra tied to mode I, II, III.
- f. Applies Palmgren-Miner LDR equivalency [2], in order to obtain constant amplitude equivalent peak stress ranges $\Delta\sigma_{eq,peak,i}$ ($i = I, II, III$) [2].
- g. Combines the calculated constant amplitude equivalent peak stress ranges into the damage equivalent peak stress range accounting for multiaxial VA local stresses, according to [2].
- h. Calculates the local biaxiality ratio λ , according to [1].

- i. Depending on the material and the local biaxiality ratio λ , performs fatigue life estimation addressing the proper PSM-based fatigue design curve [1].

The analysis tool allows to visualize the results in terms of nodal equivalent peak stresses or expected fatigue life at the V-notch lines (i.e. the weld toes and weld roots) of the 3D FE model by means of contour plots over a wireframe view of the examined model (Fig. 1).

In this work, a case study coming from an industrial application is presented, where the PSM tool has been employed to analyze a complex welded joint subjected to variable amplitude multiaxial loads.

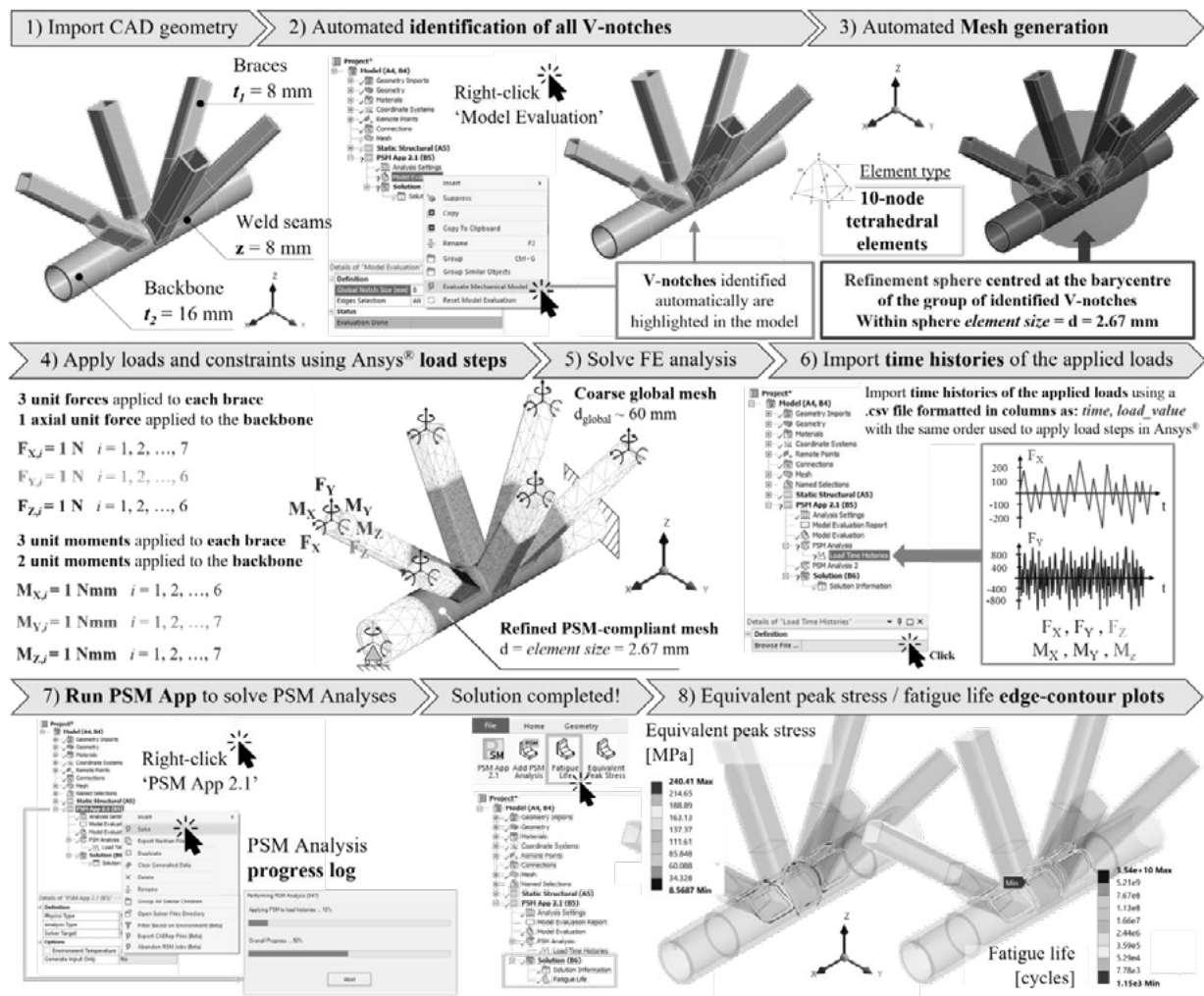


Figure 1. The automated PSM tool implemented in Ansys® Mechanical. General overview of the automated analysis workflow for analysing welded structures subjected to VA loadings.

REFERENCES

1. Meneghetti, G.; Campagnolo, A. State-of-the-art review of peak stress method for fatigue strength assessment of welded joints. *Int. J. Fatigue*, 139, 105705 (2020).
2. Campagnolo, A.; Vecchiato, L.; Meneghetti, G. Multiaxial variable amplitude fatigue strength assessment of steel welded joints using the Peak Stress Method. *Int. J. Fatigue*, 163, 107089 (2022).
3. Visentin, A.; Campagnolo, A.; Babini, V.; Meneghetti, G. Automated implementation of the Peak Stress Method for the fatigue assessment of complex welded structures. *Forces in Mechanics*, 100072 (2022).

A unified non local approach to interpret defect size and shape effects on fatigue strength

Pierre MEROT¹, Franck MOREL¹, Camille ROBERT¹, Etienne PESSARD¹, Linamaria GALLEGOS MAYORGA¹, Paul BUTTIN²

¹ Arts et Métiers Institute of Technology, LAMPA, HESAM Université, Angers, France

² CEA, CEA Pays de la Loire, Bouguenais, France

franck.morel@ensam.eu

High Cycle Fatigue (HCF) behaviour of metallic material with defects (cast alloys, Additively Manufactured (AM) alloys, ...) is still a critical issue for industrial applications. Such defects are in many cases identified as the root cause of crack initiation leading to failure and can significantly decrease the fatigue strength. The origin of defects is nevertheless diverse and often unique to each industrial application. They may be induced by the manufacturing process (Lack of Fusion (LoF) pores, gas pores, microshrinkage pores,...) or by external environmental factors (scratches, corrosion pits, ...). Different types of defects usually lead to distinct defect populations in terms of spatial distribution, shape and size.

The scientific literature contains a lot of studies using Linear Elastic Fracture Mechanics (LEFM) to interpret fatigue limit and considering defect as pre-existing cracks whose size is not large enough to exceed the stress intensity factor threshold [1]. Other works, based on a continuum mechanics approach, make use of the Finite Element Method (FEM) to get a proper description of the mechanical fields around defects [2-3]. In order to infer fatigue strength based on the FEM resolution, multiaxial Fatigue Indicators Parameters (FIPs) are computed.

The objective of this work is to present a comprehensive FE simulation study of the effect of defect shape and size on the fatigue strength using a multiaxial fatigue criterion [4] and a non-local approach [5]. A large range of defect shape and size is investigated under fully alternate uniaxial and pure shear loading modes. As this paper aims at tackling the defect effect from a general point of view (i.e. relevant for many alloys and processes), simplified geometries are used. The influence of the characteristic length introduced in the non local approach is largely discussed together with the effect of the loading mode.

A relative defect size based on a ratio between the defect size and a characteristic length introduced by the non-local approach is defined. A normalized Kitagawa-Takahashi diagram is then obtained (figure 1). A competition between the highly stressed volume size and the local maxima due to the defect is observed and seem dependent on the relative defect size. The effects of the loading mode (uniaxial and pure shear) and of the plasticity are discussed. It is found that, under uniaxial loading, a defect seems more critical than under pure shear (figure 1). The role of plasticity is more significant for large than for small defects. A normalized Frost type diagram is also built from the simulation results and the tendencies observed are in very good agreement with the experimental results available in the literature. Finally, a comparison of the simulation results with experimental data on a 316L L-PBF [6] demonstrates the robustness of the proposed approach and explains the negligible effect of the defect morphology compared to its size for the smallest defects.

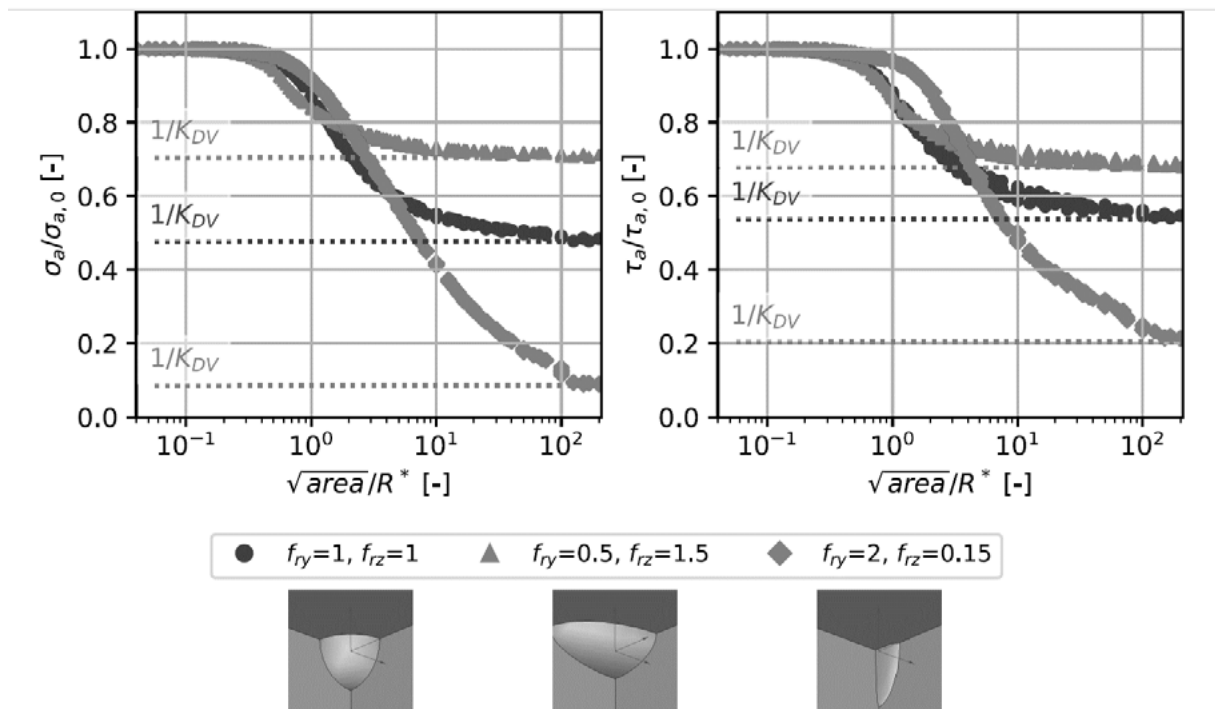


Figure 1. Effect of the defect morphology on the normalized fatigue strength assessment under uniaxial (left curve) and pure shear loading (right curve). The abscissa axes are the normalized size of the defect by the R^* value (sphere radius over which the stress field is averaged around the defect). The color and shape of the points correspond to three extreme cases described in the legend.

REFERENCES

1. Murakami, Y.; Endo, M. Effects of defects, inclusions and inhomogeneities on fatigue strength. *Int. J. Fatigue*, 16(3), 163–182 (1994).
2. McDowell, D.; Dunne, F. Microstructure-sensitive computational modeling of fatigue crack formation. *Int. J. Fatigue*, 32(9), 1521–1542 (2010).
3. Guerchais, R.; Morel, F.; Saintier, N. Effect of defect size and shape on the high-cycle fatigue behavior. *Int. J. Fatigue*, 100, 530–539 (2017).
4. Dang-Van, K. Macro-Micro Approach in High-Cycle Multiaxial Fatigue. In McDowell, DL. and Ellis, JR., editors, *Advances in Multiaxial Fatigue*, pages 120–130. ASTM International, West Conshohocken, PA (1993).
5. Taylor, D. The theory of critical distances. *Eng. Fract. Mech.*, 75(7), 1696–1705 (2008).
6. Mérot, P.; Morel, F.; Gallegos Mayorga, L.; Pessard, E.; Buttin, P.; Baffie, T. Observations on the influence of process and corrosion related defects on the fatigue strength of 316L stainless steel manufactured by Laser Powder Bed Fusion (L-PBF). *Int. J. Fatigue*, 155, 106552 (2021).

Why does the theory of critical distance work?

Antonio Carlos de Oliveira MIRANDA¹, Mengen LIU², Marco Antonio MEGGIOLARO²,
Jaime Tupiassú PINHO DE CASTRO²

¹ Department of Civil and Environmental Engineering, University of Brasília

² Mechanical Engineering Department, Pontifical Catholic University of Rio de Janeiro

acmiranda@unb.br, meng9644@yahoo.com, meggi@puc-rio.br, jtcastro@puc-rio.br

This work demonstrates that the so-called stress gradient factor K_{gr} can explain in a sound mechanical way why the critical distance theory works for estimating fatigue strengths and lives of notched components. K_{gr} s are used to correctly calculate stress intensity factors (SIFs) of cracks that depart from notch tips considering notch stress gradients effects on their behavior. This is done by assuming SIFs can be written in the form $K_I = K_{gr} \cdot \sigma \sqrt{\pi a} \cdot g(a/w)$, where K_{gr} considers stress concentration effects on K_I when the crack a is short, and $g(a/w)$ quantifies effects of the cracked piece geometry when it is long. This way, $K_{gr} \rightarrow K_t$, the stress concentration factor of the notch, when $a \rightarrow 0$, and $K_{gr} \rightarrow 1$ when $a \gg b$, where b is the notch depth. On the other hand $g(a/w) \rightarrow 1.12$, the free surface effect when $a \rightarrow 0$, and tends to grow as a grows, at least when the loads are not applied at the crack faces.

Calculations based on classic Linear Elastic Fracture Mechanics concepts, and on the ETS short crack theory, allow the derivation of fatigue stress concentration factors $K_f \leq K_t$ for notched components, when the notch tip remains elastic. The elastic fatigue SCF K_f is then obtained by:

$$K_f = K_{gr} (a_{max}/w) \cdot \left[1 + (a_R/a_{max})^{\gamma/2} \right]^{1/\gamma} / \sqrt{a_R/a_{max}} \quad (1)$$

where where $a_R = (1/\pi) \cdot (\Delta K_{thR} / \eta \Delta S_{LR})^2$ is the characteristic short crack size, w is characteristic width of geometry, a_{max} is the maximum size that a non-propagating short crack can reach under these loading and resistance conditions, and γ is Bažant's parameter [1].

Rewritten K_{gr} using the weight function method [2]:

$$K_{gr}(a/w) = \frac{\int_0^a \sigma_y(x) \cdot m(x, a) \cdot dx}{\int_0^a \sigma_n \cdot m(x, a) \cdot dx} \quad (2)$$

it is possible to write a K_{gr} considering only the stress components and make $m(x,a) = 1$, similar to definition of TCD line method.

$$K_{gr}(a/w) = \frac{\int_0^a \sigma_y(x) \cdot dx}{\int_0^a \sigma_n \cdot dx} \quad (3)$$

Moreover, the proposed K_f equation allows as well the derivation of the point and line method equations in the critical distance theory within 5% to 10%. For example, Figure 1 shows the comparison between the equations (2) and (3) for tension strip geometry $K_t = 3.26$. Figure 2 shows the difference of equation (3) in relation to equation (2).

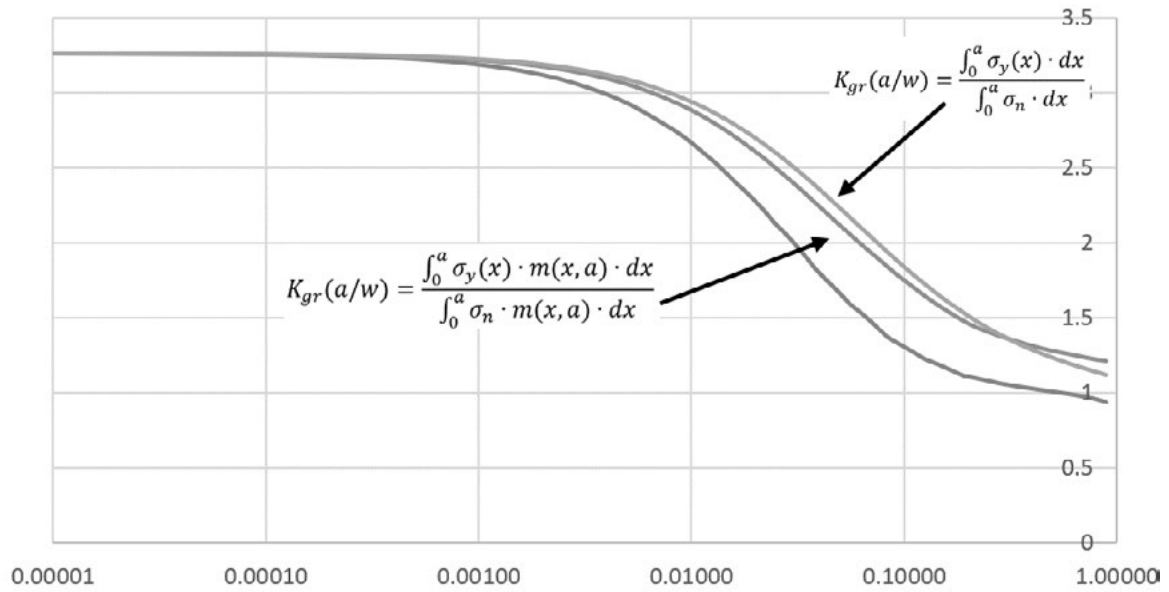


Figure 1. comparison between the equations (2) and (3) for tension strip geometry $K_t = 3.26$.

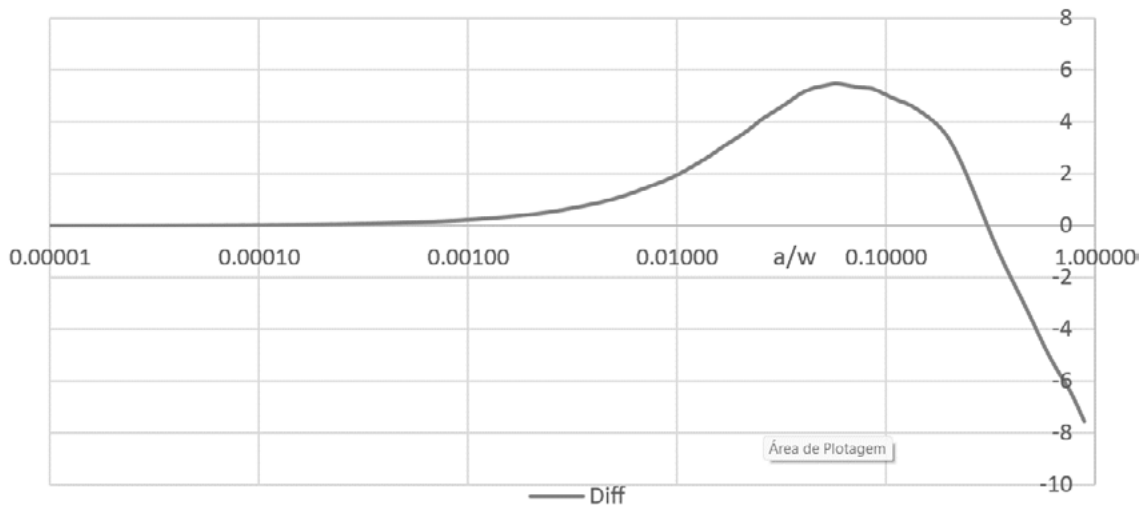


Figure 2. Diference of equation (3) in relation to equation (2) for tension strip geometry $K_t = 3.26$.

Additionally, this work studies plasticity effects around notch tips on the fatigue strength of notched components, and verifies experimentally the estimations proposed here through the tolerance to fatigue growth of short crack that depart from LE and EP notch tips.

REFERENCES

1. Bažant, Z. P. Scaling of quasibrittle fracture: asymptotic analysis. *Int. J. Fract.*, 83, (1997)
2. Glinka, G.; Shen, G. Universal features of weight functions for cracks in mode I. *Eng. Fract. Mech.*, 40, 1135–1146 (1991)

Fatigue life prediction of holed laminated composites based on Finite Fracture Mechanics

Amir Mohammad MIRZAEI¹, Pietro CORNETTI¹, Alberto SAPORA¹

Department of Structural, Geotechnical and Building Engineering, Politecnico di Torino, Italy

alberto.sapora@polito.it

Finite Fracture Mechanics (FFM) is a failure criterion that assumes a discrete crack extension of amount L by coupling stress and energy conditions. The distance L is not just a material property, but depends on the geometry as well. In the static framework, the FFM approach writes as follows:

$$\begin{cases} \frac{1}{L} \int_0^L \sigma dx = \sigma_u \\ \frac{1}{L} \int_0^L K_I^2 da = K_{Ic}^2 \end{cases} \quad (1)$$

The first equation consists of a stress criterion, which states that failure occurs when the (average) stress ahead of the notch tip over L achieves the critical value of the strength, namely the ultimate tensile stress σ_u . The second condition represents the discrete energy balance: failure happens when the available energy for a finite crack extension L reaches the a critical threshold. In Eq. 1, the latter condition is rewritten in terms of the stress intensity factor (SIF) and fracture toughness K_{Ic} by means of Irwin’s relationship.

The FFM was generalized to the fatigue limit regime as follows:

$$\begin{cases} \frac{1}{L} \int_0^L \Delta \sigma dx = \Delta \sigma_0 \\ \frac{1}{L} \int_0^L \Delta K_I^2 da = \Delta K_{Ith}^2 \end{cases} \quad (2)$$

where $\Delta \sigma_0$ represents the fatigue limit or the high-cycle fatigue strength of the material, and ΔK_{Ith} is the threshold value of the SIF range.

Since finite fatigue life lies in between static and fatigue limits, the basic idea behind the FFM extension to fatigue life estimation consists in varying the critical stress and SIF amplitude on the number of cycles to failure [1]. For this purpose, Basquin equation can be used to describe their dependency on the number of cycles, using both plain and cracked (or notched) geometries, respectively:

$$\sigma_c = \sigma_c(N) = a_s N^{-b_s} \quad (3)$$

$$K_{I_f} = K_{I_f}(N) = a_k N^{-b_k} \quad (4)$$

All in all, to estimate the lifetime of notched structures, FFM can be recast as follows:

$$\begin{cases} \frac{1}{l} \int_0^l \sigma_y(x) dx = \sigma_c(N) \\ \frac{1}{l} \int_0^l K_I^2(a) da = K_{ff}^2(N) \end{cases} \quad (5)$$

The set of experiments we use to validate the model is related to notched laminated composites with two different lay-ups, $[0/90]_{2s}$ and $[90/0]_{2s}$, as presented in [2]. The specimens were made of carbon fiber (T300-12K, 200 g/m²) and a low viscosity epoxy resin (Araldite LY 5052) cured with Aradur 5052 Hardener in a weight fraction of 100:38, employing the vacuum-assisted resin injection method. Except the plain sample, the specimens were weakened by a crack with total length of $a = 15.4$ mm, and two holes with two different radii of $\rho = 2.1, 3.25$ mm. The tests were performed under tension-tension loading ($R=0.1$). We used the plain and cracked sample data to get the functions in Eqs. (3) and (4), using the holed sample data as blind predictions. Fig. 1(a) presents a depiction of a holed sample, and Fig. 1(b) illustrates the predictions by FFM for $[90/0]_{2s}$.

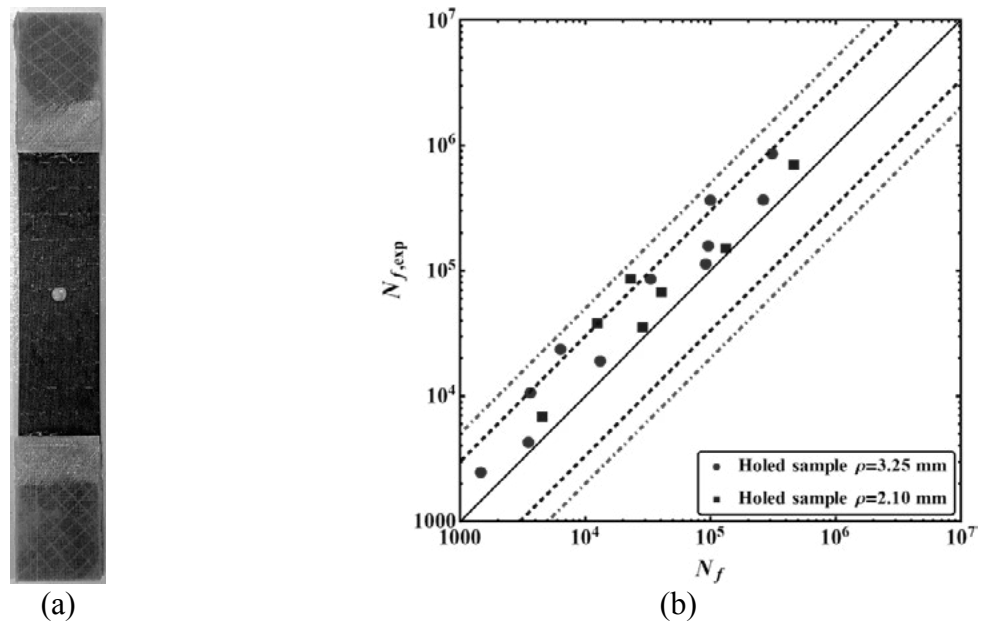


Figure 1. (a) Holed specimen (b) Estimated fatigue lives for $[90/0]_{2s}$ vs experimental results [2].

Considering Fig. 1(b), it can be stated that the FFM model provides accurate (and conservative) predictions regarding the fatigue life across different notch geometries, given the complexity of the problem, with all results falling within the scatter band of 1/5 to 5.

REFERENCES

1. Mirzaei, A.M.; Cornetti, P.; Sapora, A. A novel Finite Fracture Mechanics approach to assess the lifetime of notched components. *Int J Fatigue*, 107659 (2023).
2. Mirzaei, A.M.; Mirzaei, A.H.; Shokrieh, M.M.; Sapora, A.; Cornetti, P. Fatigue life assessment of notched laminated composites: Experiments and modelling by Finite Fracture Mechanics. *Compos Sci Technol*, 246:110376 (2024).

Predicting the fatigue crack growth rate using the plastic strain damage at the crack tip

Diogo Mariano NETO¹, Edmundo Rafael SÉRGIO¹, Fernando Ventura ANTUNES¹

¹ CEMMPRE, ARISE, Department of Mechanical Engineering, University of Coimbra, Portugal

diogo.neto@dem.uc.pt

Fatigue crack growth (FCG) is usually studied using the stress intensity factor range (ΔK), which is a linear elastic parameter from the fracture mechanics. However, the application of this approach based on ΔK has limitations, such as: (i) constant amplitude loading assumption; (ii) geometric effects; (iii) propagation direction effects. Since FCG is linked to irreversible mechanisms happening at the crack tip, non-linear parameters must be used to study FCG. Therefore, the cumulative plastic strain at the crack tip has been used to predict FCG, which is evaluated by numerical simulation. The accurate prediction of the stress and strain distribution around the crack tip requires the use of elastic-plastic models in the finite element method.

Understanding and accurately predicting FCG rates are essential for ensuring the reliability and safety of engineering components subjected to cyclic loading. The objective of the present study is predicting FCG rates using the plastic strain damage accumulated at the crack tip during cyclic loading. Therefore, the numerical approach assumes that cyclic plastic deformation is the main damage mechanism responsible for FCG. This model includes the effects of plasticity induced crack closure, residual stresses, partial closure, crack tip blunting and material hardening. The node release technique is used to model the crack propagation. The crack tip node is released when the cumulative strain reaches a critical value, which is calibrated using a single experimental value of da/dN . This model, based on crack tip cumulative plastic strain, was able to predict qualitatively the effects of ΔK , stress ratio, stress state, overloads, and overload ratio. Besides, the direct comparisons made with experimental results validated the assumption that cyclic plastic deformation is the main crack driving force. Borges et al. [1] successfully predicted the effect of ΔK observed experimentally in AA2024-T251 and 18Ni300 steel, while Neto et al. [2] predicted the effect of stress ratio, and Neto et al. [3] predicted the effect of Superblock2020 load pattern.

Figure 1 (a) presents the effect of a single overload of $OLR = 1.5$ on the predicted FCG rate, comparing different values of baseline-level loading. The model assumes plane stress conditions in the simulation of CT specimens of Ti-6Al-4V alloy. The overload was applied only after stabilization of cyclic plastic deformation and formation of residual plastic wake. The increase of the baseline cyclic stress intensity factor (ΔK_{BL}) leads to an increase of the initial acceleration of the FCG rate occurring immediately after an overload. Besides, the magnitude and extent of retardation increases when the baseline-level loading increases. Figure 1 (b) compares FCG rates obtained with and without contact of crack flanks for $\Delta K_{BL}=18 \text{ MPa}\cdot\text{m}^{0.5}$. Without contact, there is no significant effect of overload on FCG, presenting only a small peak of da/dN when the overload is applied. On the other and, the inclusion of crack closure produces a dramatic effect on FCG rate, and the typical variation of da/dN associated with an overload is now seen.

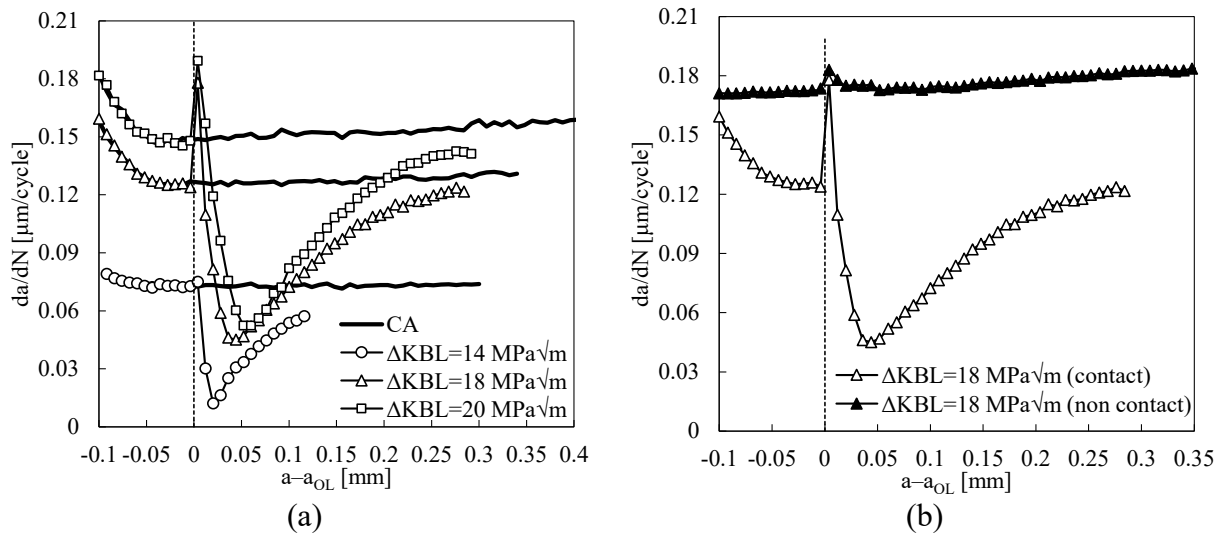


Figure 1. Predicted FCG rate for a single overload (OLR=1.5) considering plane stress conditions in CT specimens of Ti-6Al-4V alloy: (a) effect of baseline-level loading; (b) effect of neglecting the contact between crack flanks.

Considering constant amplitude loading conditions, the numerical predictions are in good agreement with the experimental measurements, which indicates that cyclic plastic deformation is the main damage mechanism. In case of single overloads, the numerical results show that crack closure is responsible for the effect of overloads on FCG rate behaviour. Identical behaviour is observed in the low-high and high-low load blocks [4]. The transient behaviour observed between loading blocks of different amplitude is strongly reduced or vanishes when the contact of crack flanks is neglected in the numerical models. Therefore, the crack closure is able to explain the retardation in both single overloads and load block patterns.

REFERENCES

1. Borges, M.F.; Neto, D.M.; Antunes, F.V. Numerical simulation of fatigue crack growth based on accumulated plastic strain. *Theor. Appl. Fract. Mech.* 108, 102676 (2020).
2. Neto, D.M.; Borges, M.F.; Antunes, F.V. Mechanisms of fatigue crack growth in single overloads, *Theor. Appl. Fract. Mech.* 114, 103024 (2021).
3. Neto, D.M.; Borges, M.F.; Antunes, F.V.; Sunder, R. Numerical analysis of SuperBlock2020 loading sequence. *Eng. Fract. Mech.* 260, 108178 (2022).
4. Neto, D.M.; Sérgio, E.R.; Borges, M.F.; Borrego L.P.; Antunes F.V. Effect of load blocks on fatigue crack growth, *Int J Fatigue*, 162, 107001 (2022).

Fatigue Crack Propagation under Non-proportional Multiaxial Loading

David NOWELL¹ and Bemin SHEEN¹

¹ Department of Mechanical Engineering, Imperial College London.

d.nowell@imperial.ac.uk

Many engineering components are subject to a number of different loads which may not always vary in proportion. Since fatigue cracks generally initiate on the surface of a component, the principal case of interest is that of non-proportional biaxial loading. Prediction of component life under these circumstances can be challenging. Both crack nucleation and propagation phases will be affected by the biaxial and non-proportional nature of the loading. A more basic question is to predict the crack propagation direction. Under proportional loading, several different criteria have been proposed, but the most popular are Maximum Tensile Stress (MTS) [1] and Maximum Strain Energy Release Rate (MSE) [2]. However these criteria were originally proposed for quasi static fracture and may not necessarily be effective under non-proportional fatigue loading.

A particular case of interest is one which arises in gas turbine engines. Here, pressures to reduce weight have resulted in the replacement of traditional bladed disks with a single integral component, or blisk, where the blades and disks are combined. The lack of an interface between blade and disk saves weight, but it removes frictional damping, so that vibration amplitudes may be larger. Further, there is no longer a barrier to fatigue crack propagation from the blade to the disk. The blades can suffer foreign object damage which results in a high stress concentration and a fatigue crack may nucleate. A key question is then to predict crack trajectory, since release of a single blade can be tolerated in a multi-engine aircraft. In contrast a crack which leads to bursting of the disk will produce an uncontained failure which can hazard the aircraft. Figure 1a shows an example of a blisk and Figure 1b illustrates the potential crack trajectories.

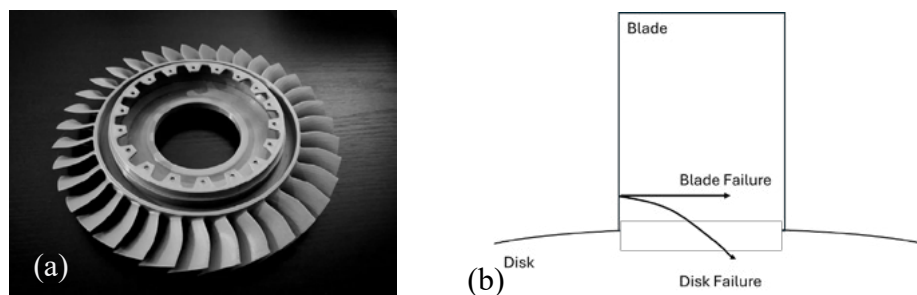


Figure 1. (a) Typical geometry of a blisk; (b) Possible fatigue crack trajectories

The example described above has two main sources of loading: (i) centrifugal body force as the disk rotates. This causes tension in the blade, but also a hoop stress in the blade; (ii) bending of the blade under both pressure loading and vibration. This leads to tension and compression on opposite sides of the blade. The centrifugal loading will vary with the square of engine speed, whereas the pressure and vibration loading will not. Hence, the overall load experienced is both multiaxial and non-proportional.

Fatigue tests on full-size blisks are expensive, so a novel test configuration has been designed, which employs a cruciform specimen loaded in the two perpendicular directions, together with an out of plane load which produces bending. To fully simulate the blisk situation at least three fatigue actuators would be required in mutually perpendicular directions. At Imperial College we have access to a two-actuator machine. Hence, a fixture was designed to apply the third load in a simple, quasi-static manner using a hydraulic cylinder. Tests were run in two configurations: (i) with the hoop load constant and (ii) with the blade centrifugal load constant. In each case the other in-plane load and the bending load were varied. Figure 2a shows an overview of the apparatus and Figure 2b shows the trajectory of a fatigue crack. In this case it has grown largely under the influence of the hoop stress.

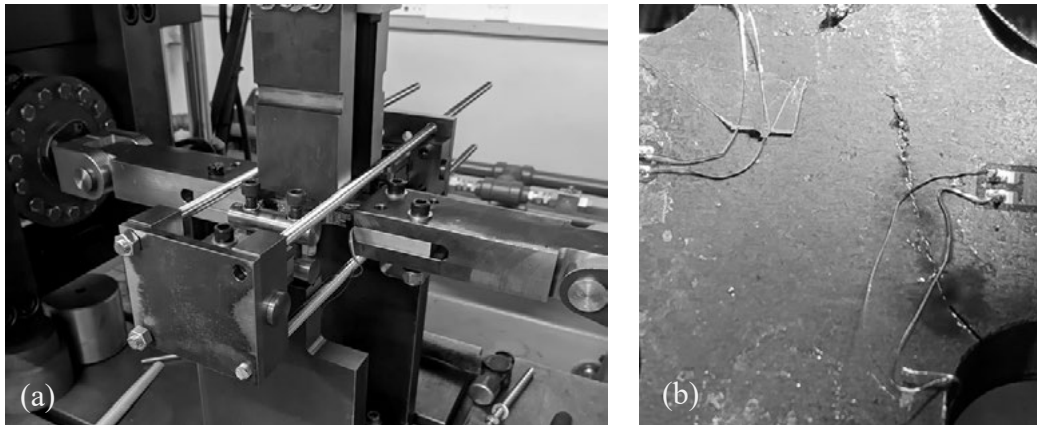


Figure 2. (a) Overview of the apparatus; (b) Experimental fatigue crack trajectory

Modelling was carried out with finite elements using the Franc3D [3] software to re-mesh for crack growth. The predicted trajectories using MTS and MSE criteria were compared to those found experimentally. Under some loading combinations reasonable agreement was found between model and experiment, but other configurations showed some discrepancies. The paper will report some of the experimental and model results and will discuss the improvements required to the criteria for predicting crack growth direction under non-proportional biaxial loading.

REFERENCES

1. Erdogan, F., and Sih, G.C.; On the crack extension in plates under plane loading and transverse shear. *J. Basic Eng*, 85(4): 519-525 (1963).
2. Hussain, M.A., Pu, S.L., and Underwood., J.; Strain Energy Release Rate for a Crack Under Combined Mode I and Mode II. 1973 National Symposium on Fracture Mechanics, Part II, 1973, Washington, United States. pp.1-27.
3. Franc3D software, Fracture Analysis Consultants, Inc., 121 Eastern Heights Drive, Ithaca, New York 14850, USA.

Cyclic R-curve measurements for structural metallic alloys

Luca PATRIARCA¹, Antonio D'ANDREA², Matteo COVA³, Lorenzo RUSNATI¹,
Stefano BERETTA¹

¹ Politecnico di Milano, Department of Mechanical Engineering, via La Masa 1, 20156 Milano, Italy

² École de technologie supérieure, 1100 Notre-Dame St W, Montreal, Quebec H3C 1K3, Canada

³ SacMi, Imola, Italy

luca.patriarca@polimi.it

Fractures nucleated from defects and subjected to cyclic loading can experience propagation for a range of stress intensity factor ΔK well below the so-called long crack threshold. This phenomenon is attributed to the development of crack closure mechanisms which may differ from those observed in laboratory tests conducted in accordance with current standards. Cracks originating from material defects require a specific degree of extension to develop the plastic wake, thus achieving a stabilized condition called the long crack threshold ΔK_{th} . However, in certain materials, this stabilization length can extend up to several millimetres, effectively encompassing a significant portion of the component’s fatigue life. Therefore, understanding and quantifying the development of ΔK_{th} with crack extension is important for implementing a reliable assessment procedure based on the fracture mechanics theory.

The concept of fatigue crack threshold has garnered significant interest over the last years due to the strong effect induced by several factors, including microstructure, load ratio, sources of crack closure, load history, etc. The complexity arising from these diverse factors makes the formulation of a comprehensive crack threshold model challenging. One practical approach to include most of these factors into a tool suitable for industrial applications is the use of the cyclic R-curve [1, 2]. The cyclic R-curve describes the increase of the crack threshold ΔK_{th} with the crack extension Δa , and it was initially observed in the 1980s [3-5]. The R-curve allows to model the behaviour of physically short-cracks that is mainly governed by the build-up of the closure mechanisms.

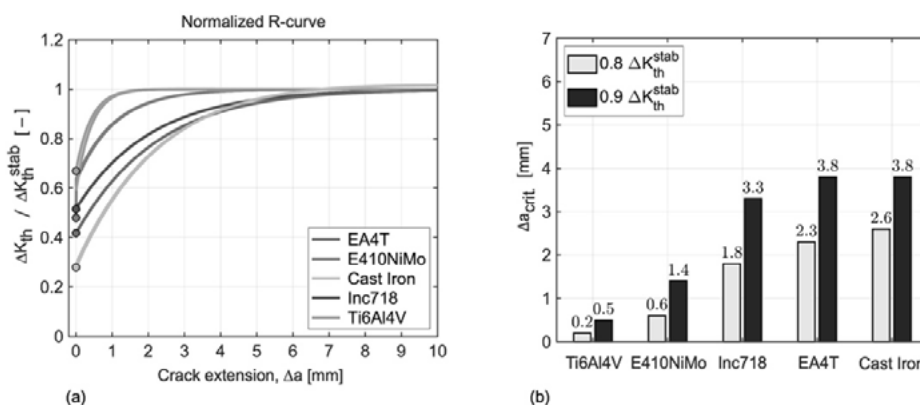


Figure 1. Crack extensions overview of the analysed alloys: a) Normalized R-curves considering the unique fitting approach; b) Detailed values of the stabilization length Δa_{crit} .

In this study, R-curve measurements are presented for five distinct structural metallic alloys widely used in various industrial applications. Figure 1 gives an overview of the normalised R-curves obtained. Despite the load ratio influences the development of ΔK_{th} , the normalised plot enables to compare the general cyclic R-curve behaviour among the presented alloys. As a matter of comparison, we defined two values of critical crack advancements Δa_{crit} that correspond, respectively, to the crack extension required to reach 80% and 90% of the asymptotic $\Delta K_{th}(\Delta a \rightarrow \infty)$. Such comparison shows that the different microstructures and crack closure mechanisms of the selected alloys have a remarkable influence on the initial $\Delta K_{th}(\Delta a=0)$ and the asymptotic $\Delta K_{th}(\Delta a \rightarrow \infty)$ thresholds. Indeed, the stabilisation lengths are also strongly influenced. The results are extremely important when the R-curves are included in a fracture mechanics-based assessment of defected components.

This study underscores the necessity of ruling new experimental techniques to measure and implement the long crack threshold, thereby ensuring the development of a reliable and robust framework for fatigue assessment.

REFERENCES

1. Zerbst, U.; Vormwald, M.; Pippan, R.; Gänser, H. P.; Sarrazin-Baudoux, C.; Madia, M. About the fatigue crack propagation threshold of metals as a design criterion—a review. *Eng. Fract. Mech.*, 153, 190-243 (2016).
2. Zerbst, U.; Madia, M.; Vormwald, M.; Beier, H. T. Fatigue strength and fracture mechanics—A general perspective. *Eng. Fract. Mech.*, 198, 2-23 (2018).
3. Tanaka, K.; Nakai, Y. Propagation and non-propagation of short fatigue cracks at a sharp notch. *Fat. Fract. Eng. Mat. Struct.*, 6(4), 315-327 (1983).
4. Sehitoglu, H. Crack opening and closure in fatigue. *Eng. Fract. Mech.*, 21(2), 329-339 (1985).
5. McEvily, A. J.; Minakawa, K. On crack closure and the notch size effect in fatigue. *Eng. Fract. Mech.*, 28(5-6), 519-527 (1987).

Residual Stress Fields of Pre-Cracks and Impact on Fracture Mechanics Properties

Reinhard PIPPAN¹, Michael PEGRITZ¹, Lukas WALCH², Anton HOHENWARTER³

¹ Erich Schmid Institute of Materials Science, Austrian Academy of Sciences, Jahnstraße 12, 8700 Leoben, Austria

² Materials Center Leoben Forschung GmbH (MCL), Roseggerstraße 12, A-8700, Leoben, Austria

³ Department of Materials Science, Chair of Materials Physics, Montanuniversität Leoben, Jahnstraße 12, 8700 Leoben, Austria

reinhard.pippan@oeaw.ac.at

Fracture mechanics considerations starts usually on plane and sharp cracks with a well-defined crack front, in addition, in plane specimens a straight crack front, free of contact stresses between the crack surfaces and free of residual stresses are assumed. In fracture mechanics testing these ideal starting conditions is hardly to fulfill. The standard procedure to generate a pre-crack was developed for ductile materials, where the pre-crack is generated by fatigue loading in a notched specimen usually at a stress ration of about 0.1 with an initial stress intensity of 3 to 5 times the threshold of stress intensity factor range, depending on the material strength and notch quality. For the determination of the fracture toughness of ductile materials the residual stresses are usually negligible, because the strains necessary for crack propagation are typically an order of magnitude or more, larger than the strains introduced during the pre-cracking. The geometric requirements are more often problematic. For fatigue crack propagation experiments, especially for the crack propagation behavior of the near threshold regime these residual stress and strain fields are very important, hence a well-defined load reduction schema has to be fulfilled in order to obtain reproducible material data. However, whether these data are really useful for a save lifetime determination is still questionable. For materials with a low fracture toughness, this procedure of pre-cracking is often difficult or impossible, because the fracture toughness is smaller than the necessary maximum stress intensity factor to generate a pre-crack. The fracture toughness of many of these brittle materials exhibits a material intrinsic R-curve behavior, i.e. a fracture toughness depends on crack extension. Such R curve behavior usually is not measurable on such standard tension pre-cracked specimens. Even the threshold of stress intensity range and the fatigue crack propagation behavior exhibits an R curve behavior, which is also not measurable standard pre-cracked specimens, due to the introduced strains, stresses and crack closure phenomena introduced by the pre-cracking load.

A technique to overcome this problem is the compression-compression pre-cracking procedure [1]. Such pre-cracks are open in the unloaded state, however even in front of these pre-cracks residual stresses remains.

The goal of these paper is now to discuss:

- What is the difference in the residual stress field of a compression-compression fatigue and a tension-tension fatigue pre-crack?
- Requirement for the determination of a R-curve for fracture toughness and R-curve for the threshold of stress intensity factor range.

- How do residual stresses affect the shape of the R-curve?
- How can we reduce the effect of the residual stresses on the R-curve?

The addressed questions will be discussed for very different materials, ductile low and high strength metals [2], brittle metals (tungsten) and intermetallics (TiAl) [3] and fracture mechanisms and crack tip shielding mechanisms, for both static and fatigue R curves.

REFERENCES

1. Pippan, R. The growth of short cracks under cyclic compression. *Fract. Eng. Mater. Struct.*, 9, 319–28 (1987)
2. Walch, L.; Klünsner, T.; Ressel, R.; Hohenwarter, T.; Marsoner, S.; Pippan, R. Refined cyclic R-curve determination through residual crack tip stress reduction by annealing. (submitted)
3. Lintner, A.; Pippan, R.; Schloffer, M.; Hohenwarter, A. Effect of a single overload on the cyclic R-curve behaviour of a γ -TiAl TNM alloy. *Int. J. Fatigue*, 163, 107083 (2022)

A comprehensive damage-based strategy to predict fatigue damage evolution in composite laminates

Marino QUARESIMIN¹, Paolo Andrea CARRARO¹, Lucio MARAGONI¹,
Michele ZAPPALORTO¹

¹ Department of Management and Engineering, University of Padova (Italy)

marino.quaresimin@unipd.it

Fatigue failure and in-service loss of stiffness of composite parts are due to a multi-mechanisms damage evolution which mainly includes cracks, delamination and fibre failures. This paper presents an innovative, comprehensive framework for the fatigue design of composite parts, based on the actual physics of damage evolution. The initiation and growth of each mechanism are described by suitable analytical models, validated on a large volume of internal and literature experimental data (Figure 1)

The interaction among the mechanisms and their effects on the strength and stiffness of the composite parts are also considered and described by analytical models (Figures 1,2).

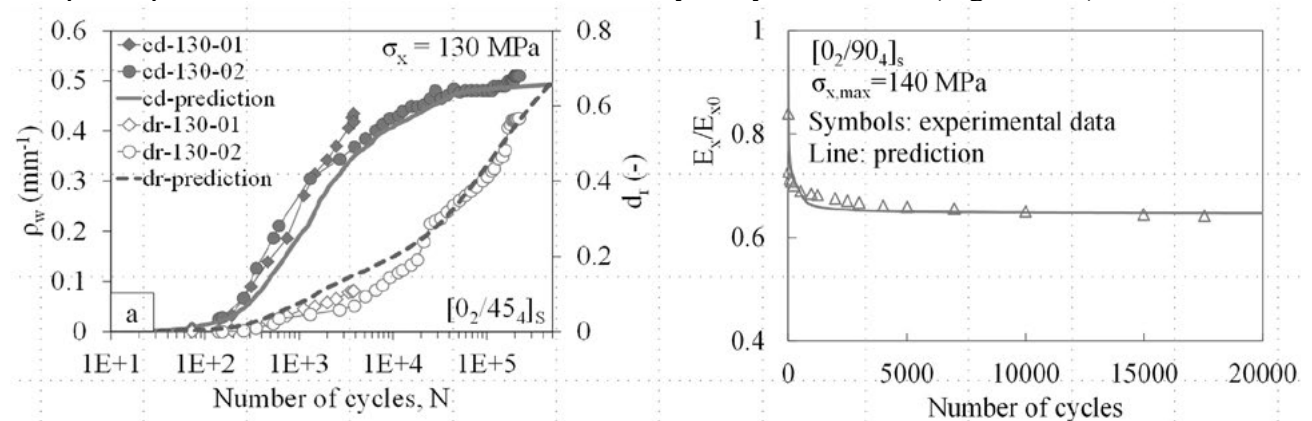


Figure 1: Experimental trends of crack density, delamination ratio and axial stiffness in glass epoxy laminates, compared with the predictions obtained by the analytical models.

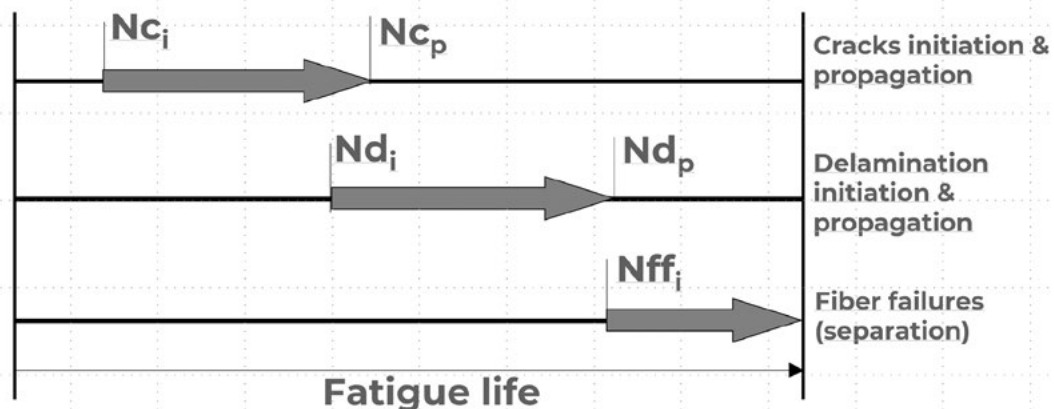


Figure 2: Schematic of the procedure for the description of the global damage evolution in a composite laminate

The combination of all these new models into a single design framework represents a significant step forward with respect to the design tools available in the literature, resulting in an enormous increase in the safeness and reliability of the structural applications made with these materials. The theoretical basis behind the approach will be briefly outlined leaving space to the discussion of the application procedure, with an example of implementation on parts of industrial interest.

REFERENCES

1. Quaresimin, M.; Susmel, L.; Talreja, R. Fatigue behaviour and life assessment of composite laminates under multiaxial loadings. *Int J. Fatigue*, 32, 2–16 (2010)
2. Quaresimin, M.; Carraro, P.A. On the investigation of the biaxial fatigue behaviour of unidirectional composites. *Compos. B Eng*, 54, 200–208 (2013).
3. Quaresimin, M.; Carraro, P.A. Damage initiation and evolution in glass/epoxy tubes subjected to combined tension-torsion fatigue loading. *Int J. Fatigue*, 63, 25–35 (2014).
4. Quaresimin, M.; Carraro, P.A.; Pilgaard, M. L.; Lucato, N.; Vivian, L.; Brøndsted, P.; Sørensen, B. F.; Varna, J.; Talreja, R. Damage evolution under internal and external multiaxial cyclic stress state: a comparative analysis. *Compos. B Eng*, 61, 282-290 (2014).
5. Carraro, P.A.; Quaresimin, M. A damage-based model for crack initiation in unidirectional composites under multiaxial cyclic loading. *Compos Sci Technol*, 99, 154-163 (2014).
6. Quaresimin, M. Multiaxial fatigue testing of composites: from the pioneers to future directions. *Strain*, 1, 16-29 (2015).
7. Quaresimin, M.; Carraro, P.A.; Maragoni, L. Early stage damage in off-axis plies under fatigue loading. *Compos Sci Technol*, 128, 147-154 (2016).
8. Carraro, P. A.; Maragoni, L.; Quaresimin, M. Prediction of crack density evolution in multidirectional laminates under fatigue loading. *Compos Sci Technol*, 145, 24-39 (2017).
9. Carraro, P.A.; Maragoni, L.; Quaresimin, M. Characterisation and analysis of transverse crack-induced delamination in cross-ply composite laminates under fatigue loadings. *Int J. Fatigue*, 129, 105217 (2019).
10. Carraro, P.A.; Maragoni, L.; Quaresimin, M. Stiffness degradation of symmetric laminates with off-axis cracks and delamination: an analytical model. *Int. J. Solids Struct.*, 213, 50–62, (2021).

Notch vs. crack effects on impact toughness of a duplex steel

Aleksandar SEDMAK¹, Srdja PERKOVIC², Zijah BURZIC², Zoran RADAKOVIC¹

¹ University of Belgrade, Faculty of Mechanical Engineering, Serbia

² Military-technical Institute, Belgrade, Serbia

aleksandarsedmak@gmail.com

This paper presents the effect of stress concentration due to notch or cracks on impact toughness of duplex steel S32750. This analysis is based on the results obtained by Charpy instrumented pendulum, enabling separation of total energy into crack initiation, E_i , and crack propagation energy, E_p .

The main goal of this paper was to evaluate the Crack Sensitivity (CS), defined here as the ratio of total impact energy (KV value), obtained by testing standard ISO-V specimen, Fig. 1, and KV1 value, obtained on a same type of specimen but with 1 mm long fatigue cracks: $CS=KV/KV1$.

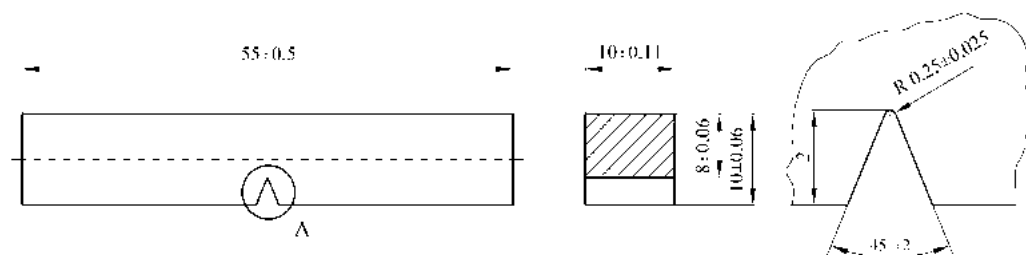


Figure 1. Standard Charpy ISO-V specimen

Notched specimens were tested in order to determine total impact energy, as well as energies for crack initiation and propagation. Testing was conducted in accordance with standard EN ISO 148-1:2017 at different temperatures: 20°C, -40°C, -60°C and -80°C.

Fatigue crack lengths ranged from 1 to 5.5 mm, as measured from the notch root on ISO-V specimen. After failure, fatigue crack length a was measured in 5 locations, and its mean value was used to make a diagram KV- a with an origin at 2 mm (the notch depth). Typical KV- a diagrams for Super Duplex steel S32750 tested at different temperatures are shown in Fig. 2. Based on these diagrams, KV1 values are obtained by interpolation of all results, as shown in Fig. 2. Results for CS are given in Tab. 1, indicating relatively low values at all tested temperatures, which can be explained by the fact that E_p was much higher than E_i , as shown in [1].

Table 1. Crack sensitivity factors for steel S32750

Testing temperature	Notched specimen KV, J	Cracked specimen KV1, J	Crack sensitivity KV/KV1
+20°C	297/245	225	1.32
-40°C	201/156	147	1.37
-60°C	125/99	98	1.28
-80°C	82/65	72	1.14

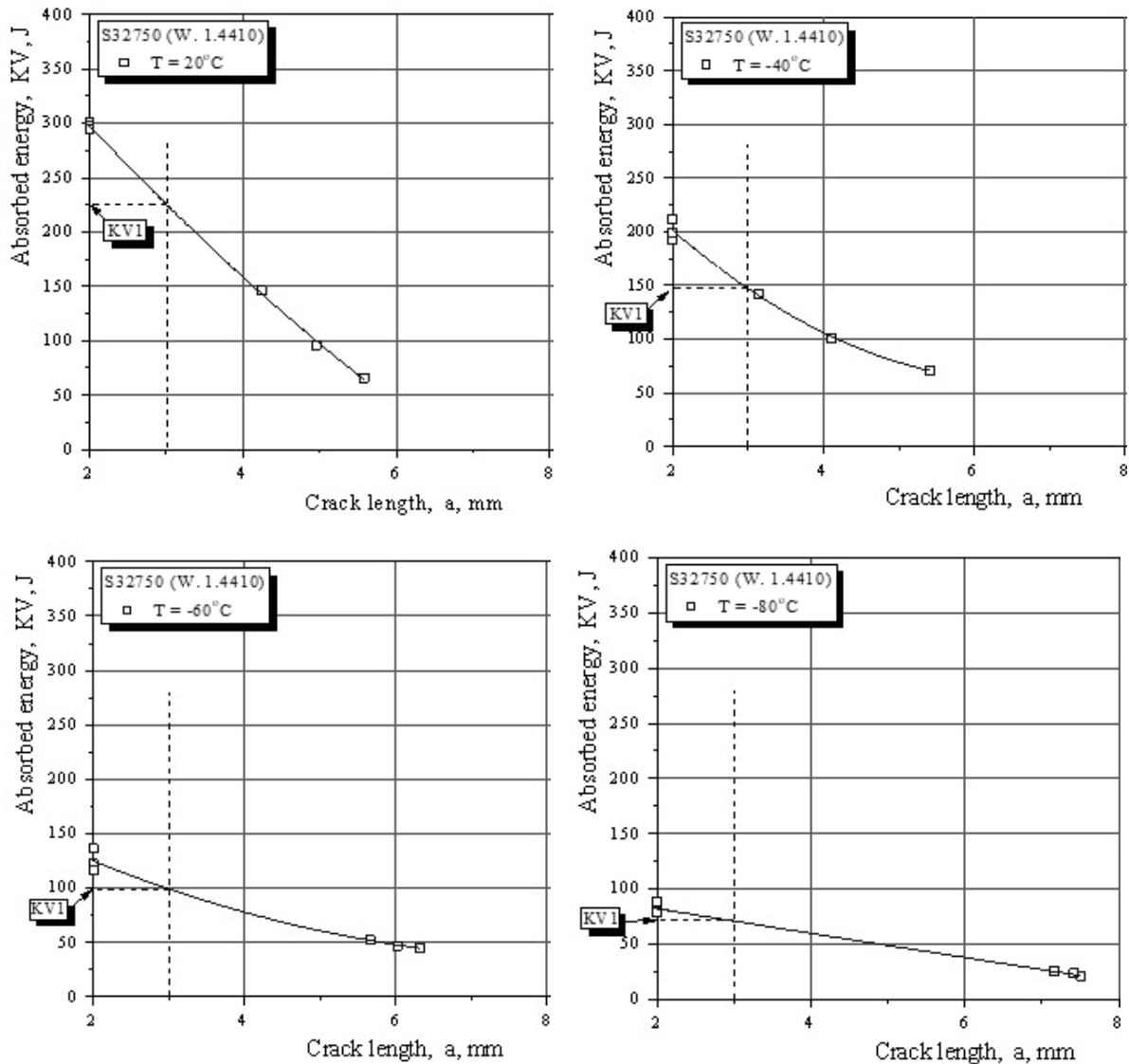


Figure 2. Impact energy, KV, vs. crack length, a , at different testing temperatures

Another interesting aspect of this analysis is to compare E_p , obtained on notched specimens, with the total energy KV1, obtained on cracked specimens. According to the results presented in [1], E_p was 245 J, 156 J, 100 J and 65 J at +20°C, -40°C, -60°C and -80°C, respectively, being in good agreement with corresponding values KV1 (225 J, 147 J, 98 J and 72 J). Therefore, one can conclude that the separation of energies on instrumented pendulum represent sound base for an analysis of notch and crack effects on impact toughness both at room and low temperature. Similar analysis was performed on a welded joint, made of duplex steel S32750, for another two zones, weld metal and heat-affected zone, as shown in [2].

REFERENCES

1. Perković, S.; Radaković, Z.; Burzić, Z.; Sedmak, S.; Sedmak, A.; Radović, Lj. Stress concentration effects on toughness value of duplex steel S32750, *Structural Integrity and Life*, 23(1), 3-7, 2023
2. Perković, S. Analysis of dynamic and impact loads influence on welded steel structures made of super duplex stainless steel (in Serbian), University of Belgrade, FME, 2023.

Dislocation Glide Theories (CRSS) Relevant to Fatigue

Huseyin SEHITOGLU¹

¹University of Illinois at Urbana- Champaign, Urbana, Illinois 61801, USA

huseyin@illinois.edu

Despite many years of research, the fundamental quantities, such as the critical resolved shear stress (CRSS) that affects the dislocation glide in metallic materials, still remain not well understood [1-6]. The theoretical results for critical stress far exceed the experimental results because of fundamental assumptions made in the development of the early theory in neglecting the elastic strain energies, the lattice types, the dislocation character, and so on. Such formulations can not predict the correct stress magnitudes for dislocation emission at crack tips. The variability of the critical stress is also essential because the slip planes exhibit compositional variations, and such variability may arise from spatial variation of short-range order in alloys. Because there are a myriad of arrangements of atoms at lattice scales, artificial neural network methodologies have been developed to capture the variability in CRSS. The determination of critical stress is also relevant to crystal plasticity models, which are widely used in fatigue. In this presentation, I will show examples of the determination of critical stress for a wide range of metallic materials, highlighting tension-compression asymmetry effects and the role of different slip systems observed in titanium.

The work is supported by the National Science Foundation (high entropy alloys) and Department of Energy-BES (titanium).

REFERENCES

1. You, D.; Celebi, O.K.; Mohammed, A. S. K.; Sehitoglu, H. Negative Stacking Fault Energy in FCC materials-Its Implications. *Int. J. Plasticity*, 103770 (2023).
2. Celebi, O. K.; Mohammed, A. S. K.; Sehitoglu, H. Effect of Dislocation Character on the CRSS. *Acta Materialia*, 254, 118982 (2023).
3. You, D.; Celebi, O. K.; Mohammed, A. S. K.; Abueidda, D. W.; Koric, S.; Sehitoglu, H. CRSS determination combining ab initio Framework and Surrogate Neural Networks. *Int. J. Plasticity*, 103524 (2023).
4. Mohammed, A. S. K.; Celebi, O. K.; Sehitoglu, H. Critical stress prediction upon accurate dislocation core description. *Acta Materialia*, 233, 117989 (2022).
5. Celebi, O. K.; Mohammed, A. S. K.; Krogstad, J. A.; Sehitoglu, H. Evolving dislocation cores at Twin Boundaries: theory of CRSS elevation. *Int. J. Plasticity*, 148, 103141 (2022).
6. You, D.; Celebi, O. K.; Gengor, G.; Mohammed, A. S. K.; Sehitoglu, H. Short-range ordering mechanics in FCC materials. *Int. J. Plasticity* (2024).

Fatigue crack growth: Effect of micro-voids damage

Edmundo Rafael SÉRGIO¹, Fernando Ventura ANTUNES¹, Diogo Mariano NETO¹

¹ CEMMPRE, ARISE, Department of Mechanical Engineering, University of Coimbra, Portugal

edmundo.sergio@uc.pt

Fatigue crack growth (FCG) in metallic materials has been studied assuming that cyclic plastic deformation is the main damage mechanism. However, considering that this the only damage mechanism behind FCG, the effect of the mean stress is null in the absence of crack closure. The present study considers an additional damage mechanism, based on the growth, nucleation and coalescence of micro-voids [1]. The introduction of this damage mechanism, in FCG studies, is justified by several works in literature. In fact, Rhodes *et al* [2] stated that for a wide range of crack growth rates, the crack extends both by the formation of ductile striations and by the coalescence of micro-voids. According to Sunder *et al* [3], the initiation, growth and coalescence of microvoids is possible in the presence of cyclic loads. Finally, Li *et al* [4] refer that the growth/coalescence of micro-scale voids become the dominant FCG mechanism at high ΔK zone.

A non-local GTN damage model was used to include the effect of micro-voids on the predicted FCG rate for a AA2024-T351 alloy in a CT50 specimen . A node release strategy was employed to simulate the propagation stage of a fatigue crack. Cyclic plastic deformation shown to be the predominant mechanism, assuming that crack grows due to striation formation. However, the GTN model shown to be relevant because it affects the plastic strain accumulation at the crack tip and the crack-closure phenomenon due to the increase in the volume of the crack flanks, which the increases the crack closure phenomenon.

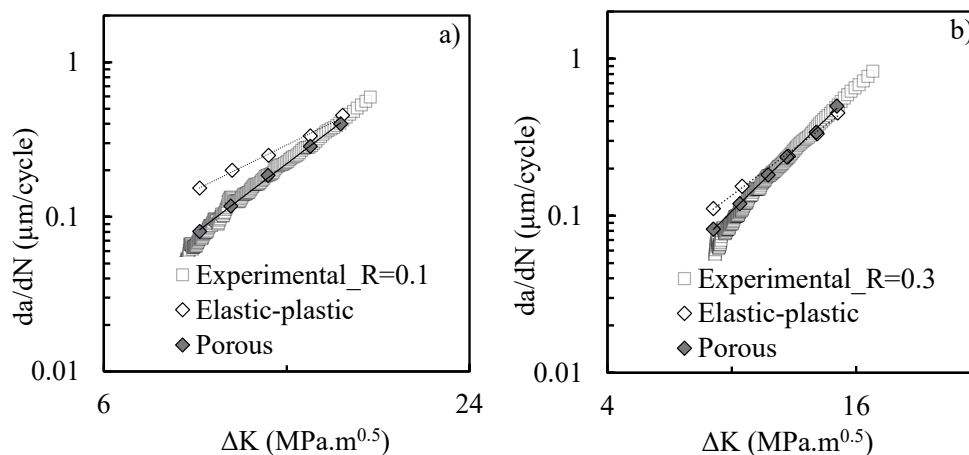


Figure 1. Numerical predictions considering both cyclic plastic deformation and GTN (Porous) compared with results based solely on cyclic plastic deformation (Elastic-Plastic).

The numerical predictions agree with the da/dN - ΔK experimental results, for distinct stress ratios, especially considering the GTN model, as shown in Figure 1 (a) and (b). The numerical da/dN - ΔK curve rotated in the anti-clockwise sense having the correct slope when considering

micro-voids damage. The effect of K_{max} was also observed considering micro-voids damage, even when crack closure was numerically disabled, as shown in Figures 2 (a) and (b). This was expected because K_{max} and stress ratio effects are linked with the mean stress, which is a very relevant parameter in porosity evolution. Accordingly, the GTN allows to capture the effect of this parameter. Nevertheless, the K_{max} dominant zones, widely discussed in the Unified Approach works, are only observed in the presence of crack closure. This indicates that a three-parameter approach (ΔK_{eff} - ΔK - K_{max}) is necessary to fully understand fatigue crack growth, as observed previously by [5]. In fact, it shows that all the mechanisms acting at the crack tip are intrinsically related.

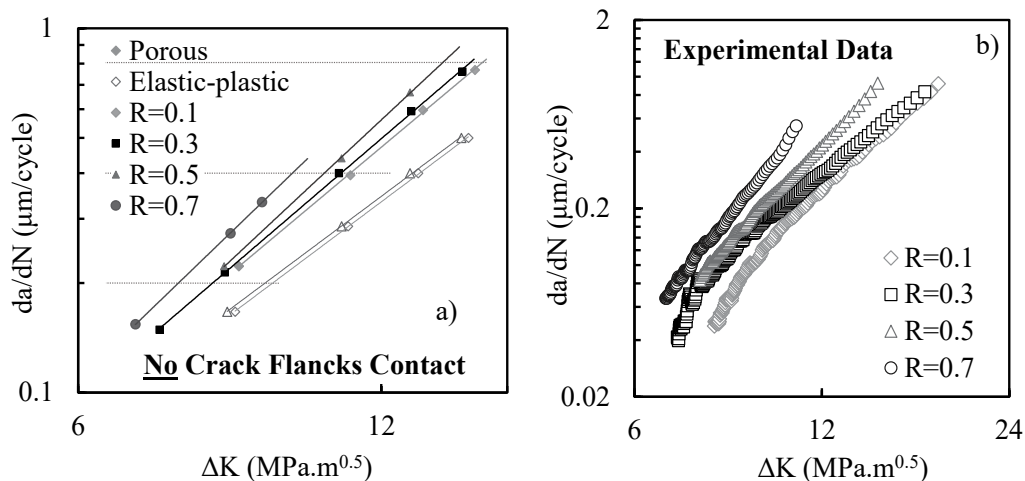


Figure 2. Effect of the stress ratio in the absence of crack closure obtained from: **(a)** numerical results, where without GTN there is no effect of R . **(b)** Experimental data.

In the authors opinion, the only way to solve the fatigue problem is to identify and understand the fundamental mechanisms acting at the crack tip zone. Porous damage shows to be one of the main mechanisms, especially in very ductile materials like the studied aluminium alloy.

REFERENCES

1. Sérgio, E.R.; Antunes, F. V.; Kujawski, D.; Neto, D.M. Fatigue crack growth: Validation of the K_{max} - ΔK approach using the GTN damage model, *Int. J. Fatigue.*, 176 (2023)
2. Rhodes, D.; Nix, K.J.; Radon, J.C. Micromechanisms of fatigue crack growth in aluminium alloys, *Int. J. Fatigue.*, 6, 3–7 (1984)
3. Ramasubbu, S.; Porter, W.; Ashbaugh, N. Fatigue voids and their significance, *Fatigue Fract. Eng. Mater. Struct.*, 25, 1015–1024 (2002)
4. Li, H.F.; Zhang, P.; Zhang, Z.F. A new fatigue crack growth mechanism of high-strength steels, *Mater. Sci. Eng. A.*, 840, 142969 (2022)
5. Riddell, W.; Piascik, R. Stress Ratio Effects on Crack Opening Loads and Crack Growth Rates in Aluminum Alloy 2024, *ASTM Spec. Tech. Publ.*, 407–425 (1999)

On the effect of triple line disclinations in intergranular cracking

Puyu SHI¹, Dirk ENGELBERG², Michael SMITH¹, Andrey JIVKOV¹

¹ School of Engineering, The University of Manchester, Manchester M13 9PL, UK

² School of Natural Sciences, The University of Manchester, Manchester M13 9PL, UK

andrey.jivkov@manchester.ac.uk

The modelling of intergranular cracking requires explicit consideration of materials' microstructure at the polycrystalline level. The now standard approach is to approximate the microstructure by a collection of polyhedrons representing grains (GRs) with polygonal faces representing grain boundaries (GBs), and to represent the mechanical behaviour of GRs by crystal plasticity models, and of GBs with cohesive zone models [1]. Microstructure approximations are typically generated using Voronoi tessellations of spatial domains with prescribed size distribution of polyhedrons and assigning crystallographic orientations to GRs, randomly or subject to prescribed texture [2]. The result is an assembly of simple polyhedrons where each internal polygonal face represents a GB, and each internal edge is the meet of exactly three GBs and three GRs. The edges represent triple lines (TLs) in the material microstructure. The crystallographic orientations assigned to GRs determine their crystal plasticity response [1,3]. The GBs can either have identical cohesive behaviour [1] or be assigned individual cohesive properties depending on the GB character [3].

TLs can be interpreted as disclinations with strengths depending on the crystallographic orientations of the three adjacent grains [4]. Disclinations break the rotational symmetry of a crystalline lattice creating strength-dependent stresses that decay with the logarithm of the distance, rather differently from dislocations, which break the translational symmetry creating stresses that decay with the inverse of the distance [5]. This suggests potentially significant effect of TLs on the deformation and intergranular cracking. Despite the experimental confirmation of TLs disclination character [6] and of their strong effect on local properties [7], they have not found their way into the existing models for intergranular fracture. Applying the rigorous mathematical approach for calculating the strength of TL-disclinations [4] on EBSD images of Cu-alloys, a recent work has shown that 30-40% of TL-disclinations have non-zero strength, i.e., they create local stress fields with different intensities that need to be considered as local residual stresses in determining the mechanical behaviour upon external loading [8].

The aim of this work is to explore the effect of TLs on intergranular cracking. Polycrystalline assemblies, including crystallographic orientations of GRs, are constructed using 3D EBSD images of Ni-based Alloy 600. The GRs are meshed with tetrahedral finite elements. Cohesive elements of zero original thickness are inserted on GBs replacing the triangles that are faces of pairs of tetrahedrons in the corresponding neighbouring GRs. Assembly construction, meshing, and cohesive element insertion are performed by Neper [2] providing the geometry information for subsequent analysis by Abaqus [9]. A well-established crystal plasticity law [10], implemented by a user material subroutine, is used for the tetrahedral elements within GRs considering their crystallographic orientations. The crystal plasticity parameters are calibrated with own experimental stress-strain behaviour of Alloy 600. A traction-separation (T-S) law with linear T-S behaviour prior to damage initiation and linear damage evolution (softening) is used for the cohesive elements with GBs [11].

Three cases for representing the cohesion of the GBs network are considered. The first uses the same T-S law for all GBs as in [1]. The second assigns different T-S laws to different GBs considering their misorientations as in [3], where the misorientations and their effect on the cohesive behaviour are calculated with an in-house procedure. The third uses the assignment of misorientation-dependent T-S laws as in [3], but further degrades the cohesion of grain boundaries adjacent to TL-disclinations depending on their strength, where the strengths and their effect on the cohesive behaviour are also calculated with an in-house procedure as in [8]. Examples intergranular cracks are shown in Fig. 1. The results to be presented will show significant differences in the crack initiation locations and propagation patterns predicted by the three studies cases. Validating the effect of TL-disclinations on the cracking patterns requires tailored experiments to record the evolution of crystallographic orientations with loading at least up to the moment of the emergence of the first crack. The work on acquiring this data is ongoing.



Figure 1. Cracks in an assembly of 700 grains (meshed by 1,000,000 elements) at 20% strain.

REFERENCES

1. Simonovski, I.; Cizelj, L. Cohesive zone modeling of intergranular cracking in polycrystalline aggregates. *Nucl. Eng. Des.*, 283, 139–147 (2015).
2. Quey, R. Neper: Polycrystal Generation and Meshing. Online: <https://neper.info/> (2023).
3. Roy, U.; McDowell, D.L.; Zhou, M. Effect of grain orientations on fracture behavior of polycrystalline metals. *J. Mech. Phys. Solids*, 151, 104384 (2021).
4. Bollmann, W. Triple-line disclinations in polycrystalline material. *Mater. Sci. Eng. A*, 113 (C), 129–138 (1989).
5. Kleman, M; Friedel, J. Disclinations, dislocations, and continuous defects: A reappraisal. *Rev. Modern Phys.*, 80 (1), 61–115 (2008).
6. Bollmann, W.; Guo, H. A study of junctions of grain boundaries by TEM. *Scr. Metall. Mater.*, 24 (4), 709–712 (1990).
7. Randle, V. On the significance of grain junction topology and crystallography in polycrystals. *Scr. Metall. Mater.*, 28 (8), 889–893 (1993).
8. Zhu, S.; Jivkov, A.P.; Borodin, E., Morozova, A.. Triple junction disclinations in severely deformed Cu-0.4%Mg alloys. *Acta Mater.*, 264, 119600 (2024).
9. Dessault Systemes. Abaqus 2022 User’s Guide (2022).
10. Rousseau, T.; Nouguiet-Lehon, C.; Gilles, P.; Hoc, T. Finite element multi-impact simulations using a crystal plasticity law based on dislocation dynamics. *Int. J. Plast.*, 101, 42–57 (2018).
11. Spring, D. W.; Paulino, G. H. A growing library of three-dimensional cohesive elements for use in ABAQUS. *Eng. Fract. Mech.*, 126, 190–216 (2014).

On the puncturing of flawed soft membranes

Andrea SPAGNOLI¹, Matteo MONTANARI¹, Roberto BRIGHENTI², Farzad TATAR¹

¹ Department of Engineering and Architecture, University of Parma, Parco Area delle Scienze 181A - 43124 Parma, Italy

² Department of Civil and Environmental Engineering, University of Florence, Via di S. Marta 3 - 50139 Firenze, Italy

andrea.spagnoli@unipr.it, matteo.montanari@unipr.it, roberto.brighenti@unifi.it, farzad.tatar@unipr.it

The mechanics of soft membranes undergoing indentation action of a rigid object is of interest in different applications, including soft devices, soft robotics, flexible electronics, and biomechanics [1-3]. Of particular interest is the failure condition related to the puncturing of membranes [4-6] and of balloons [7].

The problem of axisymmetric deformations of a compliant membrane indented by a rigid tool has been largely investigated in the literature, considering e.g. different shapes of the tip, the effect of friction, initial stretches, penetration rate [8-11].

In this paper, the seminal work of [12,13] is considered to obtain the quasi-static non-linear solution of a thin circular membrane indented by a sphere-tipped rigid object; the material is described by different hyperelastic incompressible models. The analytical solutions are compared with the results of FE simulations along with those obtained from experiments on elastomeric membranes (Fig. 1). The failure condition of puncturing of the membrane is discussed from the viewpoint of fracture mechanics in terms of energetic considerations and of the complex nearfield features [14]. Finally, particular attention is devoted to the critical conditions of fracture in the presence of initial flaws (cracks, cavities) in the membrane.

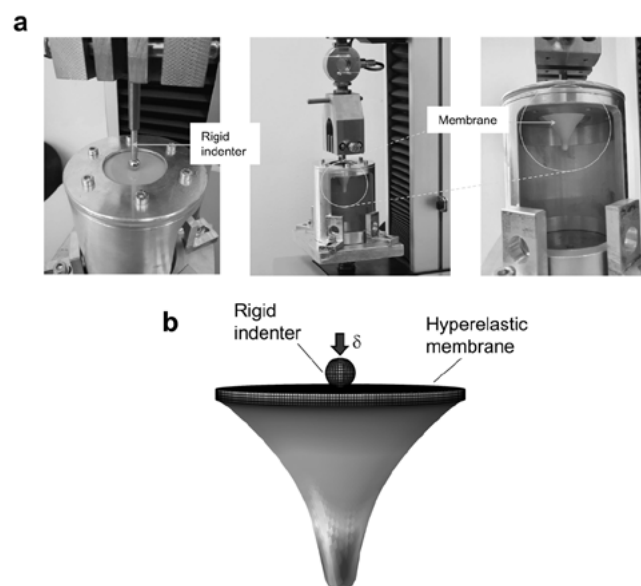


Figure 1. (a) Experimental set-up for indentation tests on circular elastomeric membranes. (b) Principal strain contour of the deformed profile of the membrane; the undeformed configuration and its mesh is also shown.

REFERENCES

1. Lu, T.; Ma, C.; Wang, T. Mechanics of dielectric elastomer structures: A review. *Extreme Mechanics Letters*, 38, 100752 (2020).
2. Polygerinos, P.; Correll, N.; Morin, S. A.; Mosadegh, B.; Onal, C. D.; Petersen, K.;... Shepherd, R. F. Soft robotics: Review of fluid-driven intrinsically soft devices; manufacturing, sensing, control, and applications in human-robot interaction. *Advanced Engineering Materials*, 19(12), 1700016 (2017).
3. Bürzle, W.; Mazza, E.; Moore, J. J. About puncture testing applied for mechanical characterization of fetal membranes. *Journal of biomechanical engineering*, 136(11), 111009 (2014).
4. Steigmann, D. J. Puncturing a thin elastic sheet. *International Journal of Non-Linear Mechanics*, 40(2-3), 255-270 (2005).
5. Nguyen, C. T. ; Vu-Khanh, T. ; Dolez, P. I.; Lara, J. Puncture of elastomer membranes by medical needles. Part I: Mechanisms. *International journal of fracture*, 155, 75-81 (2009).
6. Nguyen, C. T.; Vu-Khanh, T.; Dolez, P. I.; Lara, J. Puncture of elastomer membranes by medical needles. Part II: Mechanics. *International journal of fracture*, 155, 83-91 (2009).
7. Wang, T.; Xu, F.; Huo, Y.; Potier-Ferry, M. Snap-through instabilities of pressurized balloons: Pear-shaped bifurcation and localized bulging. *International Journal of Non-Linear Mechanics*, 98, 137-144 (2018).
8. Selvadurai, A. P. S.; Yu, Q. On the indentation of a polymeric membrane. *Proceedings of the Royal Society A: Mathematical, Physical and Engineering Sciences*, 462(2065), 189-209 (2006).
9. Pearce, S. P.; King, J. R.; Holdsworth, M. J. Axisymmetric indentation of curved elastic membranes by a convex rigid indenter. *International journal of non-linear mechanics*, 46(9), 1128-1138 (2011).
10. Pamplona, D. C.; Weber, H. I.; Sampaio, G. R. Analytical, numerical and experimental analysis of continuous indentation of a flat hyperelastic circular membrane by a rigid cylindrical indenter. *International Journal of Mechanical Sciences*, 87, 18-25 (2014).
11. Liu, J.; Zhong, D.; Yin, T.; Chen, Z.; Liu, B.; Wang, P.; ... Kang, G. Indentation of elastomeric membranes by sphere-tipped indenters: Snap-through instability, shrinkage, and puncture. *Journal of the Mechanics and Physics of Solids*, 167, 104973 (2022).
12. Yang, W. H.; Feng, W. W. On axisymmetrical deformations of nonlinear membranes. *Transactions of the ASME*: 1002-1011 (1970).
13. Yang, W. H.; Hsu, K. H. Indentation of a circular membrane. *Journal of Applied Mechanics ASME* (1971).
14. Montanari, M.; Brighenti, R.; Terzano, M.; Spagnoli, A. Puncturing of soft tissues: experimental and fracture mechanics-based study. *Soft Matter*, 19(20), 3629-3639 (2023).

Analysis of crack tip fields in a phase field model for ductile fracture

Aris TSAKMAKIS¹, Michael VORMWALD¹

¹ Materials Mechanics Group, Technische Universität Darmstadt, Germany

tsakmakis@wm.tu-darmstadt.de, vormwald@wm.tu-darmstadt.de

Phase field theories have been introduced in fracture mechanics, to capture the surface energy of cracks. The basic idea of such theories is to introduce an additional variable and its gradient in the constitutive model. The present work deals specifically with applications related to the failure of ductile materials. The basic model of phase field theories for fracture originates from a generalization of the Griffith theory for brittle materials, where the relevant crack propagation mechanism is based on the debonding of atomic planes. Consequently, plastic deformations do not influence the fracture process and established results from classic elastoplasticity are not described adequately under cyclic loading conditions [1]. In continuum damage mechanics on the other hand, the phase field corresponds to the isotropic damage variable and reflects in a natural way the physical mechanisms of crack initiation and crack propagation for ductile materials.

The aim of the present work is therefore to model the constitutive response of ductile materials within the phase field theory of fracture with contributions from classical continuum damage mechanics, cf. [2]. Accordingly, the evolution equation of the damage variables in the proposed model depends on the rate of the plastic arc length, cf. [3]. Furthermore, influences of triaxiality and Lode angle can be considered in this evolution equation. Special emphasis is also placed on the thermodynamic consistency of the model. Since the non-local influence due to the phase field part of the model cannot be captured within the framework of classical thermodynamic theories, the non-conventional thermodynamics according to Dunn and Serrin [4] is used here. The proposed material model has been developed both for general loads in three dimensions and for two-dimensional plane strain and plane stress states. For the plasticity part, a von Mises flow function with non-linear isotropic and non-linear kinematic hardening with one backstress tensor is assumed.

The numerical integration of the material model is carried out in a so-called staggered algorithm. In the first step of an increment of a finite element calculation, a pure deformation problem with constant damage is solved based on the radial return for plasticity. For the second step, the displacement is kept constant, and a pure damage problem is solved. To be more specific, the evolution equation for the phase field variable is discretised over time using an implicit Euler method and a corresponding weak form of the governing equation is established.

The capabilities of the proposed model are analysed based on numerical and experimental results with respect to cracked and notched specimens. In a first step, experimentally determined strain fields in the vicinity of a crack tip are compared with corresponding numerical predictions of the model. To that end, a thin-walled tube containing a notch under cyclic tension/compression loading is considered. Figure 1(a) shows an emanating fatigue crack after 9000 load cycles with a length of 2.4mm. The strain fields are determined experimentally in terms of the digital image correlation technique (depicted in the coloured contours) and compared to the finite element predictions (grey-scaled isolines). It can be concluded that the model is very well capable to reproduce the strain distribution. Next, a connection between possible crack path trajectories and the distribution of relevant state variables is established for the case of monotonic tension loading

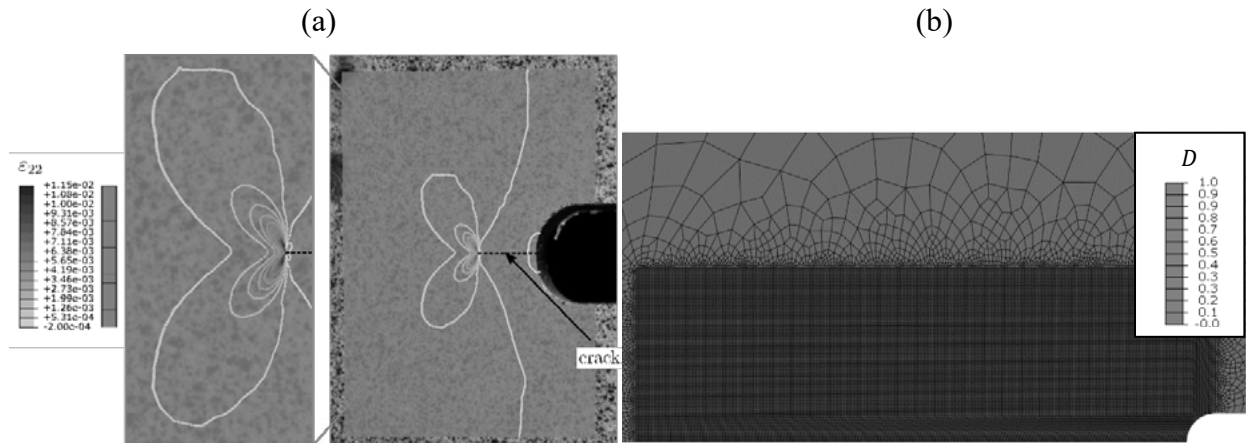


Figure 1. (a) Distribution of the strain component ε_{22} in the vicinity of a crack tip (experimental results in coloured contours and numerical results in grey-scaled isolines). (b) Predicted crack path for a notched specimen under monotonic tension.

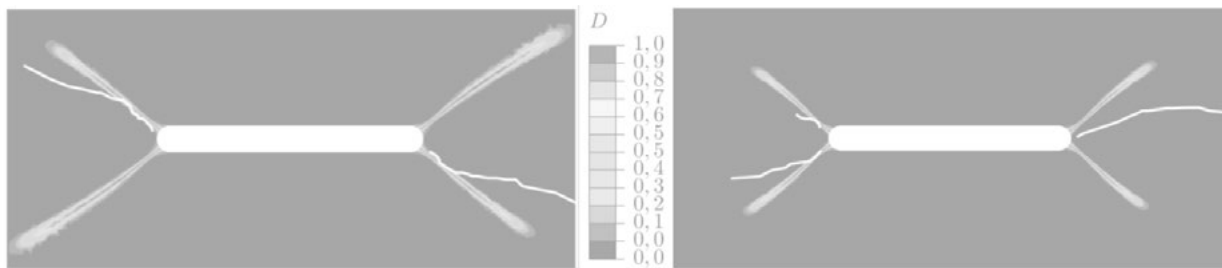


Figure 2. Experimental (white) and predicted crack paths in a notched, thin-walled tube for two different combinations of non-proportional cyclic tensions/compression and torsional loading.

on a notched specimen, see Figure 1(b). The kinking of the crack path is a result of high plastic strains under approximately 45° angle to the symmetry axis. Very similar experimental results are reported in the literature, cf. [6]. Finally, predicted crack paths are compared with experimentally determined crack paths in thin-walled tubes under combined tension/compression and torsional loading. Both proportional and non-proportional cyclic loads are analysed. To reduce the numerical effort for the time being, plane stress conditions and linear kinematic hardening are assumed for the finite element calculations. Figure 2 shows exemplarily the results for two different cases of non-proportional loading conditions. In light of the assumptions mentioned above, the experimentally determined and numerically predicted crack paths coincide very well.

REFERENCES

1. Tsakmakis, A.; Vormwald, M. Thermodynamics and Analysis of Predicted Responses of a Phase Field Model for Ductile Fracture. *Materials*, 14(19):5842, (2021).
2. Tsakmakis A.; Vormwald M. Phase field modelling of ductile fracture in the frameworks of non-conventional thermodynamics and continuum damage, *Int. J. Solids Struct.*, 262-263, (2023).
3. Lemaitre, J.; Chaboche, JL. *Mechanics of solid materials*, Cambridge University Press, (1998).
4. Dunn, JE.; Serrin, J. On the thermomechanics of interstitial working, In *The Breadth and Depth of Continuum Mechanics*, pages 705–743. Springer, (1986).
5. Dixon, J.; Visser, W. An investigation of the elastic–plastic strain distribution around cracks in various sheet materials, *Photoelasticity*, pages 231–250, Elsevier, (1963).

Effect of wake of plasticity on the residual crack closure and determination of crack tip opening loads using compliance-based methods

James VIDLER¹, Andrei KOTOUSOV¹

¹School of Electrical and Mechanical Engineering, The University of Adelaide, SA 5005, Australia

andrei.kotousov@adelaide.edu.au

A wake of plasticity forms during fatigue crack propagation due to the large stress concentration at the crack tip, and its shape is mainly determined by the loading history and plastic behaviour of the material. It has long been recognised that the plasticity induced crack closure phenomenon, which leads to the reduction of the fatigue driving force, is primarily associated with the wake of plasticity [1]. However, analytical and numerical modelling of this phenomenon is very challenging due to the highly complex nature of the underlying physical mechanisms. Therefore, many important effects of the wake of plasticity on fatigue crack behaviour remain unexamined or are simply disregarded. For example, the wake of plasticity makes fatigue cracks to be partially closed in the absence of the applied stress; and the shape of the wake of plasticity (history of loading) can affect the value of the offset compliance threshold, which is often used to determine crack tip opening loads. Accounting for these effects is important, particularly for an accurate evaluation of fatigue cracks using non-destructive techniques or experimental measurements of the crack tip opening loads with compliance-based methods.

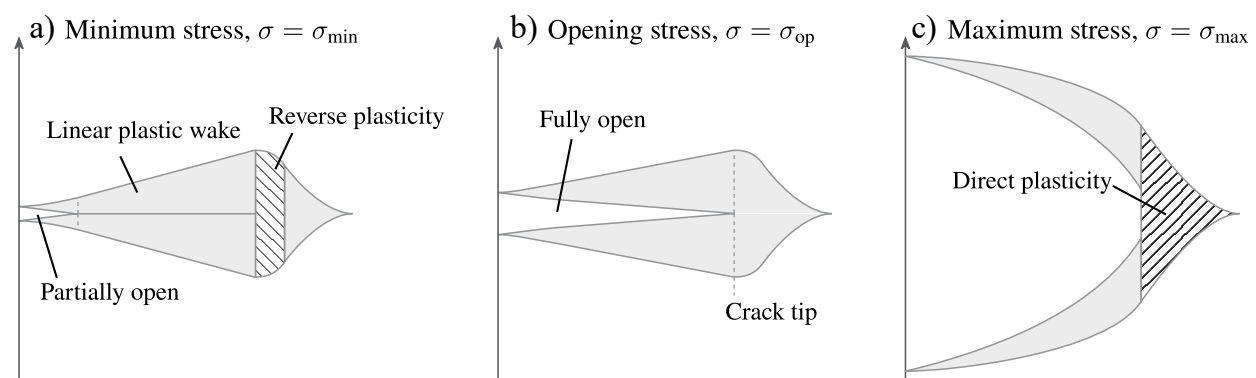


Figure 1. Crack opening process at (a) the minimum stress, (b) the opening stress, (c) the maximum stress. Deformations are exaggerated for clarity.

In this work we utilise the yield-strip (Dugdale) model and distributed dislocation technique to simulate a straight edge fatigue crack propagating in semi-infinite plate under constant amplitude loading conditions. Under these conditions, the crack growth is self-similar, and the wake of plasticity increases linearly with the propagation [2]. Diagrams of the crack opening process during a loading cycle are shown in Figure 1. Using the distributed dislocation technique, the angle of the plastic wake, the sizes of the direct and reverse plasticity zones and the opening stress can be calculated. The present solution is in a general agreement with previous numerical results, which were also based on the yield-strip methodology. The developed analytical model is then

applied to obtain the residual fatigue crack closure length for a broad range of R and σ_{\max}/σ_Y – ratios. It is demonstrated that in the absence of the applied stress up to half of the fatigue crack can be closed, though the presence of residual stress or surface roughness may affect the closure.

Analytical results have also been obtained for the crack tip opening loads. The effect of the wake of plasticity on the compliance offset threshold for an edge fatigue crack was investigated in detail. Current experimental measurements of the crack tip opening loads [3] are based on ASTM standard E647-08 [4], which provides general recommendations for compliance-based measurement of the crack tip opening load. The critical parameter, the compliance offset threshold, is typically set at 1%, 2% or 4% for CT specimens, irrespective of the cyclic loading parameters. The results obtained using the present approach (Table 1) show that R and σ_{\max}/σ_Y have a significant impact on the offset values corresponding to the crack tip opening, which are generally below the values recommended in the standard for fatigue test specimens. It was also observed that small changes in the definition of the fully-open crack compliance can lead to large variations in the threshold, particularly for large values of σ_{\max}/σ_Y .

Table 1. Compliance offset thresholds (%) calculated using the present approach for an edge crack in infinite plate and several different values of R and σ_{\max}/σ_Y . Fully open crack compliance calculated from the unloading curve at the bottom range according to ASTM E647-08 standard.

R	$\sigma_{\max}/\sigma_Y = 0.1$	$\sigma_{\max}/\sigma_Y = 0.3$	$\sigma_{\max}/\sigma_Y = 0.5$	$\sigma_{\max}/\sigma_Y = 0.7$
-0.1	0.0471	0.383	1.131	2.294
0.1	0.0333	0.262	0.807	1.369
0.3	0.0228	0.157	0.479	0.937
0.5	0.0126	0.0899	0.241	0.365

In general, the past research indicates that the yield-strip (Dugdale) model is a useful idealisation, which captures various plasticity phenomena associated with fatigue cracks, however it is still an approximation, first of all because crack opening/closure is a 3D process, and plastic deformations occupy a volume rather than a narrow strip. Therefore, all analytical (as well as numerical) results, which utilise this popular model must be treated with caution and mostly in terms of dependencies rather than absolute values. It is believed that the obtained theoretical dependencies apply to fatigue test specimens with finite geometry. It is also hoped that the current modelling study can help to develop more adequate experimental and numerical procedures for the evaluation of crack tip opening loads and fatigue life in the presence of crack-like defects [5].

REFERENCES

1. Khanna, A.; Kotousov, A. The potential for structural simulation to augment full scale fatigue testing: A review. *Progress in Aerospace Sci.*, 121, 10064 (2020).
2. Vidler, J.; Kotousov, A.; Ng, C.T. Analysis of crack closure and wake of plasticity with the distributed dislocation technique. *Theoretical and Appl. Fract. Mech.*, 127, 104034 (2023).
3. Wallbrink, C.; Hughes, J.M.; Kotousov, A. Experimental investigation of crack opening loads in an aircraft load spectrum. *Int. J. of Fatigue*, 171, 107560 (2023).
4. ASTM E 647-08. Standard Test Method for Measurement of Fatigue Crack Growth Rates. In *Annual Book of ASTM Standards*, vol. 03.01 (2011).
5. Kotousov, A; Hughes, J.; Khanna, A.; Moreno, B.; Wallbrink, C. Experimental Data-Driven approach for the evaluation of crack tip opening loads under variable amplitude loading. *Int. J. of Fatigue*, 180, 108108 (2024).

Analytical stress field solutions for radiused notches in orthotropic solids

Michele Zappalorto¹

¹ University of Padova, Department of Management and Engineering, Stradella San Nicola 3 – 36100 Vicenza (Italy)

michele.zappalorto@unipd.it

Geometrical variations, such as holes and notches, cannot, by nature, be avoided in mechanical components and represent preferable sites for the nucleation of cracks, leading to the overall failure of the part either under static or fatigue loadings.

Different from the isotropic case, where, for a certain loading mode, the notch stress fields strictly depend on the notch geometry only, in the case of anisotropic or orthotropic solids, the stress distribution is strongly influenced by the elastic properties of the material.

Indeed, for an orthotropic material, the differential equation governing the elastic problem is no longer biharmonic; it becomes quasi-biharmonic and gives to the following characteristic equation (under plane stress conditions):

$$S_{11}\mu^4 + (2S_{12} + S_{66})\mu^2 + S_{22} = 0 \quad (1)$$

Whenever $(2S_{12} + S_{66})^2 \geq 4S_{11}S_{22}$ (condition usually verified in conventional composite materials), Eq. (1) presents conjugate roots in the form $\mu_{1,3} = \pm i\beta_1$ and $\mu_{2,4} = \pm i\beta_2$ [1], and parameters β_i significantly affect the stress distribution due to notches.

In the case of pure mode I loadings, the combined effects of notch root radius, notch opening angle and material elastic properties on the stress distributions due to lateral radiused V-notches (see figure 1) can be assessed taking advantage of the following analytical solution [1]:

$$\begin{aligned} \sigma_{rr} &= \frac{\sigma_{tip}}{\tilde{A}} \left\{ \left(\frac{r_0}{r_1} \right)^{1-\lambda} \left[k_{11} \cos(1-\lambda)\theta_1 + k_{12} \sin(1-\lambda)\theta_1 \right] + \chi \left(\frac{r_0}{r_2} \right)^{1-\lambda} \left[k_{21} \cos(1-\lambda)\theta_2 + k_{22} \sin(1-\lambda)\theta_2 \right] \right\} \\ \sigma_{\theta\theta} &= \frac{\sigma_{tip}}{\tilde{A}} \left\{ \left(\frac{r_0}{r_1} \right)^{1-\lambda} \left[m_{11} \cos(1-\lambda)\theta_1 + m_{12} \sin(1-\lambda)\theta_1 \right] + \chi \left(\frac{r_0}{r_2} \right)^{1-\lambda} \left[m_{21} \cos(1-\lambda)\theta_2 + m_{22} \sin(1-\lambda)\theta_2 \right] \right\} \\ \tau_{r\theta} &= \frac{\sigma_{tip}}{\tilde{A}} \left\{ \left(\frac{r_0}{r_1} \right)^{1-\lambda} \left[n_{11} \cos(1-\lambda)\theta_1 + n_{12} \sin(1-\lambda)\theta_1 \right] + \chi \left(\frac{r_0}{r_2} \right)^{1-\lambda} \left[n_{21} \cos(1-\lambda)\theta_2 + n_{22} \sin(1-\lambda)\theta_2 \right] \right\} \end{aligned} \quad (2)$$

For the explicit meaning and values of all the involved parameters, the reader is referred to the original works. However, it is important to mention that in Eq. (2) the effect of the material properties is accounted for thanks to the eigenvalue λ and parameters r_i and θ_i defined as:

$$\xi_j = x' + r_0\beta_j^t \quad \eta_j = \beta_j y' \quad r_j = \sqrt{\xi_j^2 + \eta_j^2} \quad \theta_j = \text{Arg}(\xi_j + i\eta_j) \quad (3)$$

where x' and y' are the distance from the notch tip in the x and y direction, whereas t depends on β_i and λ .

The effect of the material properties on the notch stress distribution is evident from the relevant example shown in Figure 2, where it can be noted that the stiffer the material in the loading

direction, the steeper the stress distribution is.

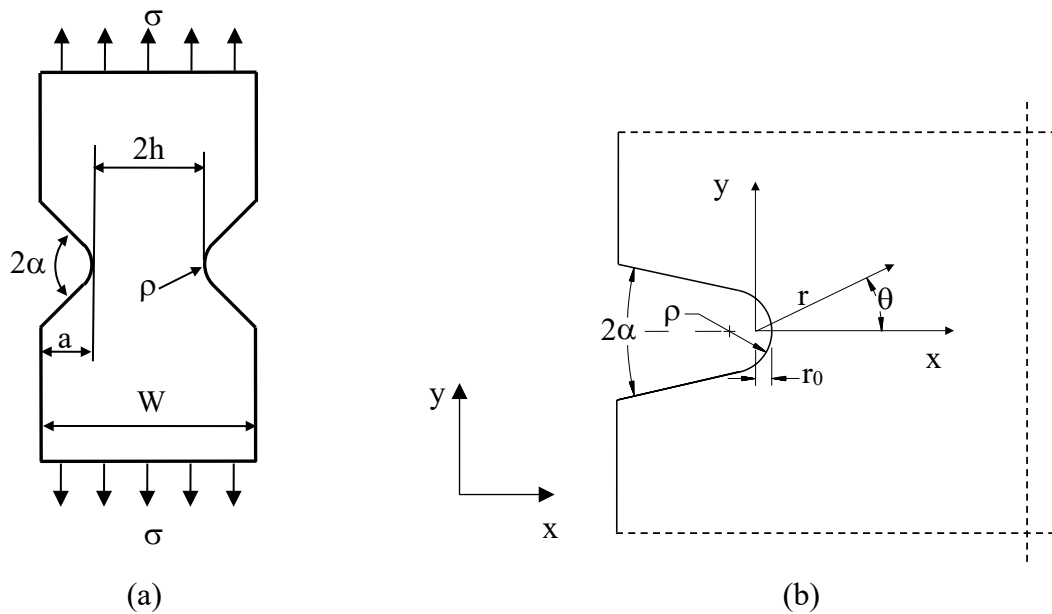


Figure 1. (a) Mode I loaded orthotropic plate weakened by symmetric lateral blunt V-shaped notches. (b) Local geometry of a rounded V-shaped notch and reference system to be used for Eq. (2).

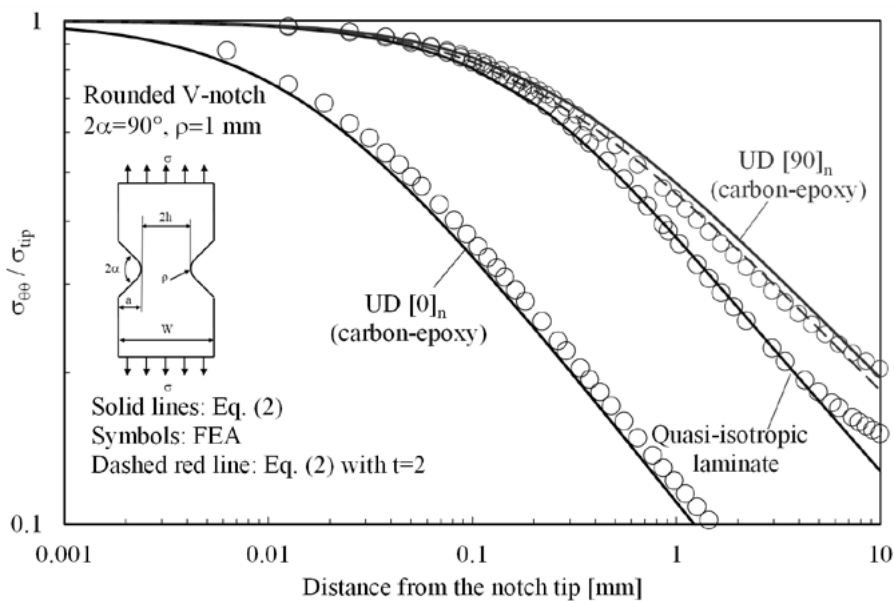


Figure 2. Plot of the normal stress $\sigma_{\theta\theta}$ along the notch bisector line and comparison with Eq. (2). Blunt V-shaped notch with an opening angle $2\alpha=90^\circ$, $a/\rho=10$. Different material systems.

The main aim of the present contribution is to provide a comprehensive discussion on this topic, presenting the relevant results obtained by the authors in the recent ten years.

REFERENCES

1. Zappalorto, M.; Carraro, P.A. Two-Dimensional Stress Distributions in Tensioned Orthotropic Plates Weakened by Blunt V-Shaped Notches. *Fatigue Fract Eng Mater Struct* 40, 804–819, (2017)

Microstructure-based fatigue life prediction of additively manufactured AlSi10Mg specimens

Ningyu ZHANG^{1,2}, Youshi HONG^{1,2}, Guian QIAN^{1,2}

¹ State Key Laboratory of Nonlinear Mechanics (LNM), Institute of Mechanics, Chinese Academy of Sciences, Beijing 100190, China

² School of Engineering Science, University of Chinese Academy of Sciences, Beijing 100049, China

qianguian@imech.ac.cn

About 80~90% of fatigue life is consumed in the crack initiation and small crack growth (SCG) stage in high-cycle fatigue (HCF) and very-high-cycle fatigue (VHCF) [1-2]. It is thus utmost significant to accurately predict the life of both in the safety evaluation of industrial field. A crack initiation life prediction model was proposed based on the modification of the Tanaka and Mura’s [3] model, which included the consideration of defect interaction and location. At the same time, the initial size corresponding to crack initiation is obtained, which is used as the relevant parameter for predicting the SCG life. The fatigue life obtained is the sum of the above two model predictions. The availability of the model was verified by the ultrasonic fatigue test of AlSi10Mg material manufactured by laser powder bed fusion (LPBF). Figure 1 shows the predicted probability distribution and experimental results under three stress ratios of 0.5, 0 and -1. The predicted probability distribution follows lognormal distribution and becomes more dispersed as the load decreases. The competition of crack initiation between surface and interior and the rough area (RA) near the location of internal crack initiation observed on the fracture surface can be well explained by the model.

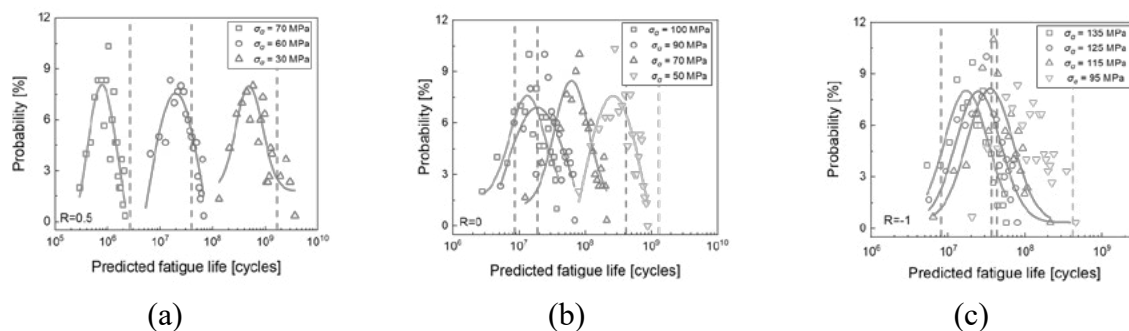


Figure 1. The probability distribution of the predicted fatigue life under three stress ratios and the comparison with experimental results represented by the dash-dotted lines.

The consideration of pore location and morphology in the proposed crack initiation life prediction model is included in the stress concentration factor (SCF) term. Figure 2(a) shows the maximum SCF considering the real defect and specimen size under different pore morphology and inclination. It is observed on the fracture surface that the surface crack initiation will transfer to the interior when the fatigue failure are about 10^7 cycles. Combined with the prediction model of crack initiation, the local stress of pore is the dominant factor for crack initiation under high fatigue loading, and the higher degree of freedom of surface pore

which will lead to the preferential initiation of crack on the surface. However, as the load decreases, the influence of local stress decreases, which together with the matrix determine the location of crack initiation. Nevertheless, the effect of surface crack oxidation to the competition phenomenon is not considered in this paper and needs further study.

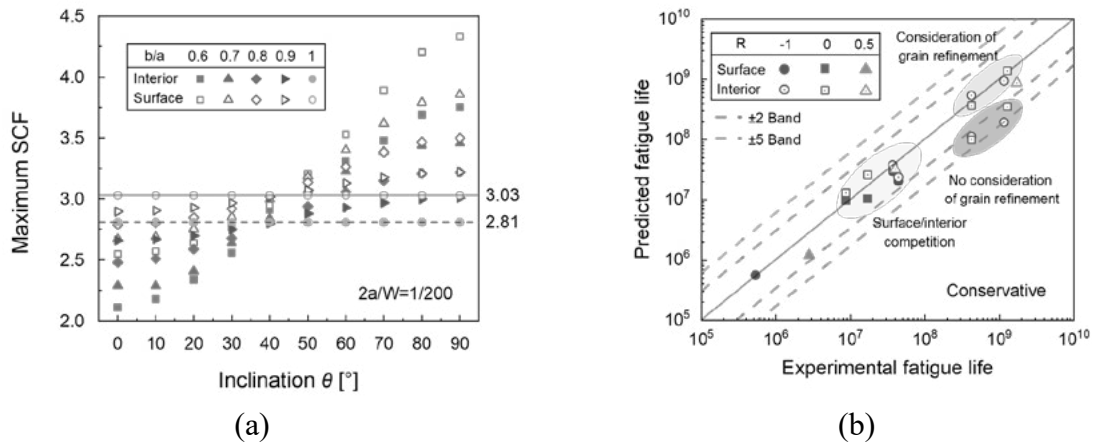


Figure 2. (a) The maximum SCF considering the real defect and specimen size under different pore morphology and inclination, and (b) the comparison between predicted and experimental results and the results of considering grain refinement (in green area).

Figure 2(b) shows the comparison between predicted and experimental results, which shows a good prediction effect when the failure life is lower than 10^8 cycles. But the results in the gray area are conservative when the failure life is higher than 10^8 cycles under the stress ratios of -1 and 0. The RA containing fine grains was observed at the crack initiation position of the corresponding fracture surface. According to the study of researchers [4-5], grain refinement will lead to the reduction of the threshold value of the stress intensity factor (SIF), so that the crack in this region can firstly propagate. Considering the Hall-Petch effect, the crack propagation in the RA needs more cycles. The predicted results after considering this effect in the short crack growth life prediction model are shown in the green area in Figure. 2(b). Overall, the predicted results are in good agreement with the experimental ones.

REFERENCES

1. Tridello, A.; Niuitta, C.B.; Haghshenas, M.; Berto, F.; Paolino, D.S.. Very High Cycle Fatigue (VHCF) of Materials: An Overview. Reference Module in Materials Science and Materials Engineering (2023).
2. Spriestersbach, D.; Kerscher, E. The role of local plasticity during very high cycle fatigue crack initiation in high-strength steels. *Int. J. Fatigue*, 111, 93–100 (2018).
3. Tanaka, K.; Mura, Y. A. A dislocation model for fatigue crack initiation. *J Appl Mech.* 48, 97-103 (1981).
4. Mughrabi, H.; Höppel, H. W. Cyclic deformation and fatigue properties of very fine-grained metals and alloys. *Int. J. Fatigue*, 32, 1413–1427 (2010).
5. Hockauf, K.; Halle, T.; Hockauf, M.; Wagner, M. F. X.; Lampke, T. Near-threshold fatigue crack propagation in an ECAP-processed ultrafine-grained aluminum alloy. *Materials Science Forum*, 667-669, 873-878 (2010)

Towards modeling hydrogen-stabilized vacancy complex interactions in crack tip fatigue of austenitic stainless steels

Theodore ZIRKLE^{1,2}, Ting ZHU¹ and David McDOWELL¹

¹ Woodruff School of Mechanical Engineering, Georgia Institute of Technology, Atlanta, GA 30332-0405 USA

² Exponent, Philadelphia, PA USA

david.mcdowell@me.gatech.edu

Hydrogen embrittlement of metallic materials is widely observed, but remains a challenge for predictive computational modeling. Multiscale modeling initiates with atomistic modeling of H-mediated dislocation plasticity for the Fe-Ni-Cr-H alloy system. A cyclic crystal plasticity model is formulated with input from the atomistic reaction pathway modeling of dislocation mobility that also considers strong pinning effects of high concentration of hydrogen-stabilized vacancy complexes [1] in addition to effects of deformable dislocation cell walls on cyclic plastic response [2] and solute drag effects of hydrogen [3]. Crystal plasticity finite element simulations reveal the effects of coupling hydrogen diffusion and plastic deformation at the crack tip, including pipe diffusion [4].

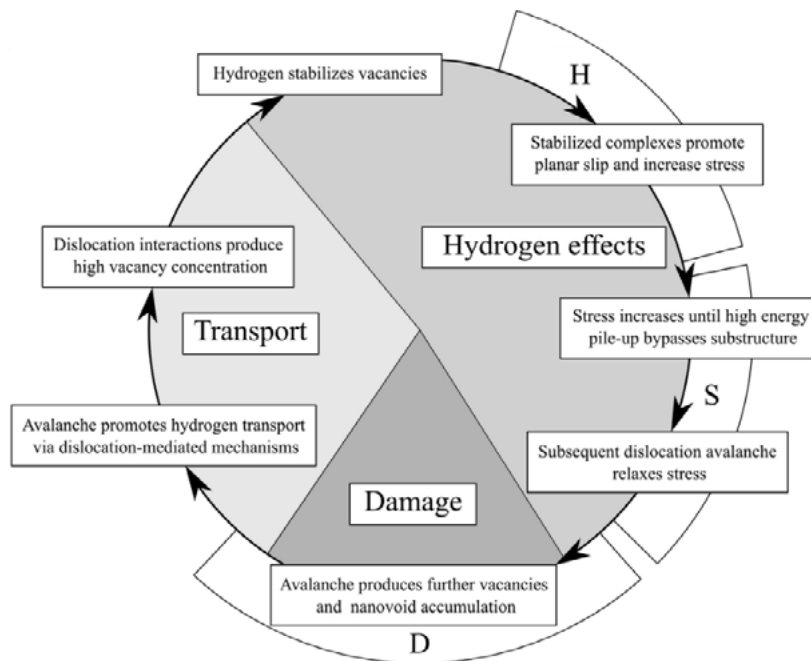


Figure 1. Schematic explaining the progression of hydrogen effects on crack tip damage evolution. Recurrent mechanisms in episodic crack advance are designated via clockwise arrows denoting the sequential activation and development of various hydrogen-related defect mechanisms (redistribution with crack advance, transport, inelastic deformation, nanovoid formation/coalescence into vacancy sheets, and crack advance) [5].

A fully two-way coupled chemomechanical model is introduced [5] to model dislocation-enhanced hydrogen transport and effects on dislocation activity and damage that is pertinent to high strain and strain gradient fields near crack tips under cyclic loading. The logic and

elements of the model are shown schematically in Figure 1. Evolution equations are based on multiscale modeling strategies drawing from atomistic simulations and unit process models for dislocation-obstacle interactions, consistent with experimental information. Vacancies generated via dislocation interactions are stabilized by hydrogen, affecting transport and serving as obstacles to dislocation glide that promote increased slip planarity. Mechanisms of vacancy coalescence into nanovoid sheets and intermittent dislocation avalanching are introduced near the crack tip as pertinent additional failure processes that accelerate crack growth in the presence of hydrogen. It is shown that the enhancement of the fatigue crack growth rate can be predicted using this methodology, as highlighted in Figure 2.

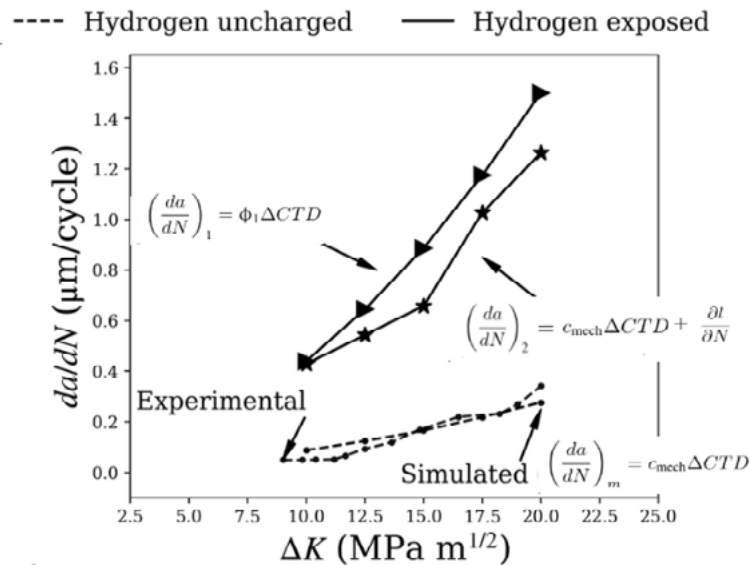


Figure 2. Estimated fatigue crack growth rates calibrated to experiments without hydrogen and prediction of the hydrogen-enhanced growth rate for two model frameworks based on chemomechanical irreversibility factor ϕ_1 (upper left) and superposition of the purely mechanical model with a nanovoid sheet-based crack extension increment $\delta l / \delta N$ per cycle [5].

REFERENCES

1. Chen, D.; Costello, L.L.; Geller, C.B.; Zhu, T.; McDowell, D.L. Atomistic modeling of dislocation cross-slip in Nickel using free-end nudged elastic band method. *Acta Materialia*, 168, 426-447 (2019).
2. Zirkle, T.; Zhu, T.; McDowell, D.L. Micromechanical crystal plasticity back stress evolution within fcc dislocation substructure. *International Journal of Plasticity*, 146, 103082 (2021).
3. Zirkle, T.; Costello, L.; McDowell, D.L.; Crystal plasticity modeling of hydrogen and hydrogen-related defects in initial yield and plastic flow of single crystal stainless steel 316L. *Metall MaterTrans A*, 52, 3961-3977 (2021).
4. Zirkle, T.; Costello, L.R.; Zhu, T.; McDowell, D.L.; Modeling dislocation-mediated hydrogen transport and trapping in fcc metals. *ASME Journal of Engineering Materials and Technology*, 144(1), 011005 (2022).
5. Zirkle, T.; Zhu, T.; and McDowell, D.L. Multiscale modeling of hydrogen-affected crack tip damage using a fully coupled chemomechanical crystal plasticity framework for austenitic stainless steel. *International Journal for Multiscale Computational Engineering*, 21(2), 21-65 (2023).



ISBN 9788869384080